Probing the nature of electroweak symmetry breaking with Higgs boson pair-production at ATLAS

IHEP Beijing

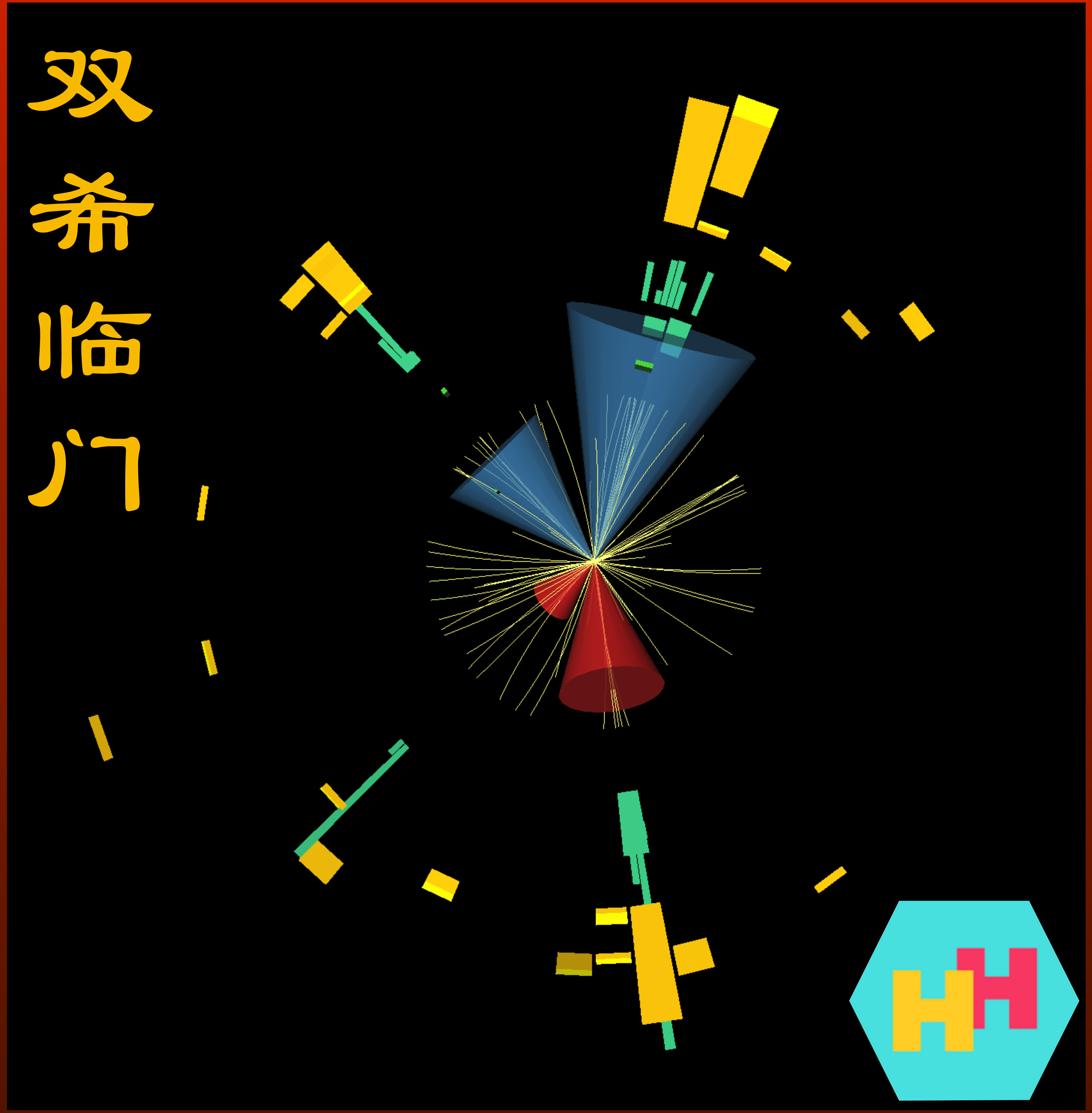

KHOO Teng Jian
(邱鼎坚)

Why HH?

Ellis, arXiv:1312.5672

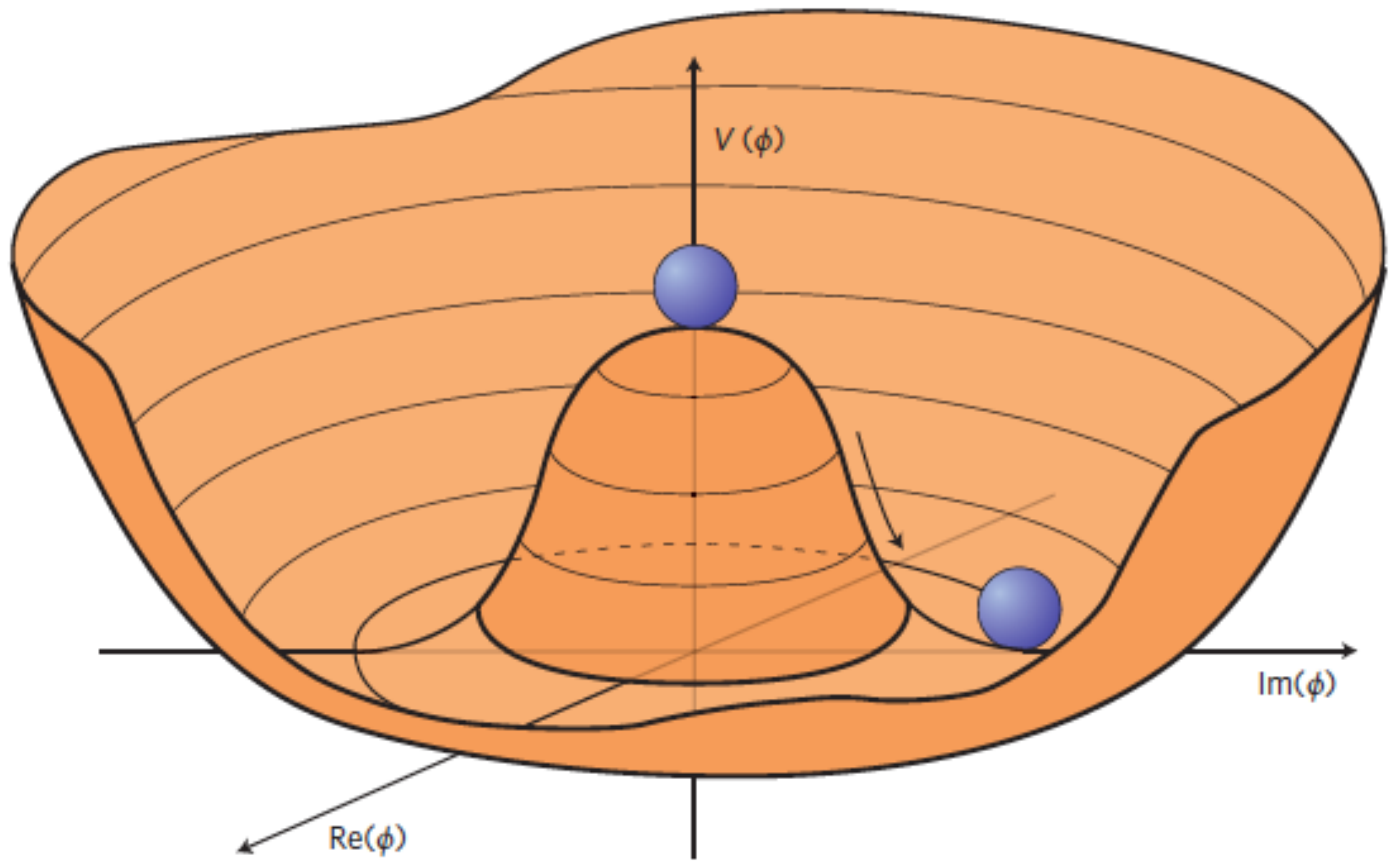

Classic 'Mexican Hat'
Higgs potential

Minimum displaced from origin causes
ElectroWeak Symmetry Breaking

$$V_h = \underbrace{\lambda v^2 h^2}_{m_h} + \lambda v h^3 + \frac{\lambda}{4} h^4$$

Why HH?

Ellis, arXiv:1312.5672

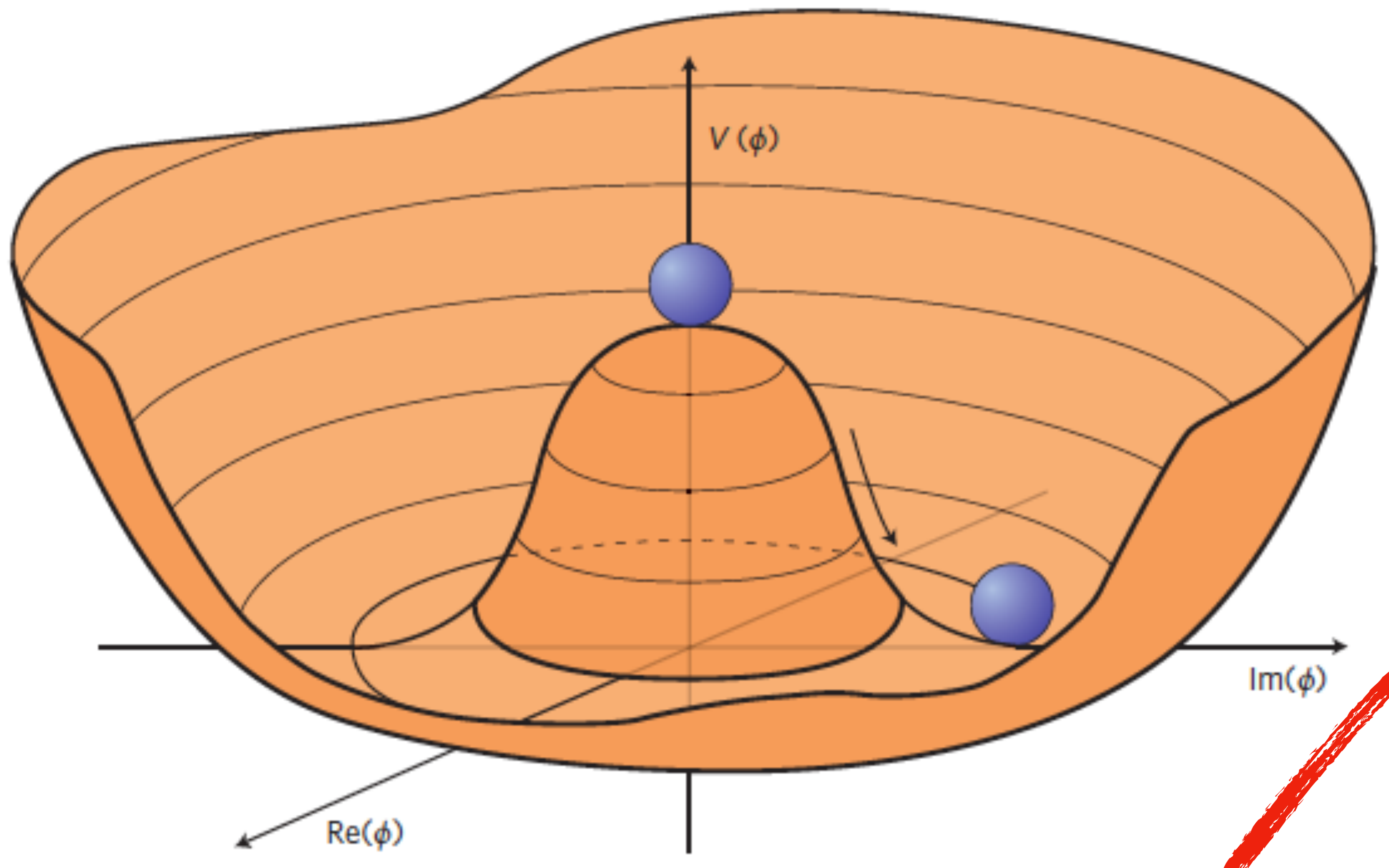

Classic 'Mexican Hat' Higgs potential

Minimum displaced from origin causes ElectroWeak Symmetry Breaking

$$V_h = \lambda v^2 h^2 + \lambda v h^3 + \frac{\lambda}{4} h^4$$

Taylor expansion indicates trilinear and quartic self-coupling terms

Trilinear self-coupling

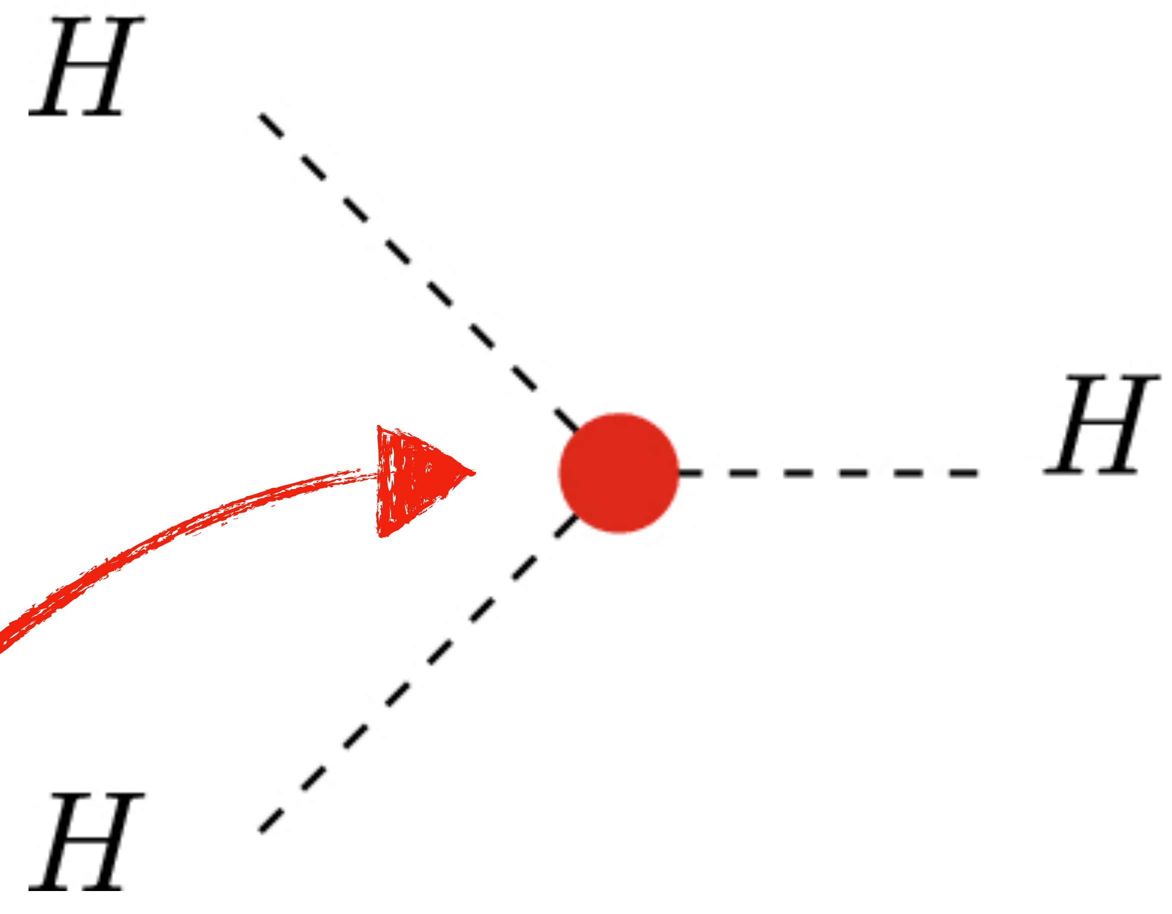

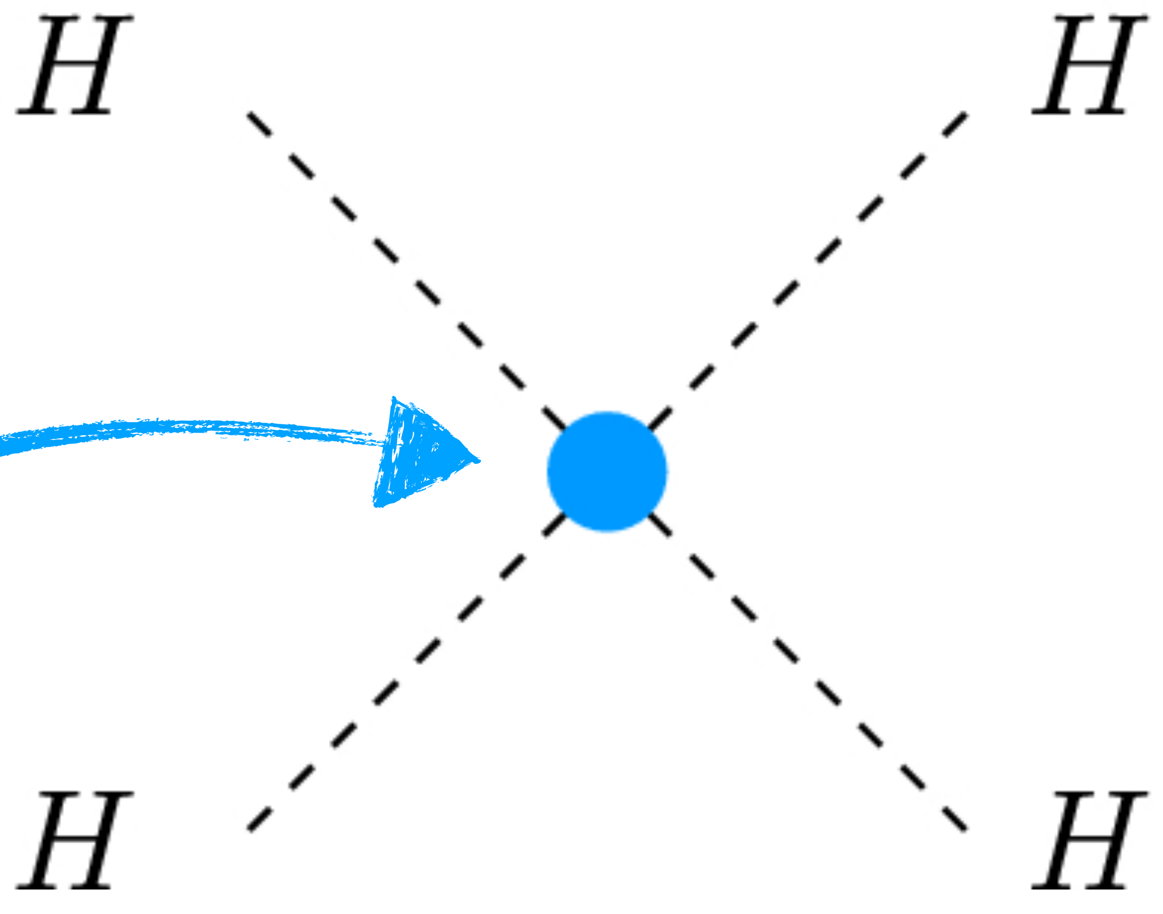

Quartic self-coupling

Why HH?

Ellis, arXiv:1312.5672

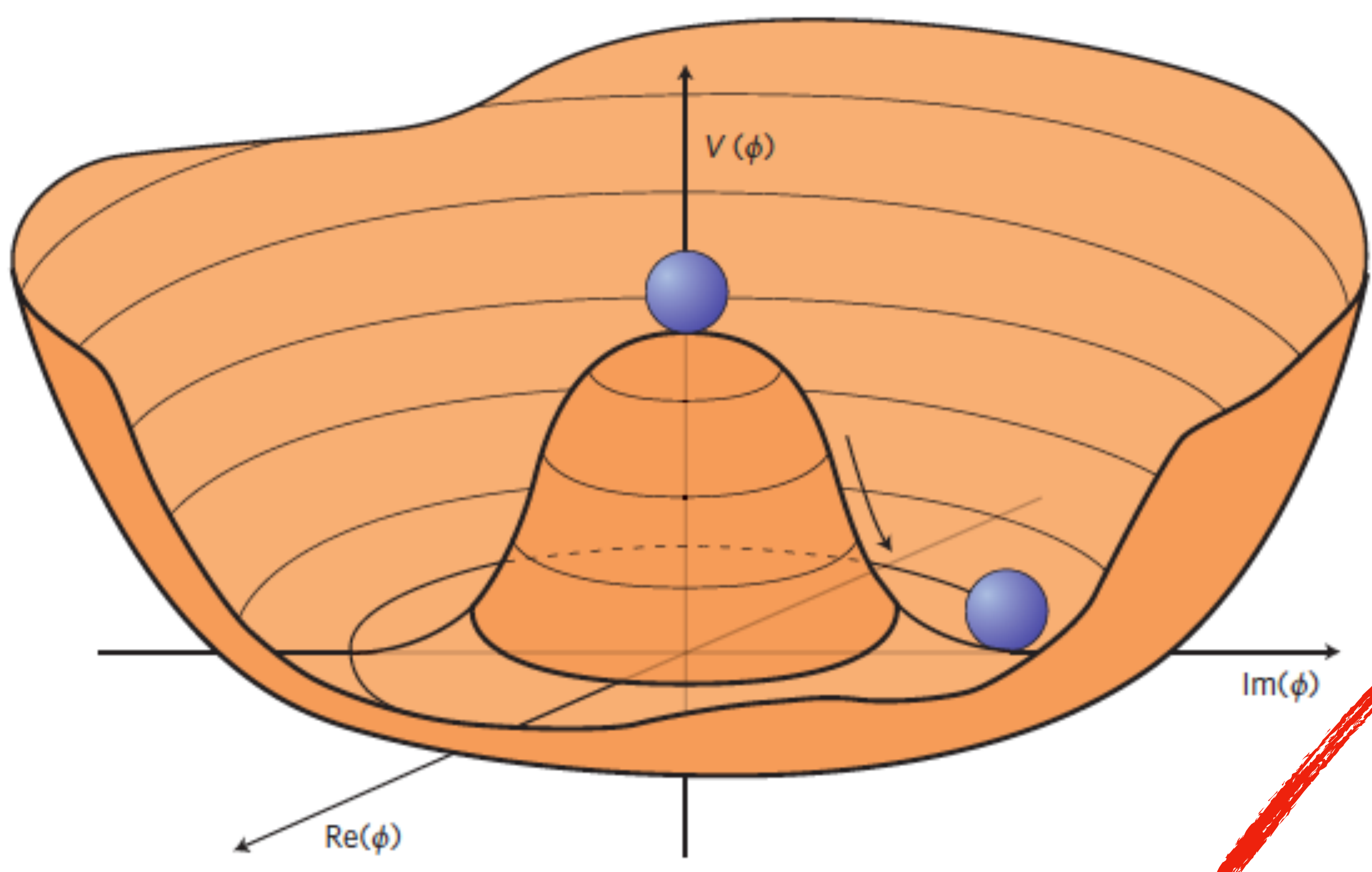

Classic 'Mexican Hat' Higgs potential

Minimum displaced from origin causes ElectroWeak Symmetry Breaking

$$V_h = \lambda v^2 h^2 + \lambda v h^3 + \frac{\lambda}{4} h^4$$

Taylor expansion indicates trilinear and quartic self-coupling terms

Trilinear self-coupling

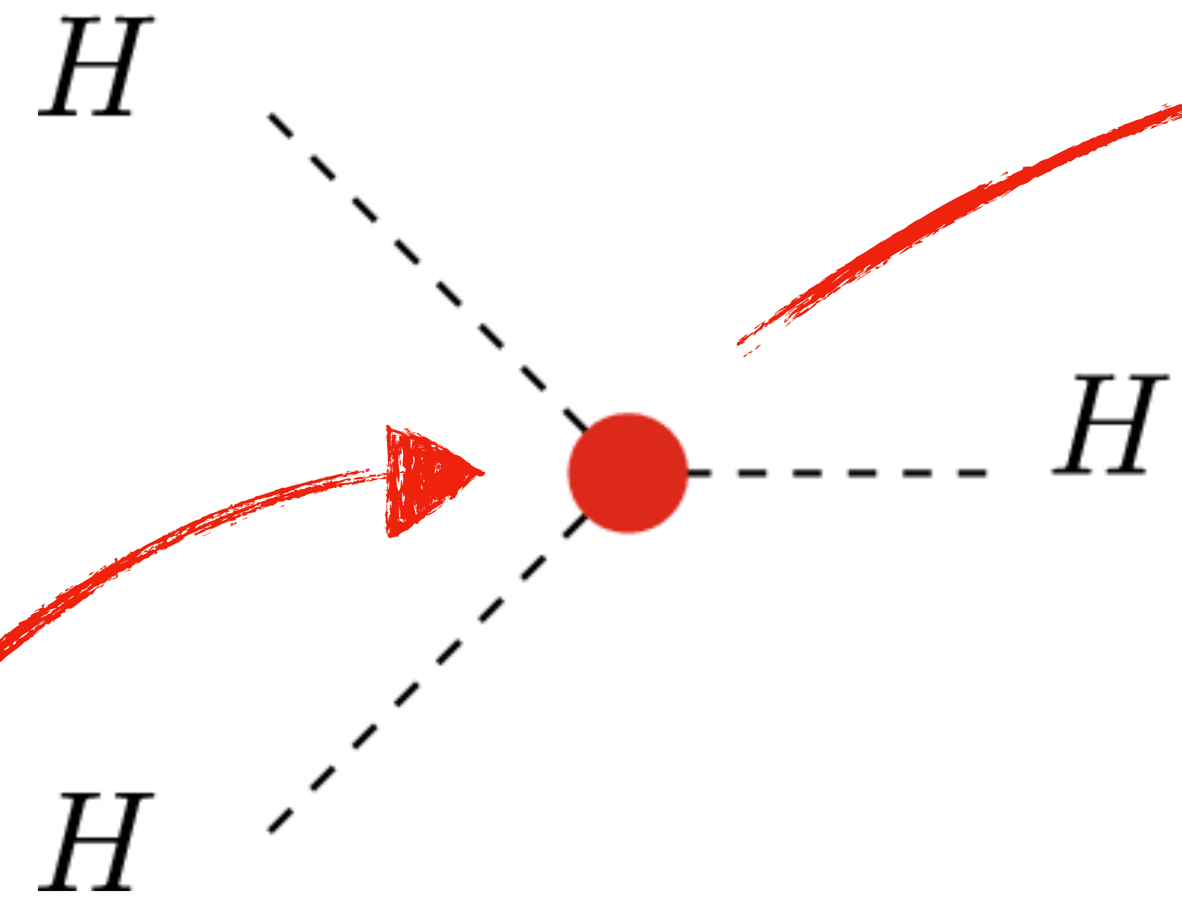

Di-Higgs production (gluon fusion)

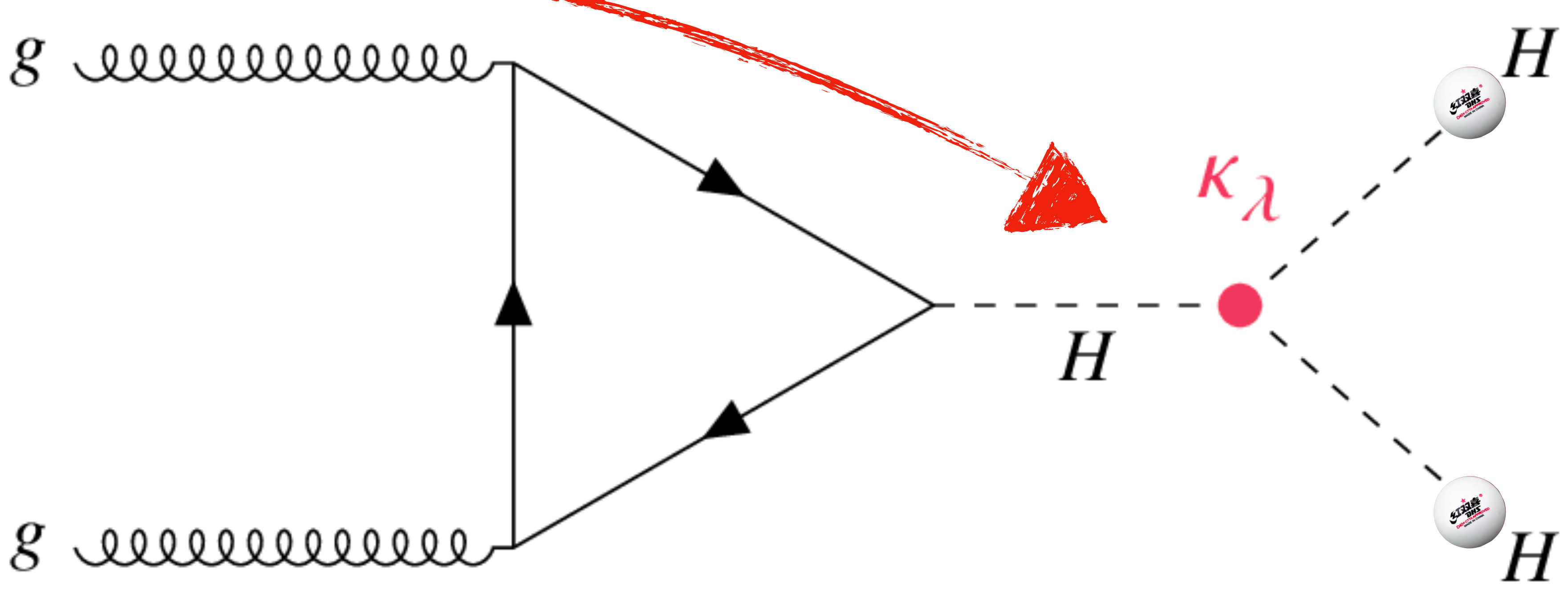

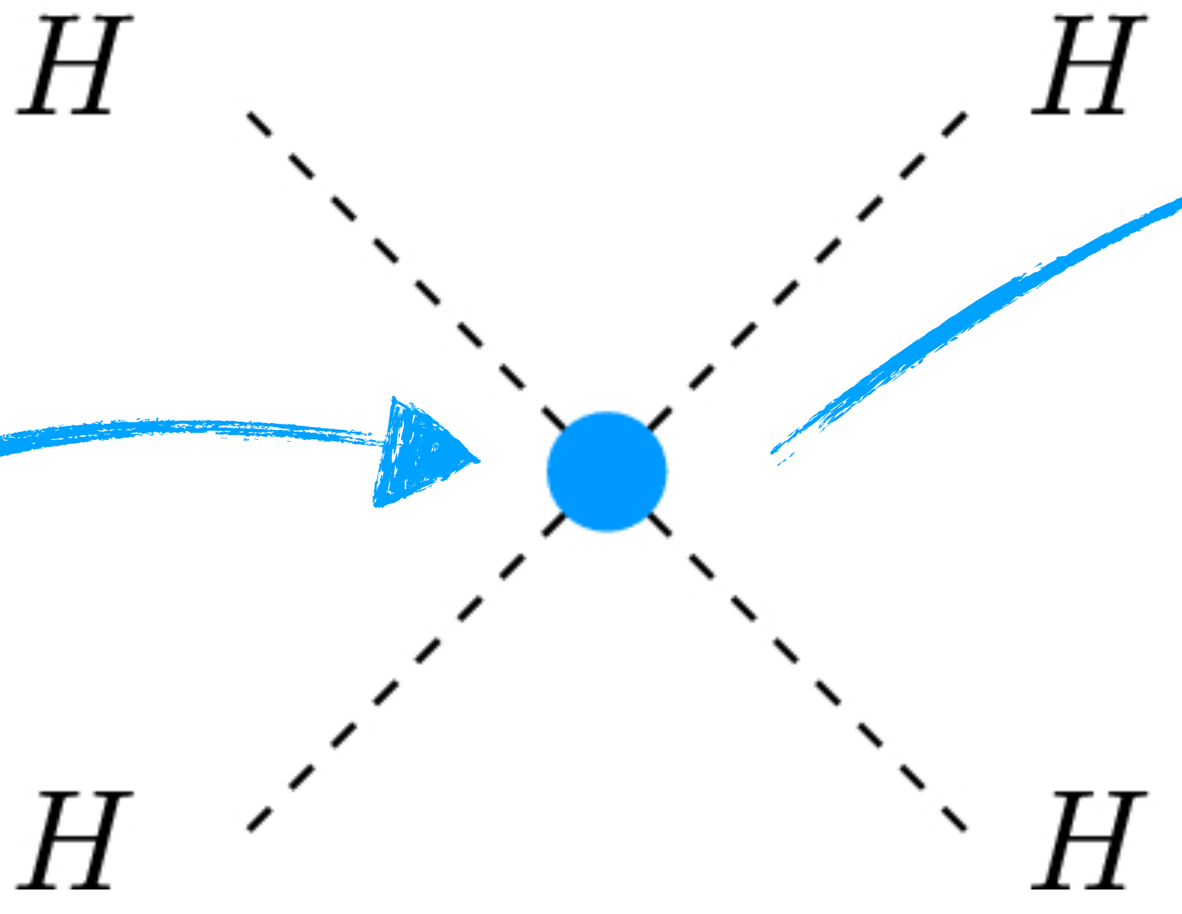

Quartic self-coupling

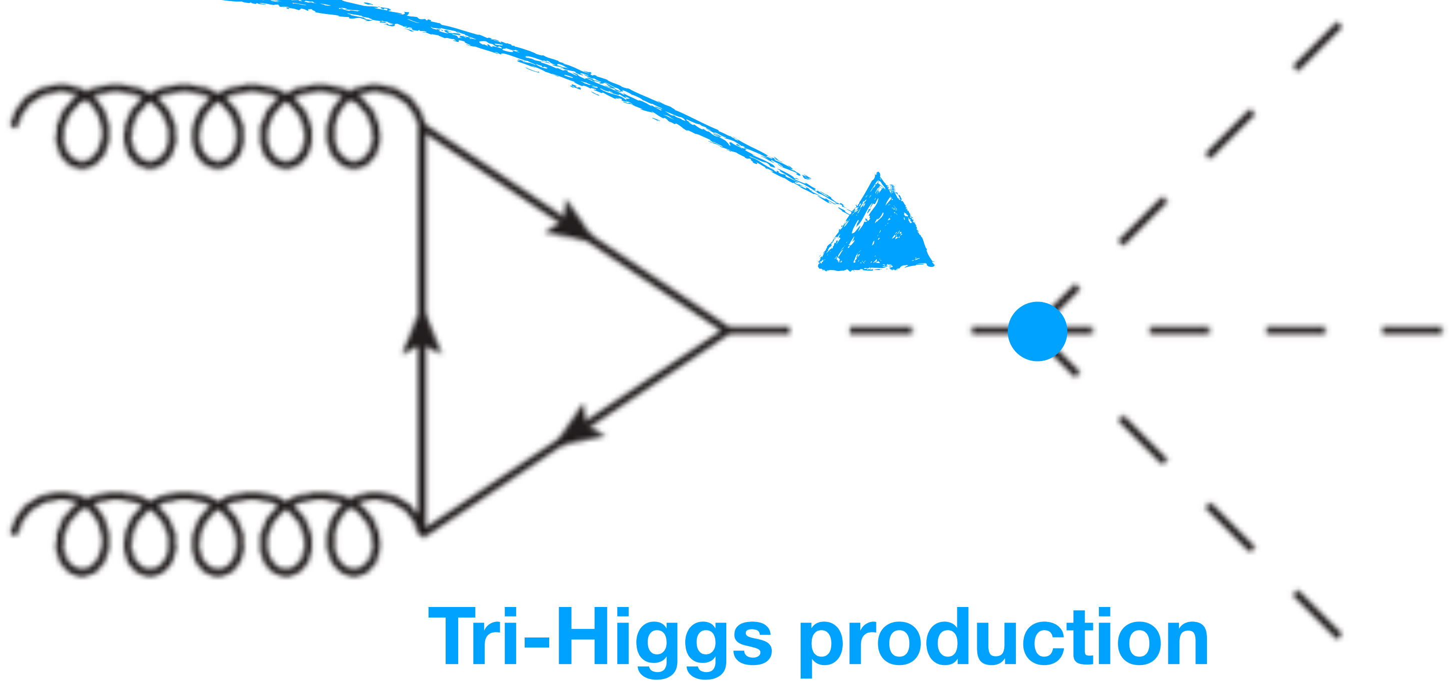

Tri-Higgs production (gluon fusion)

Why HH?

Ellis, arXiv:1312.5672

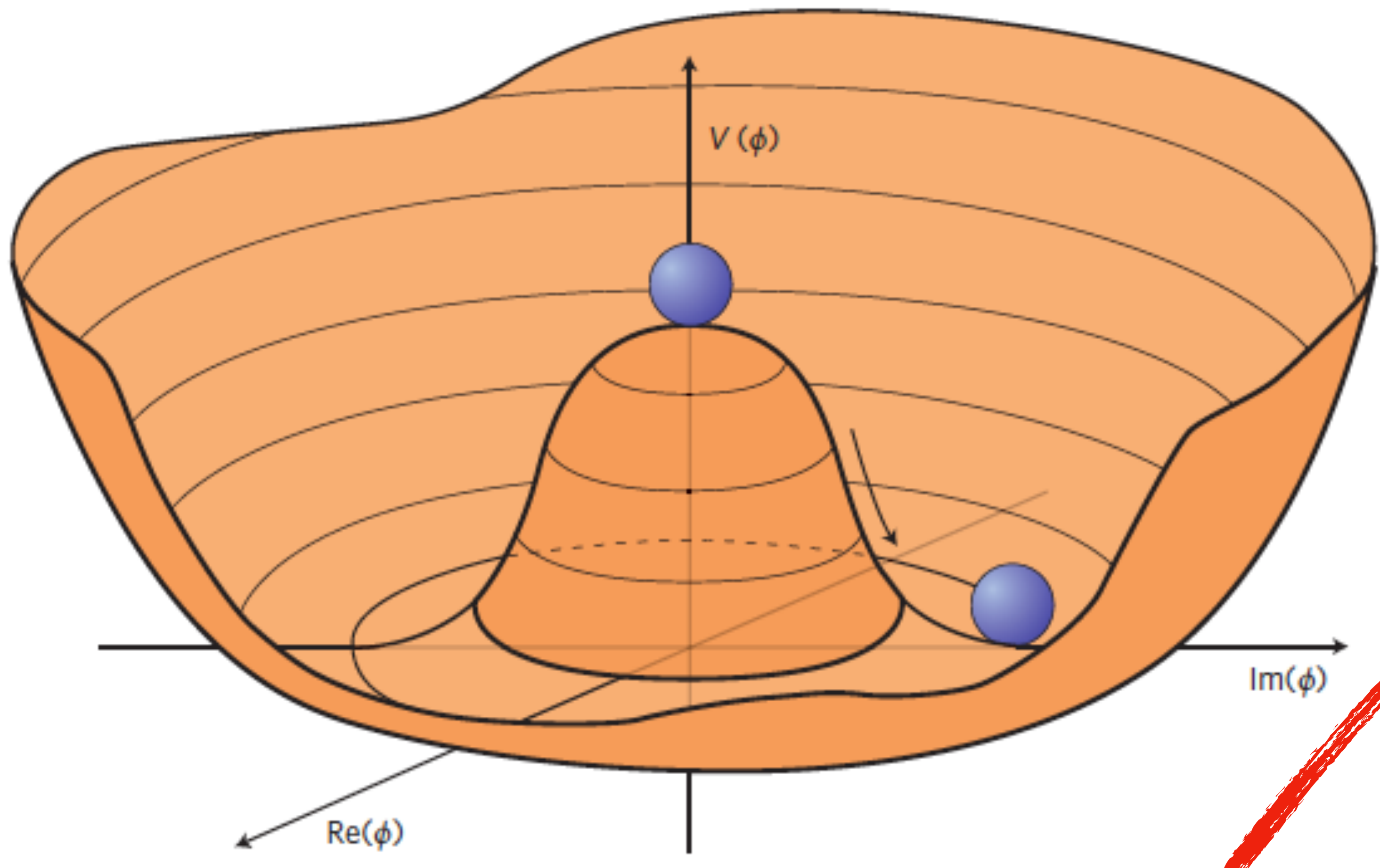

Classic 'Mexican Hat' Higgs potential

Minimum displaced from origin causes ElectroWeak Symmetry Breaking

$$V_h = \lambda v^2 h^2 + \lambda v h^3 + \frac{\lambda}{4} h^4$$

Taylor expansion indicates trilinear and quartic self-coupling terms

Trilinear self-coupling

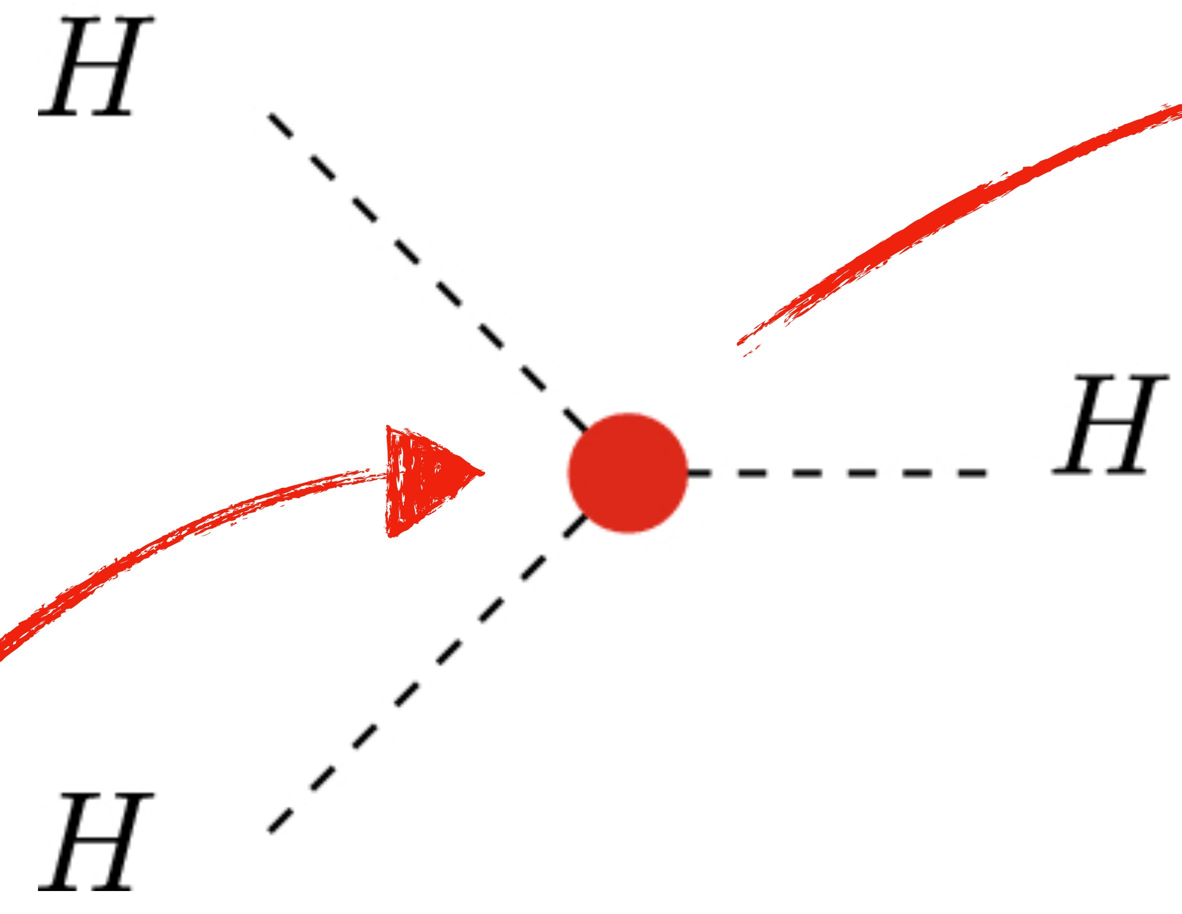

Quartic self-coupling

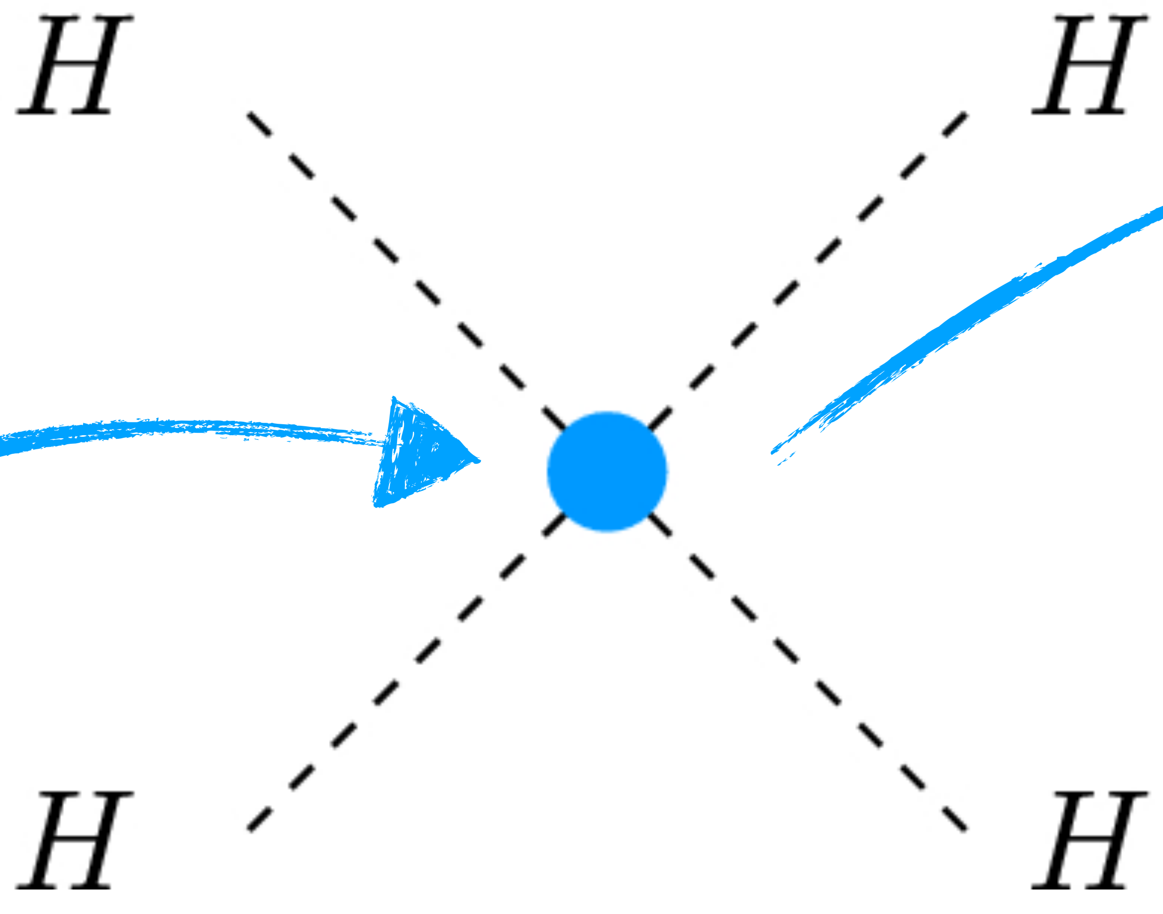

Di-Higgs production (gluon fusion)

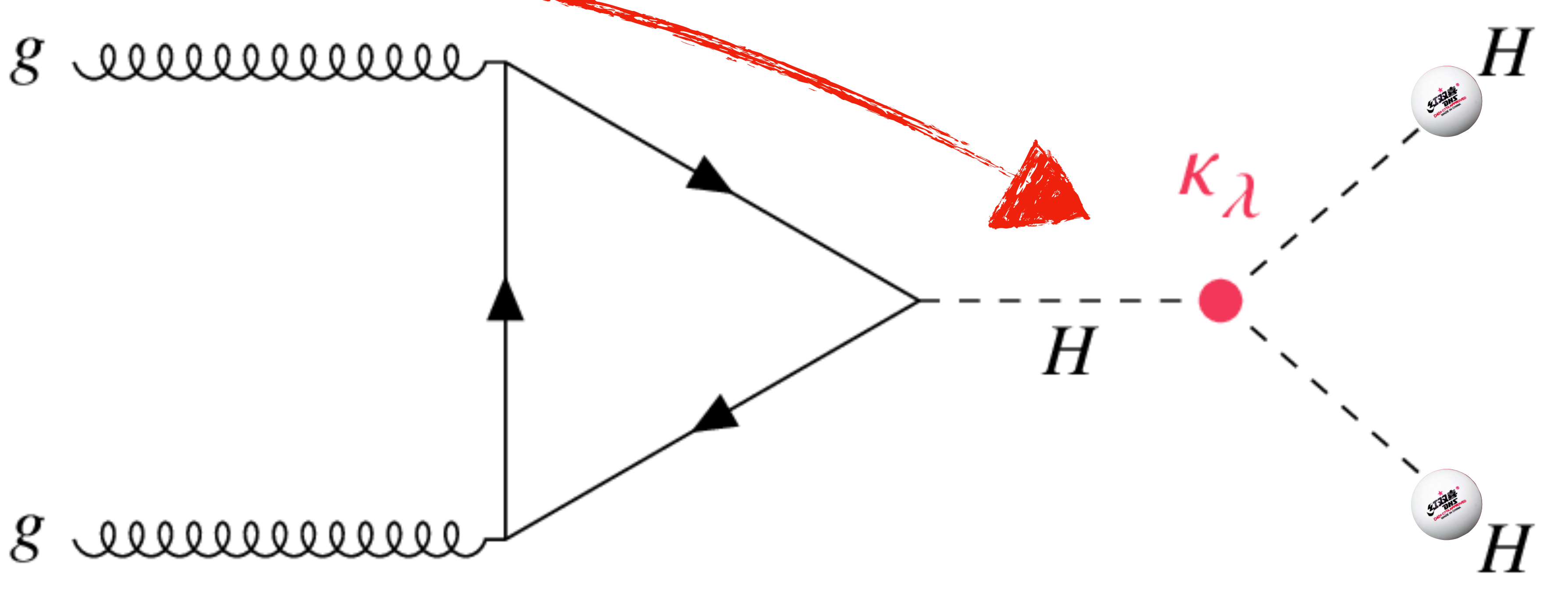

Tiny SM cross-section, inaccessible at HL-LHC

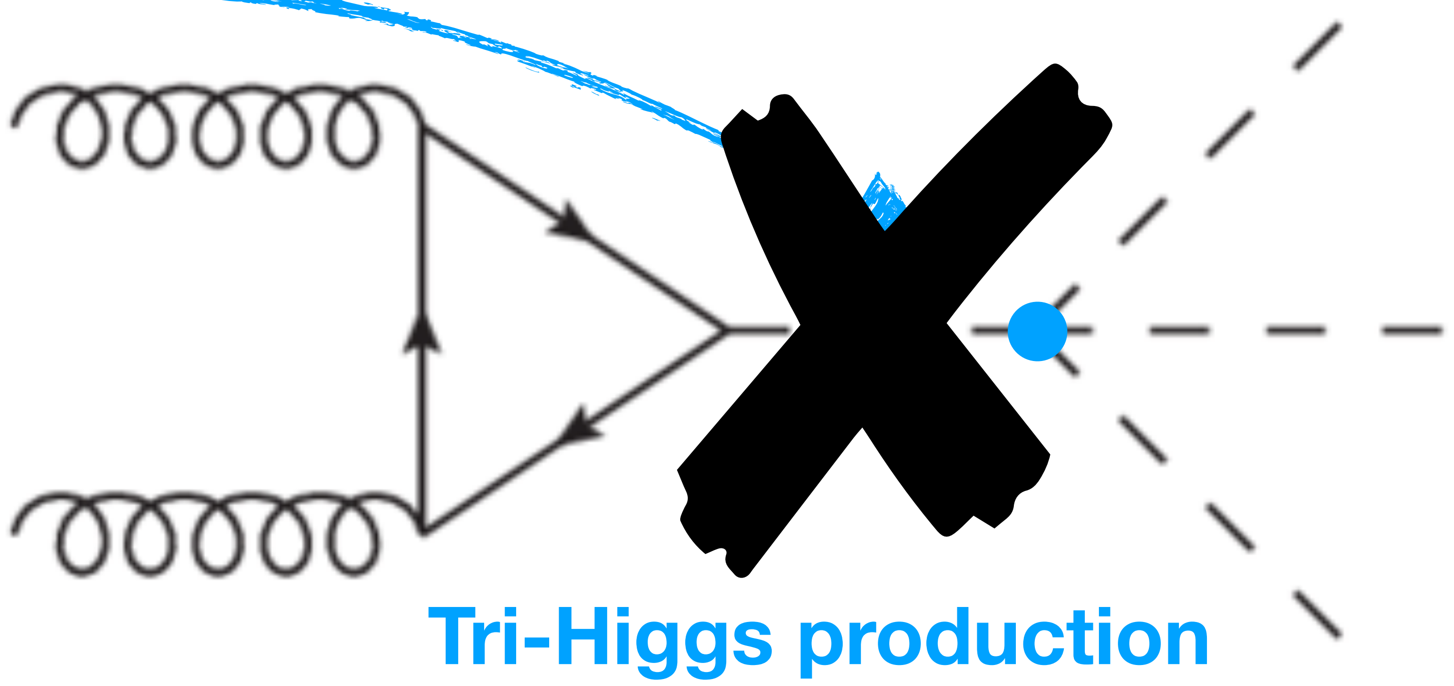

Tri-Higgs production (gluon fusion)

Why HH?

Ellis, arXiv:1312.5672

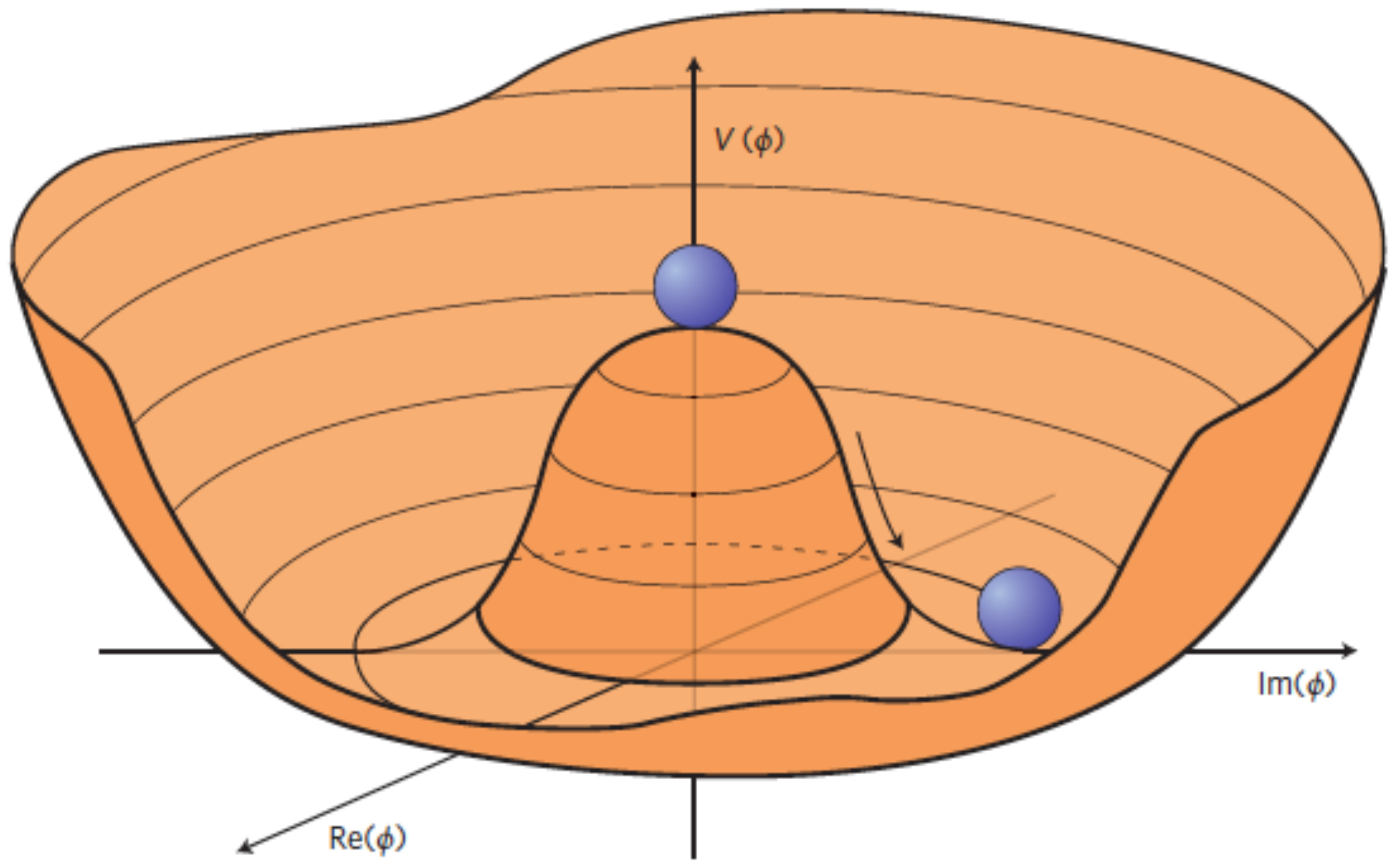

Classic 'Mexican Hat' Higgs potential

Minimum displaced from origin causes ElectroWeak Symmetry Breaking

$$V_h = \lambda v^2 h^2 + \lambda v h^3 + \frac{\lambda}{4} h^4$$

Taylor expansion indicates trilinear and quartic self-coupling terms

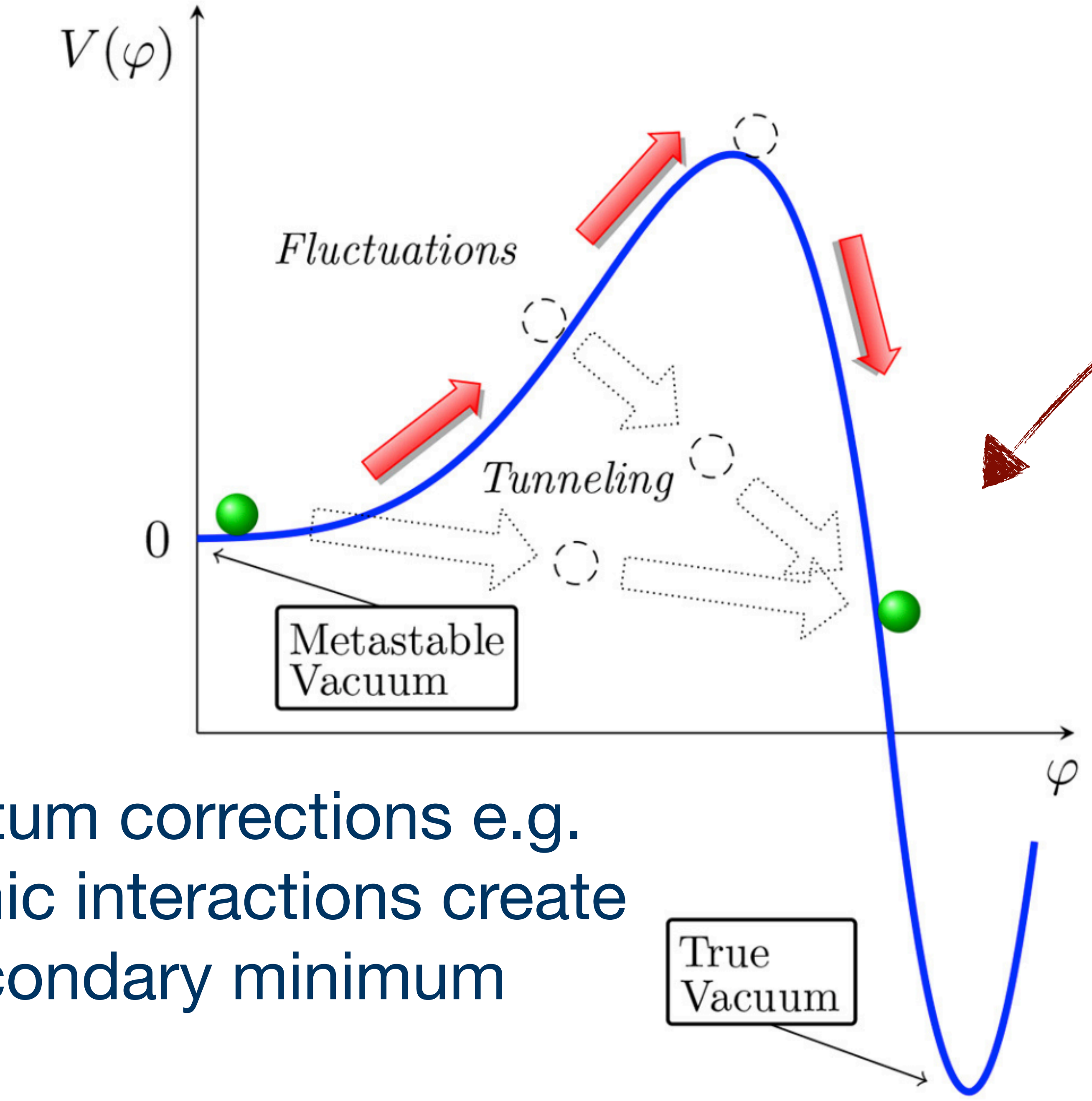

Quantum corrections e.g. fermionic interactions create secondary minimum

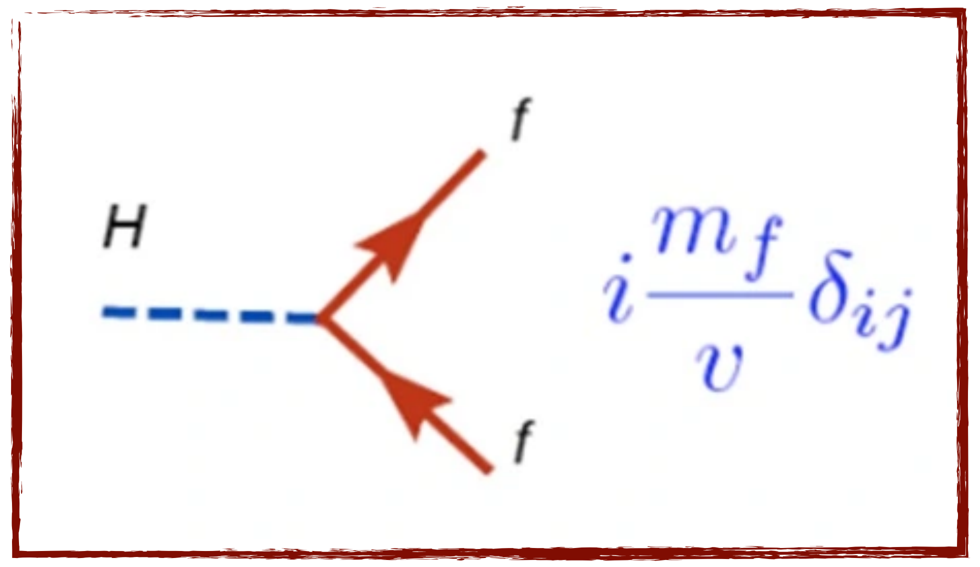

Fermions gain mass through Yukawa coupling, also generate corrections to V_h

EW vacuum is metastable, could tunnel to true vacuum

→ modify VEV ∝ $\sqrt{m_h}$

→ incompatible with observed universe!

Markkanen et al, 2018 [Front. Astron. Space Sci., 18 December 2018]

Why HH?

Ellis, arXiv:1312.5672

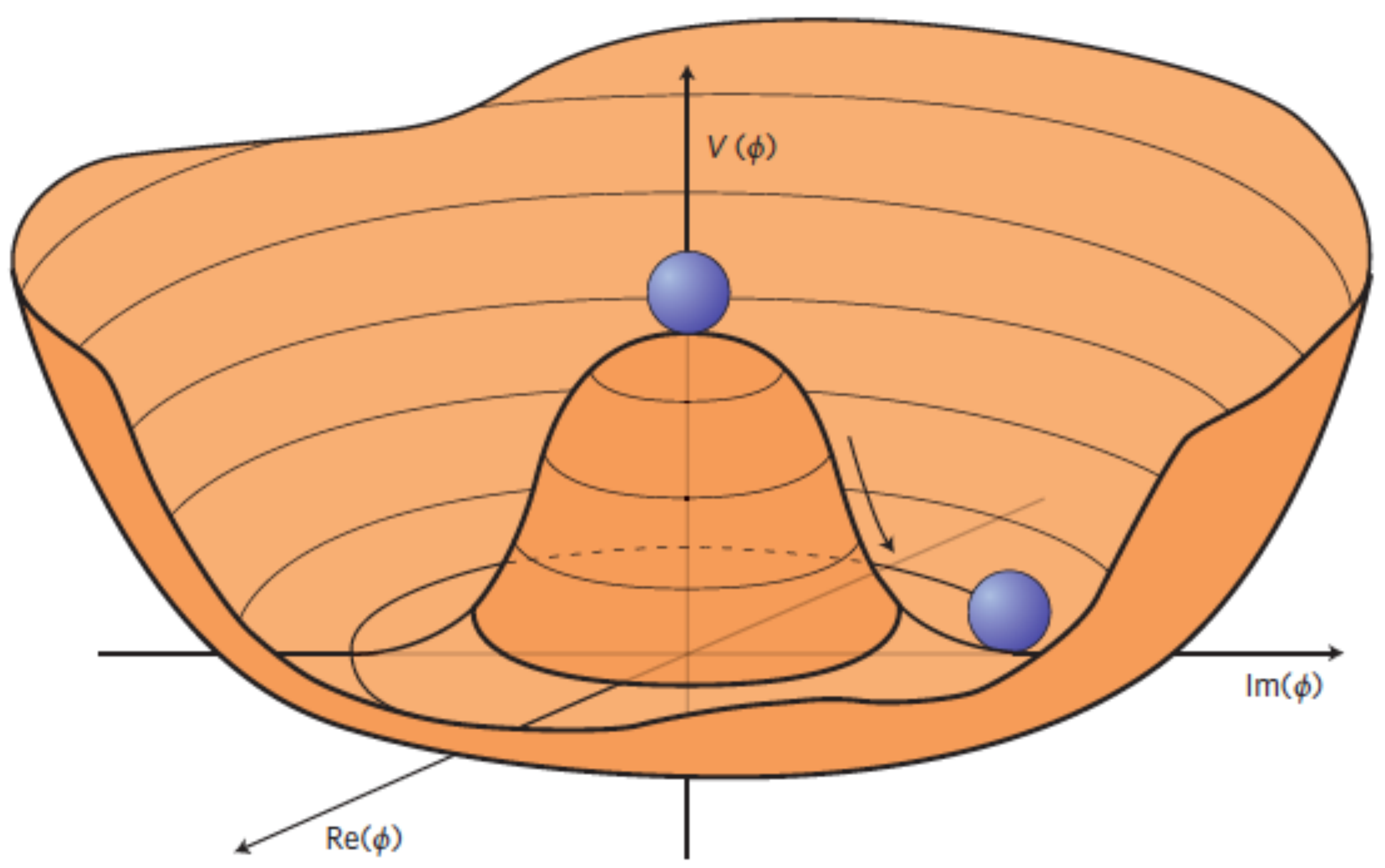

Classic 'Mexican Hat' Higgs potential

Minimum displaced from origin causes ElectroWeak Symmetry Breaking

$$V_h = \lambda v^2 h^2 + \lambda v h^3 + \frac{\lambda}{4} h^4$$

Taylor expansion indicates trilinear and quartic self-coupling terms

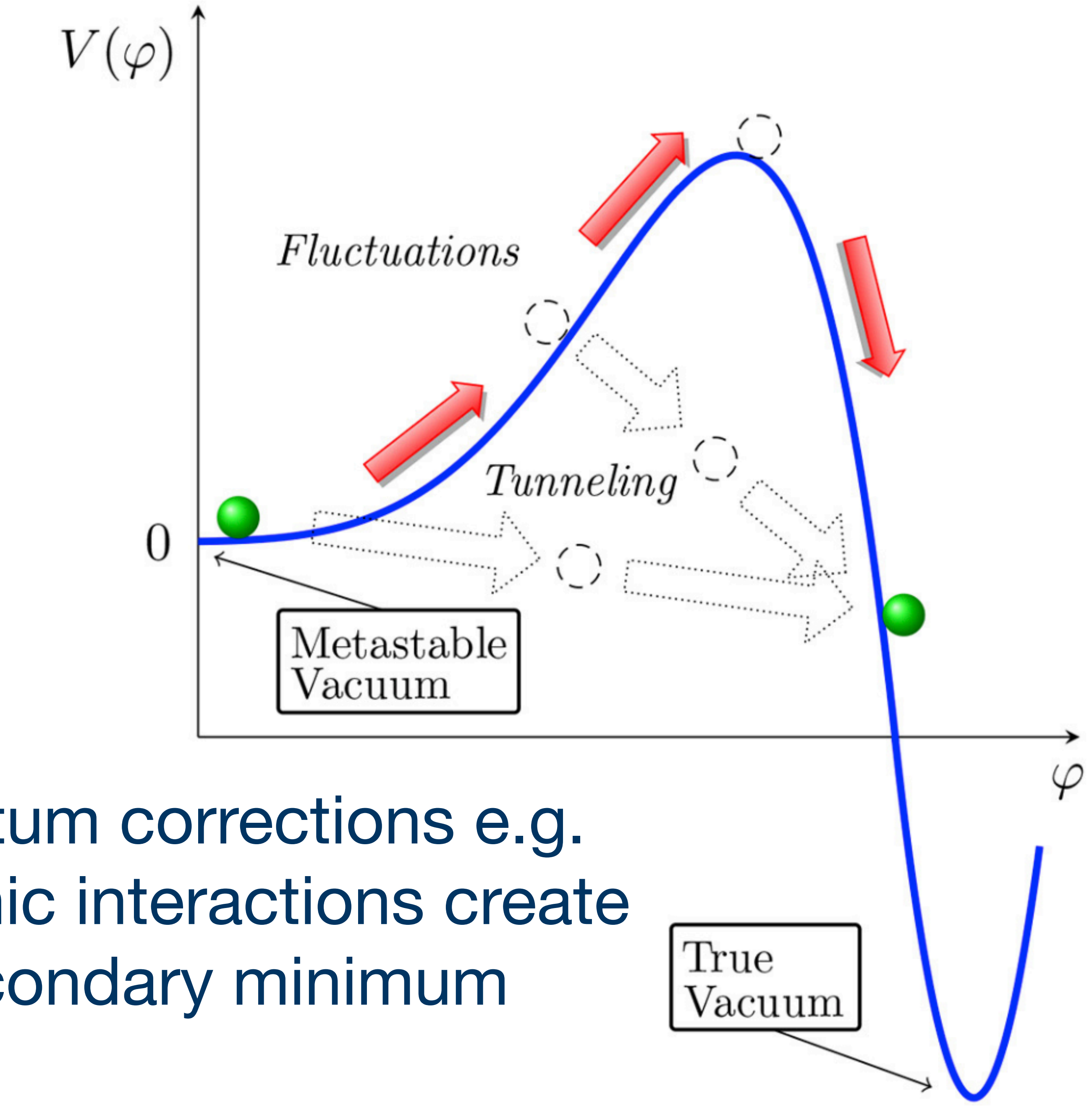

Quantum corrections e.g. fermionic interactions create secondary minimum

EW vacuum is metastable, could tunnel to true vacuum

→ modify VEV ∝ √m_h

→ incompatible with observed universe!

False vacuum lifetime > lifetime of Universe

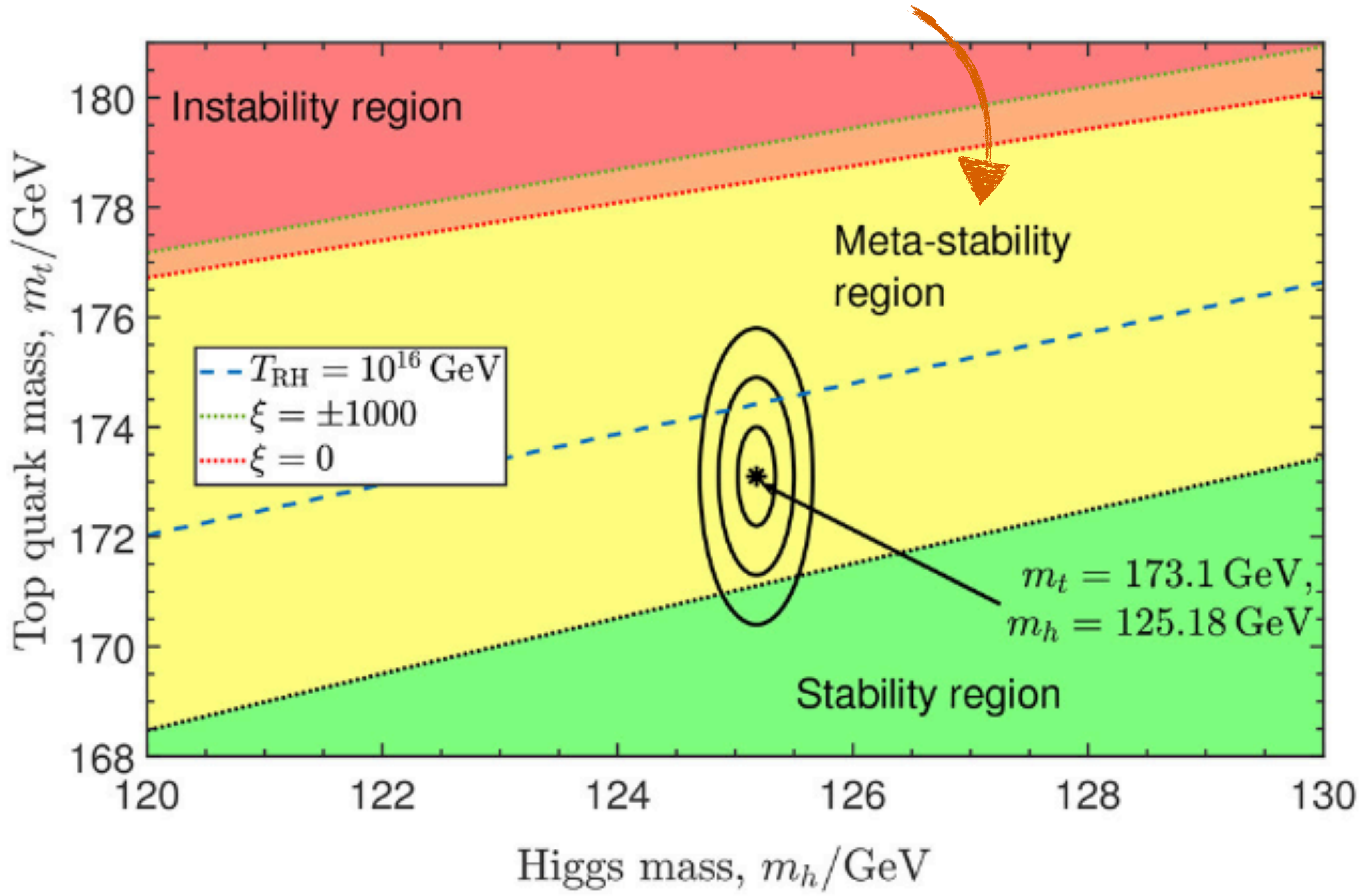

Measurements of m_t, m_h indicate Higgs potential in metastable region

Measure HH production to understand shape of V_h

Deviations from SM σ_{HH} indicate modifications to V_h

Markkanen et al, 2018 [Front. Astron. Space Sci., 18 December 2018]

DiHiggs @ LHC

NNLO: arXiv:1311.2931
LO: arXiV:1504.02334

Trilinear coupling

4.36 fb (LO) @ 13 TeV

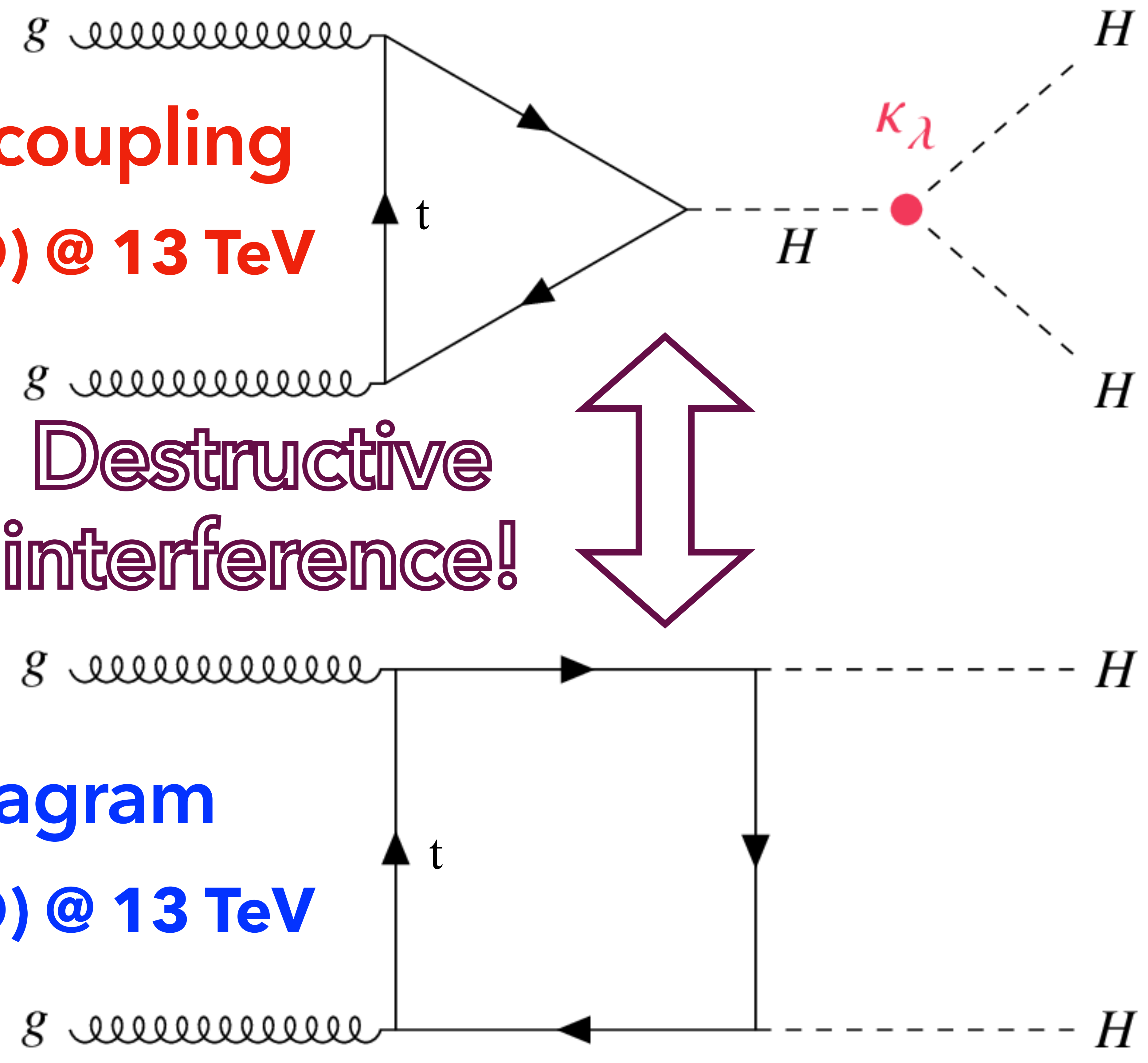

Box diagram

31.6 fb (LO) @ 13 TeV

Total σ_{HH} @ 13 TeV:

15 fb @ LO
31 fb @ NNLO

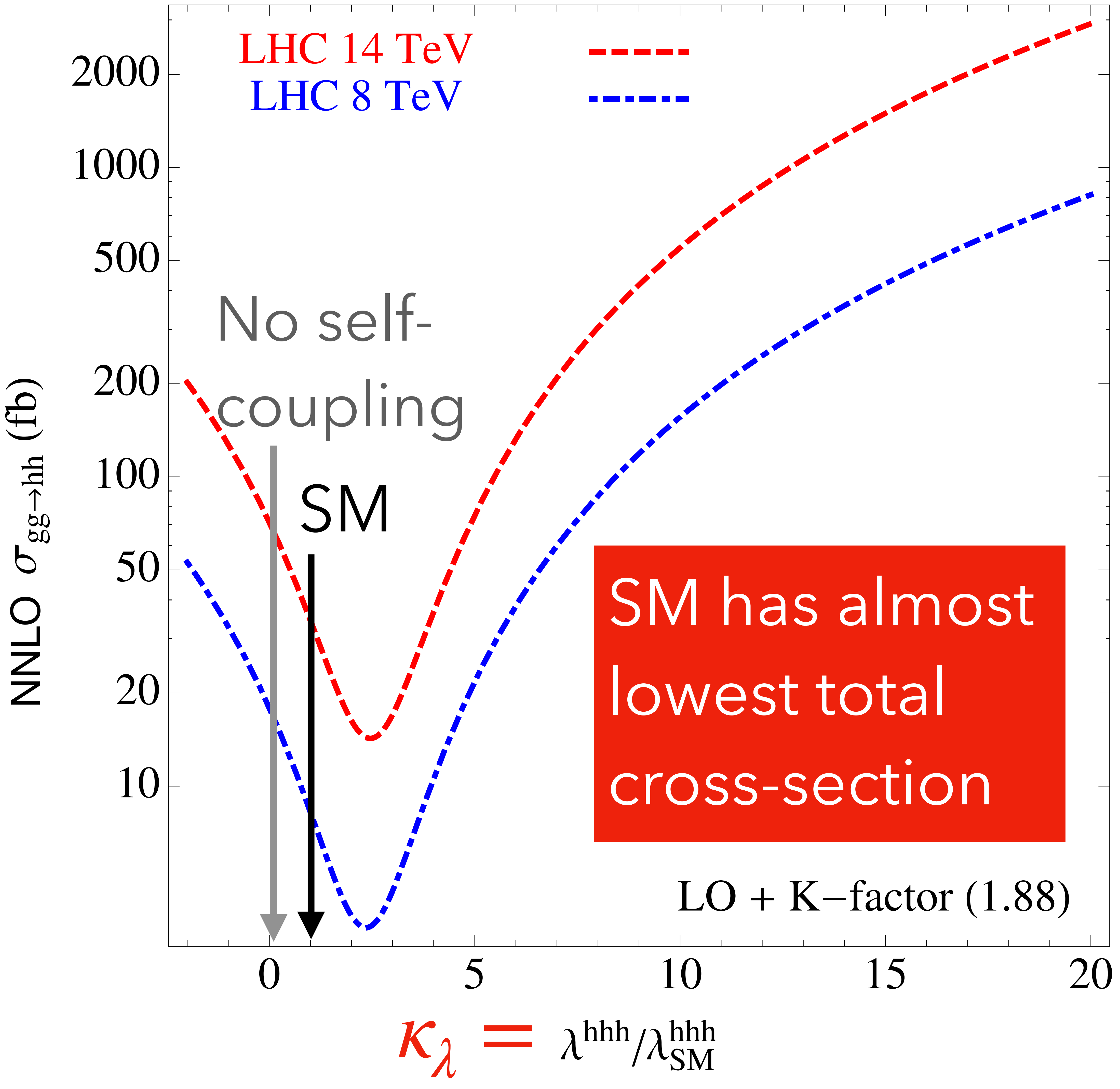

Primary experimental signatures

bb$\tau\tau$

➡ Mixed leptonic/ hadronic decays

bbbb

➡ Largest statistics

➡ Challenging background

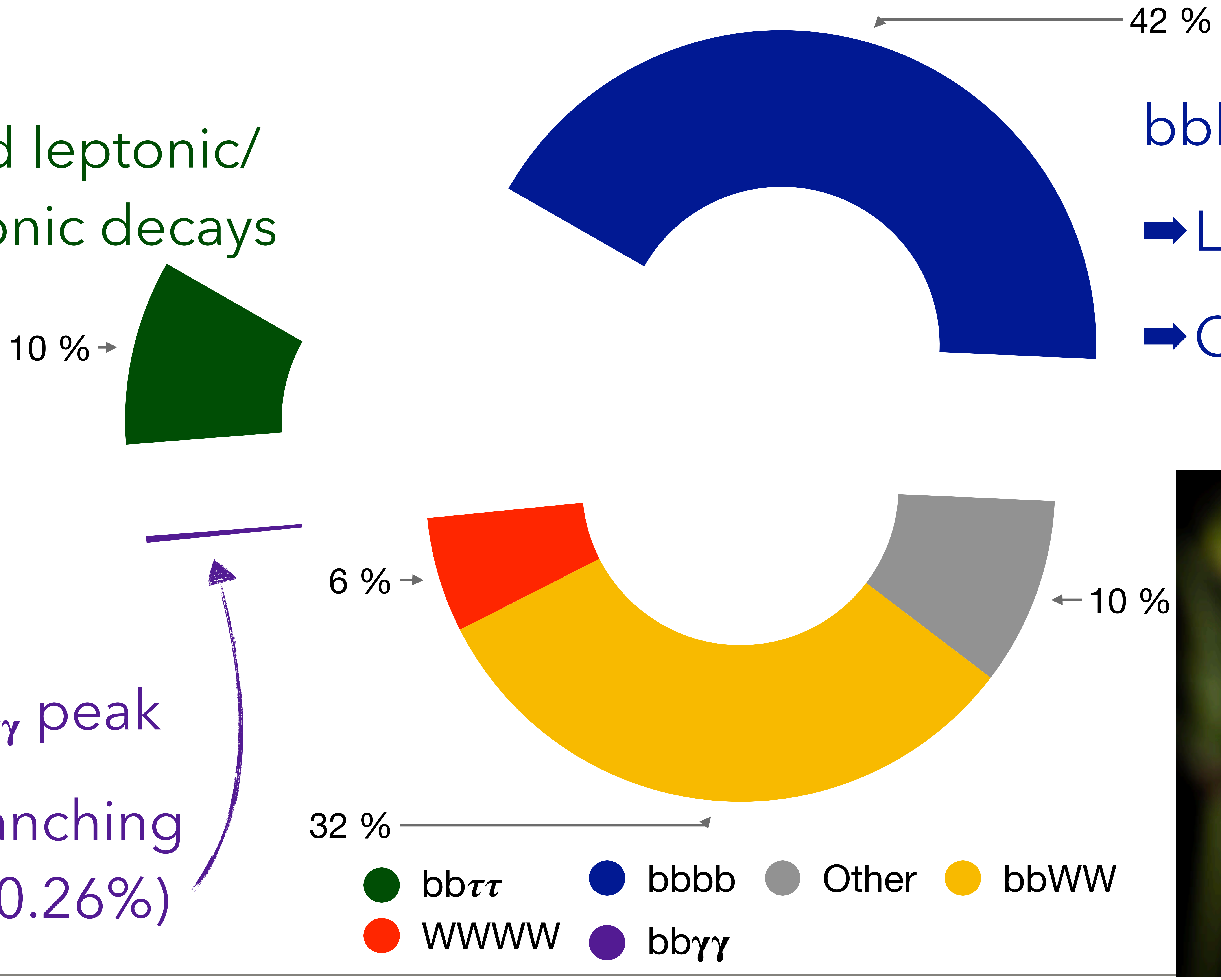

bb$\gamma\gamma$

➡ Clean $m_{\gamma\gamma}$ peak

➡ Small branching fraction (0.26%)

Primary experimental signatures

bb$\tau\tau$ [UPDATED!]

➡ Mixed leptonic/ hadronic decays

bbbb

➡ Largest statistics

➡ Challenging background

NEW @ ATLAS: bb$\ell\ell$ + E^T_{miss}

➡ $\ell\ell\nu\nu$ from ($\tau\tau$ + WW + ZZ)

➡ Clean $\ell\ell$ + E^T_{miss}

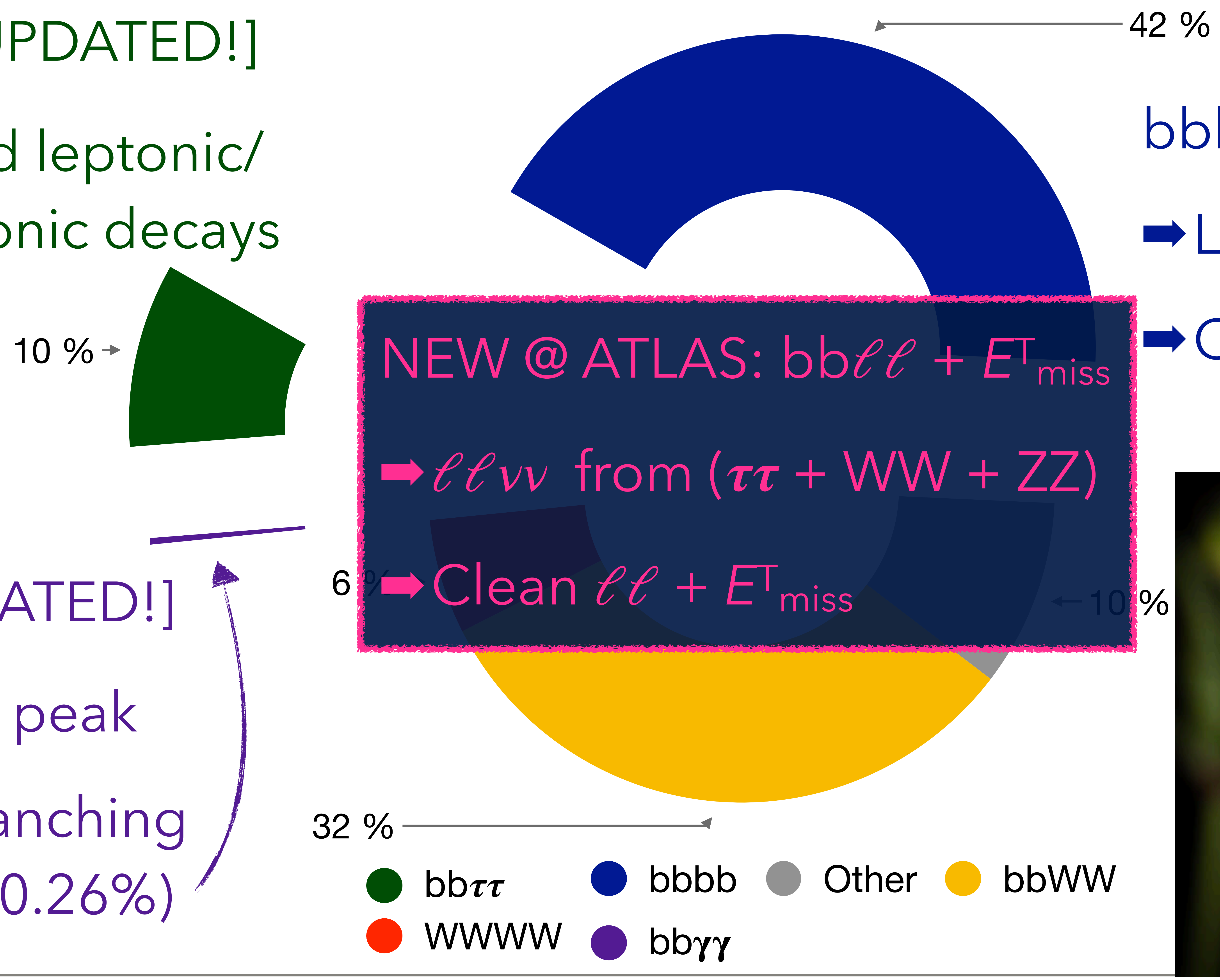

bb$\gamma\gamma$ [UPDATED!]

➡ Cleanest peak

➡ Small branching fraction (0.26%)

Related talks

$bb\tau\tau$ ATLAS EXPERIMENT

➡ B. Moser, this session

$bb\gamma\gamma$ ATLAS EXPERIMENT

➡ E. Mazzeo, tomorrow afternoon

NEW @ ATLAS: $bb\ell\ell + E_T^{miss}$

➡ $\ell\ell\nu\nu$ from $(\tau\tau + WW + ZZ)$

➡ Clean $\ell\ell + E_T^{miss}$

bbbbackgrounds

➡ M. Roguljic, N. Hartman

afternoon session today

CMS non resonant HH

B. D'Anzi, next talk

Full Run 2 (126-140 fb^{-1})

Analysis strategies

bbγγ

BDT — distinguish HH(bbγγ) from continuum γγ (+tt/jets)

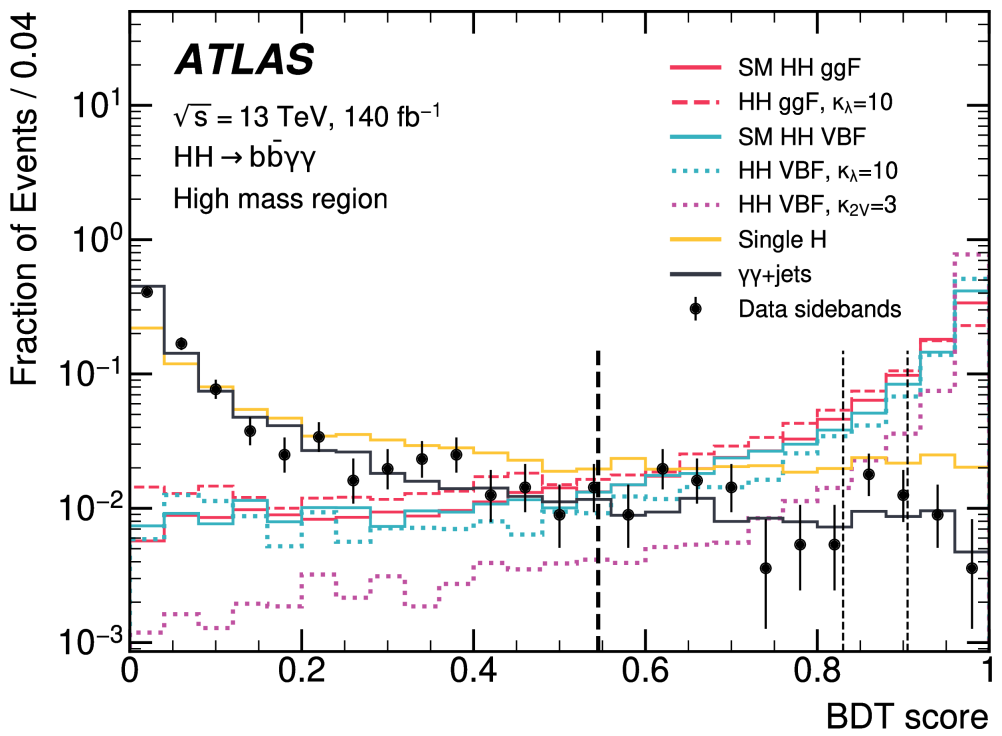

High/low m_{HH} categories

Fit $m_{\gamma\gamma}$ sidebands in BDT score categories

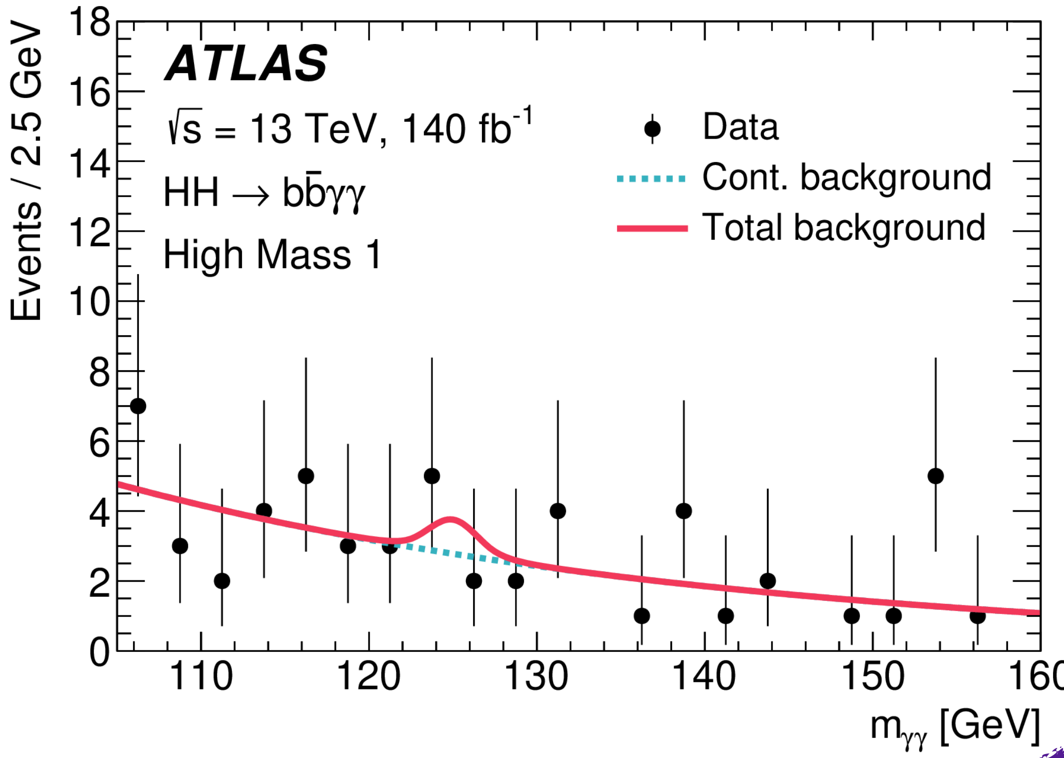

bbττ

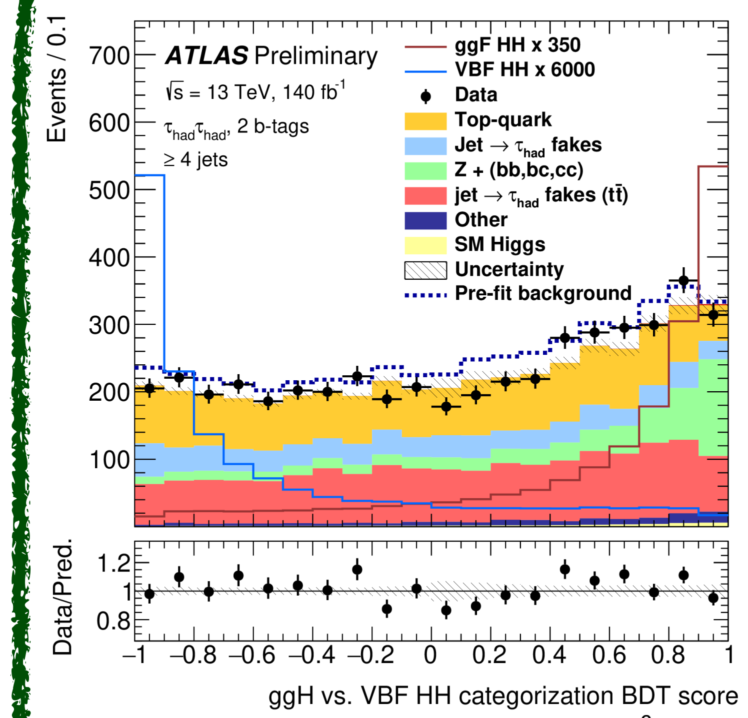

$m_{\tau\tau}$ (MMC) + $m_{bb} \Rightarrow m_{HH}$

+ other kine. variables

BDT

Signal extraction & categorisation

Fit MVA output distributions

Illustrated in merged bins of increasing signal significance

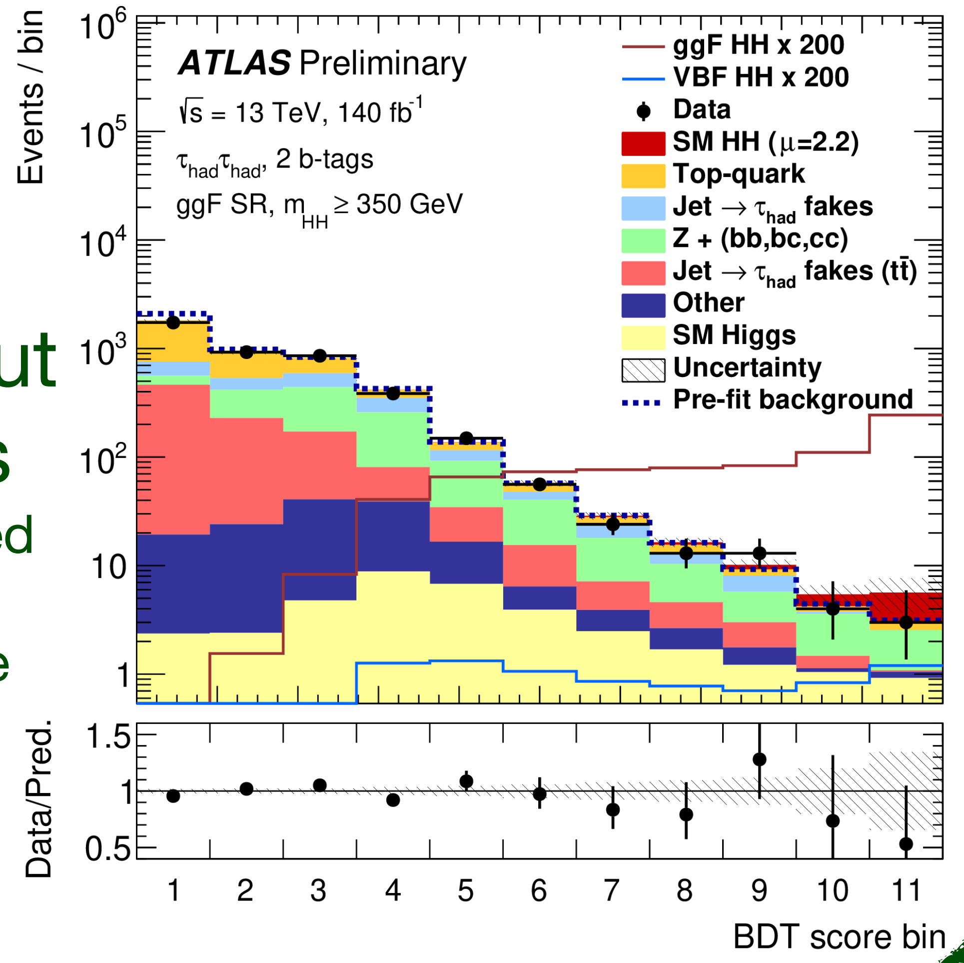

bbbb

Data-driven background estimate

Neural Network reweighting (2b → 4b)

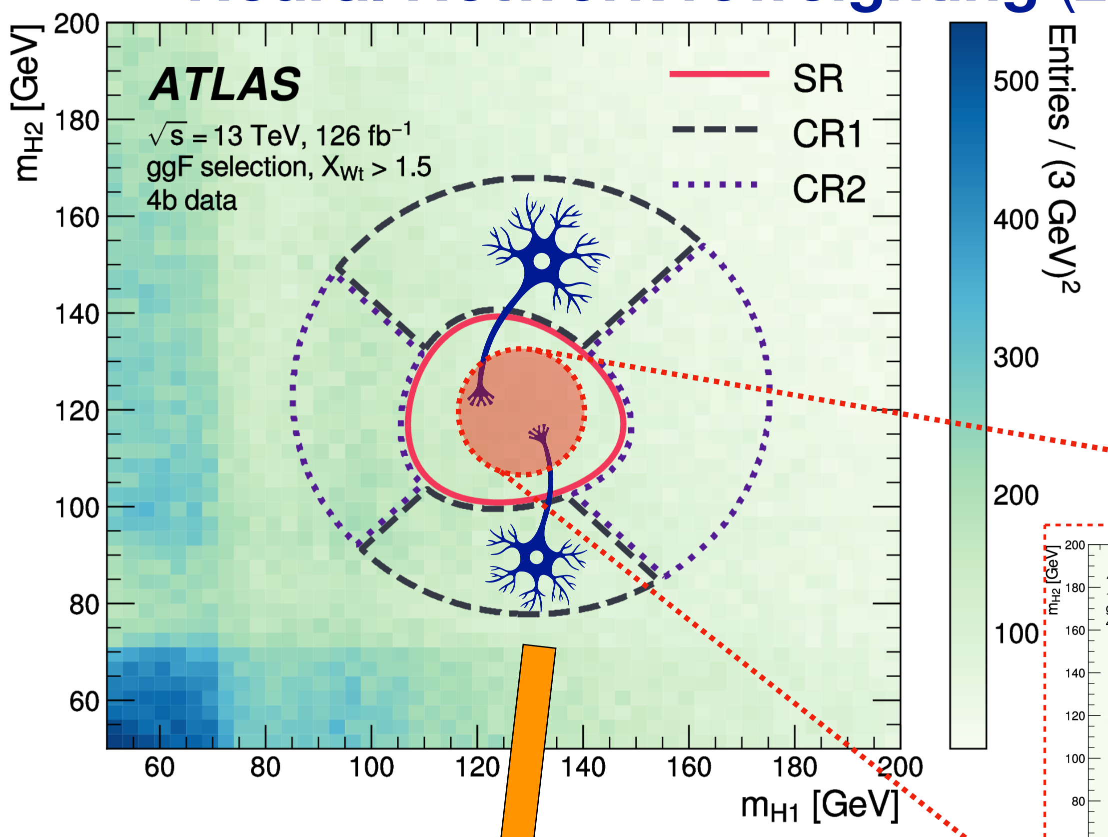

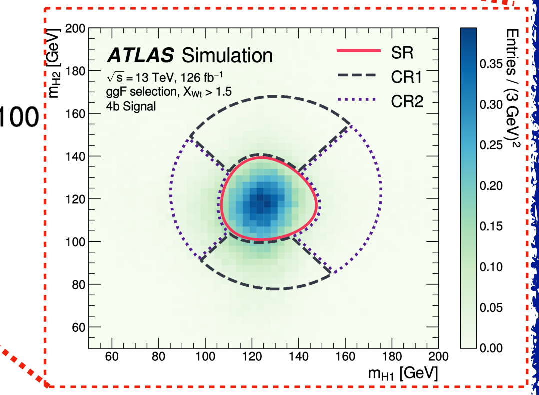

Signal centred in m_{H1}-m_{H2} plane

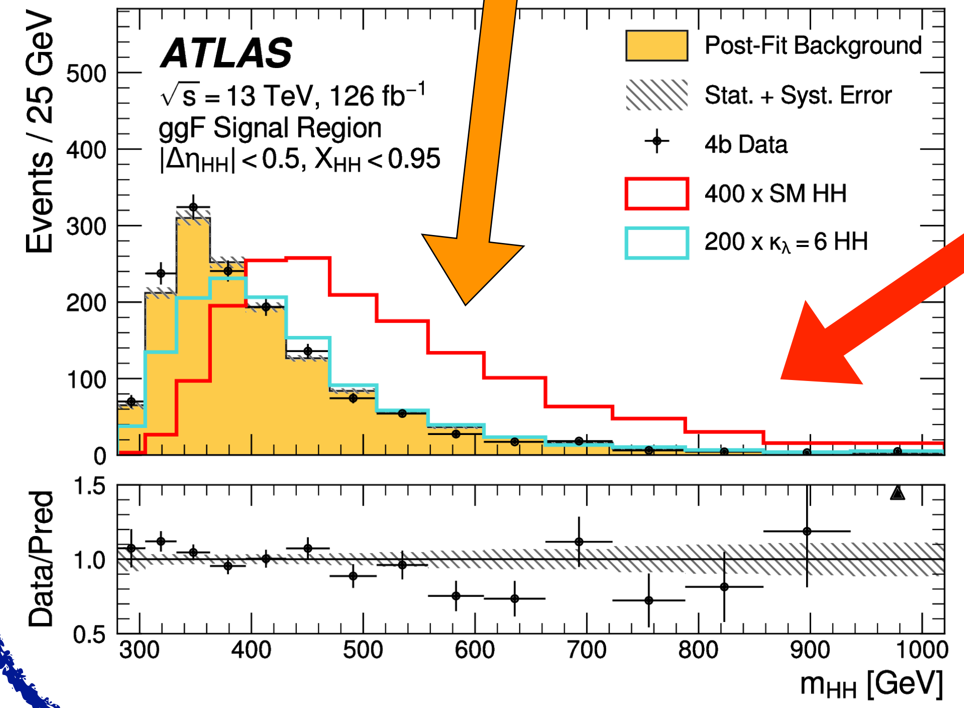

Fit signal in m_{HH} distribution

arXiv:2310.12301 | ATLAS-CONF-2023-071/ | Phys. Rev. D 108 (2023) 052003

Full Run 2 (126-140 fb^{-1})

Analysis strategies

bb$\gamma\gamma$

BDT — distinguish HH(bb$\gamma\gamma$) from continuum $\gamma\gamma$ (+tt/jets)

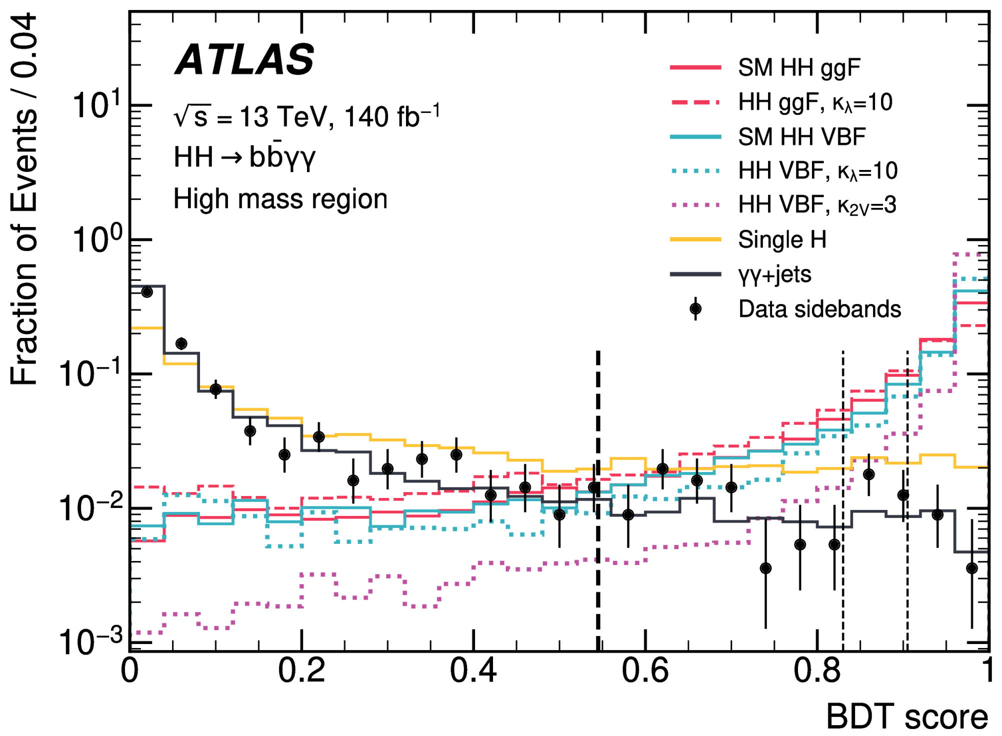

High/low m_{HH} categories

Fit $m_{\gamma\gamma}$ sidebands in BDT score categories

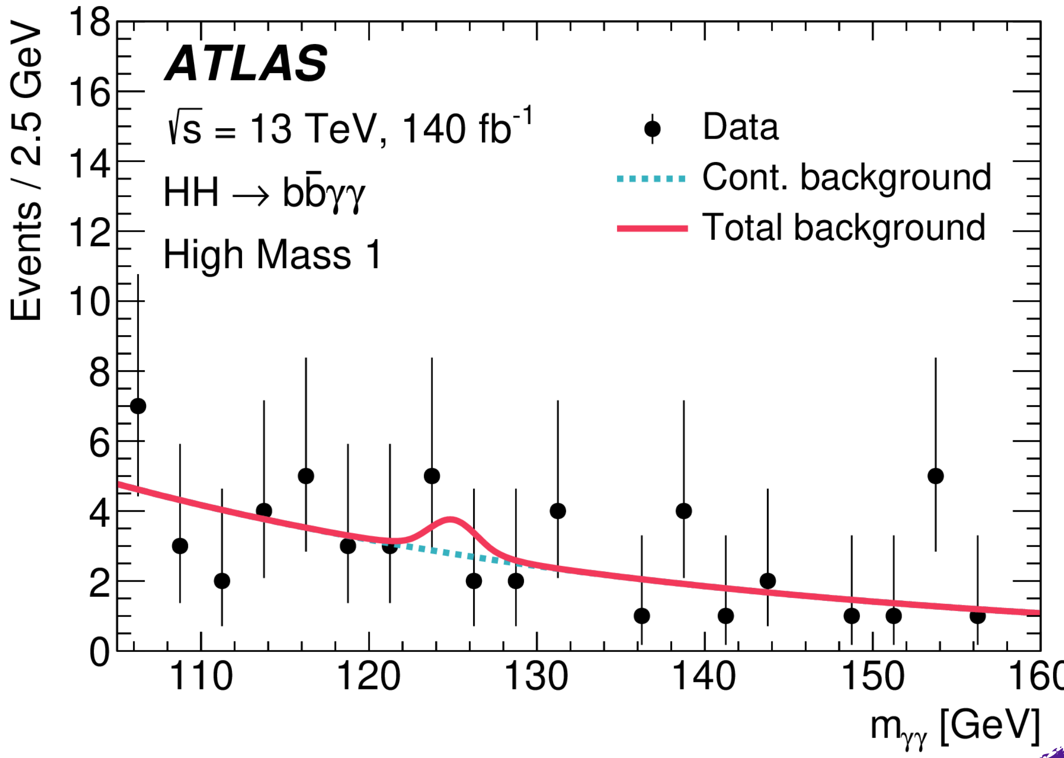

[arXiv:2310.12301]

bb$\tau\tau$

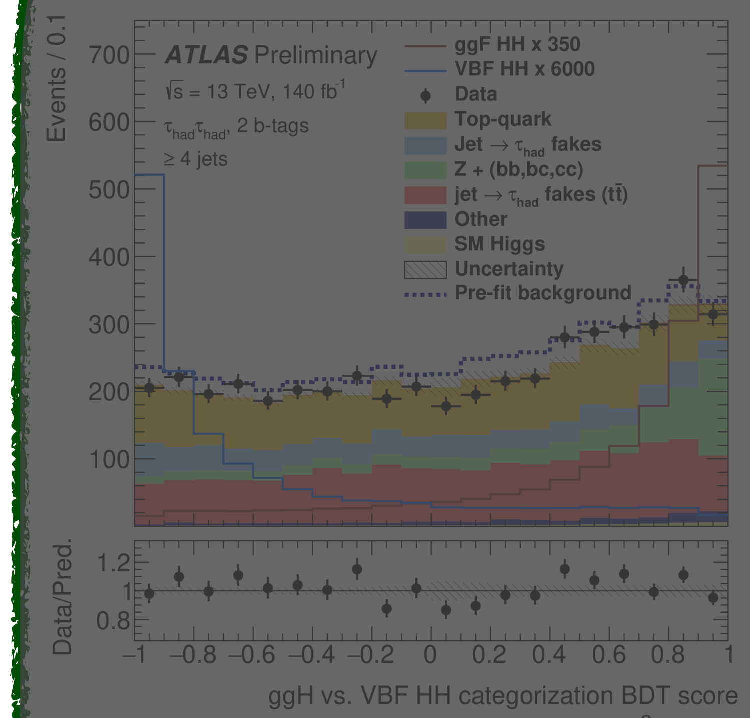

$m_{\tau\tau}$ (MMC) + m_{bb} ⇒ m_{HH}

+ other kine. variables

BDT

Signal extraction & categorization

Fit MVA output distributions

Illustrated in merged bins of increasing signal significance

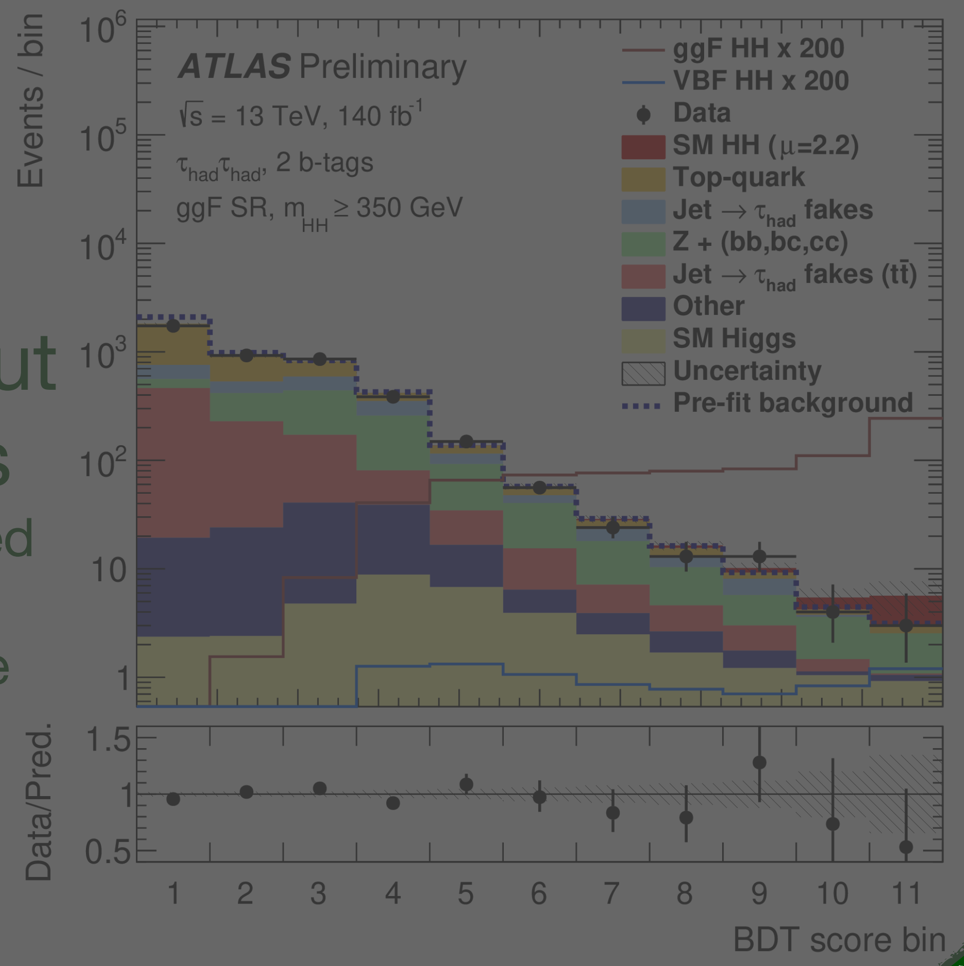

[ATLAS-CONF-2023-071/]

bbbb

Data-driven background estimate

Neural Network reweighting (2b → 4b)

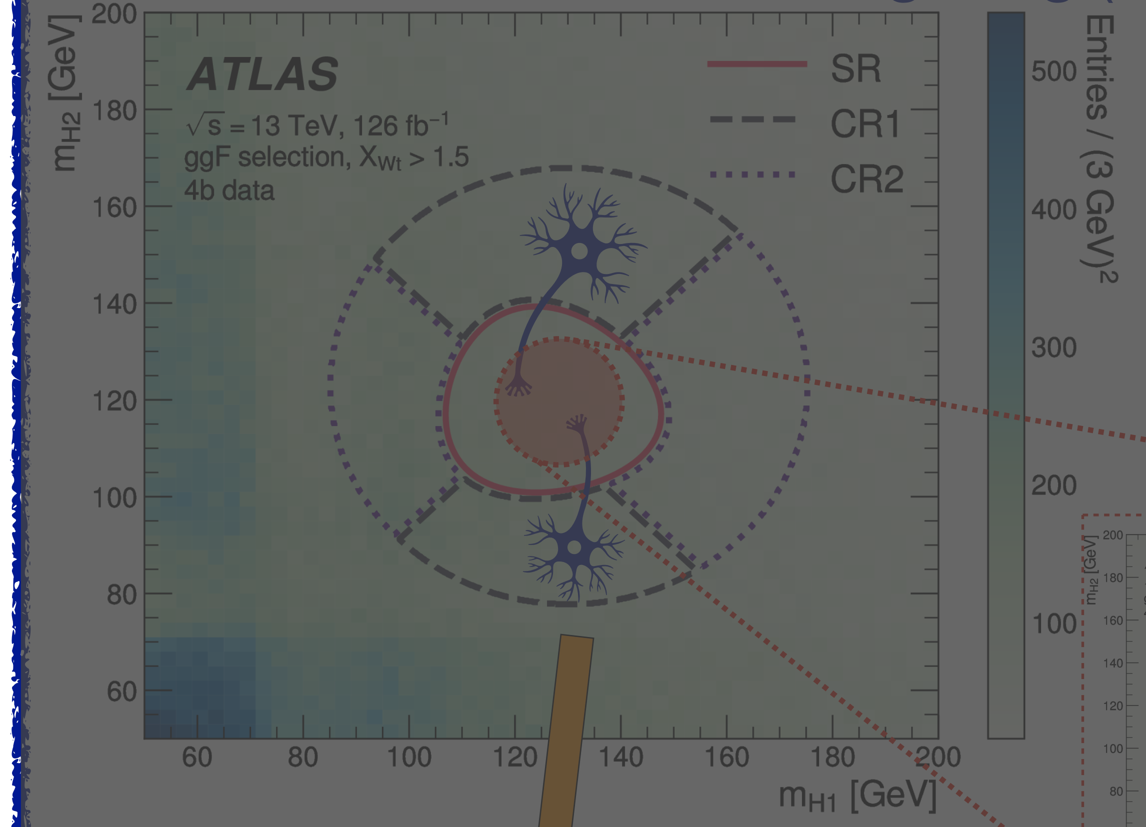

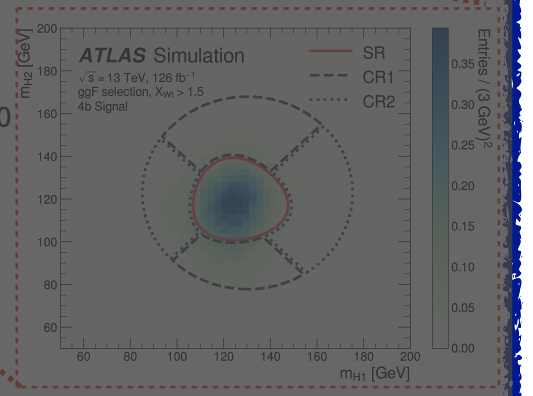

Signal centred in m_{H1}-m_{H2} plane

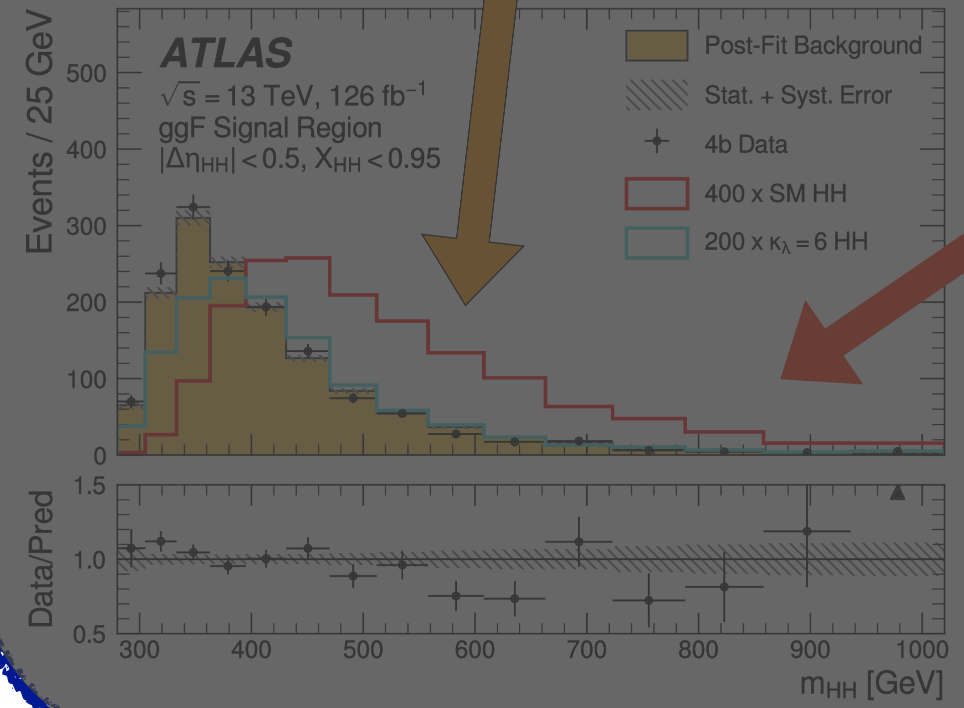

Fit signal in m_{HH} distribution

[Phys. Rev. D 108 (2023) 052003]

Full Run 2 (126-140 fb^{-1})

Analysis strategies

$bb\gamma\gamma$

BDT — distinguish HH($bb\gamma\gamma$) from continuum $\gamma\gamma$ (+tt/jets)

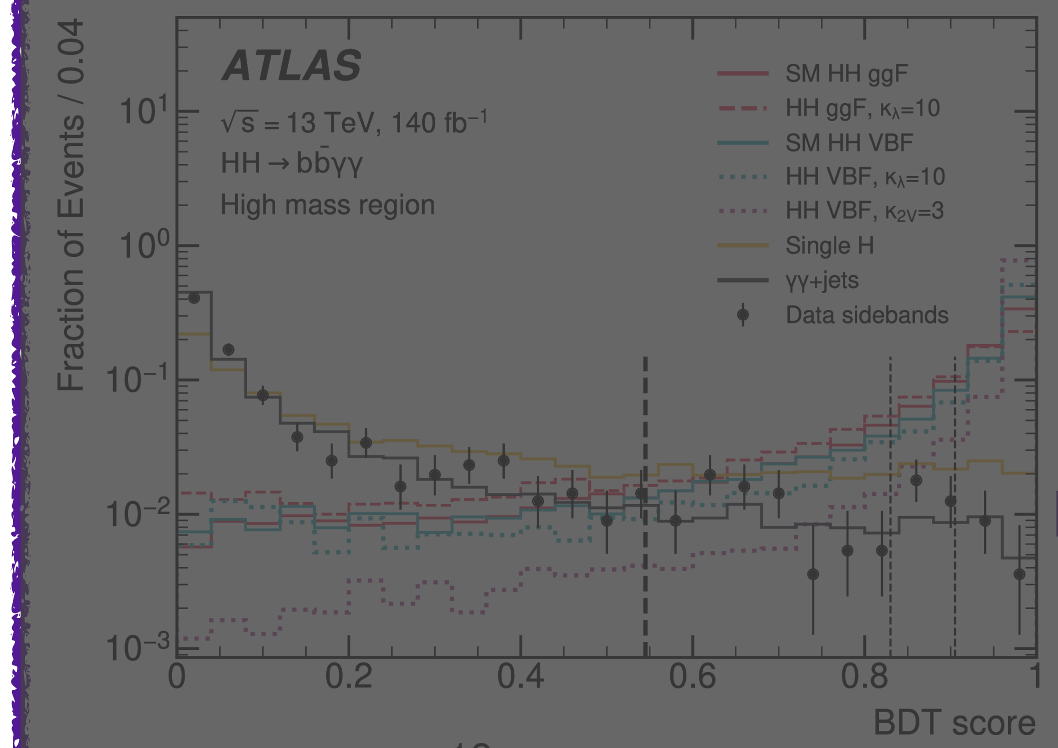

High/low m_{HH} categories

Fit $m_{\gamma\gamma}$ sidebands in BDT score categories

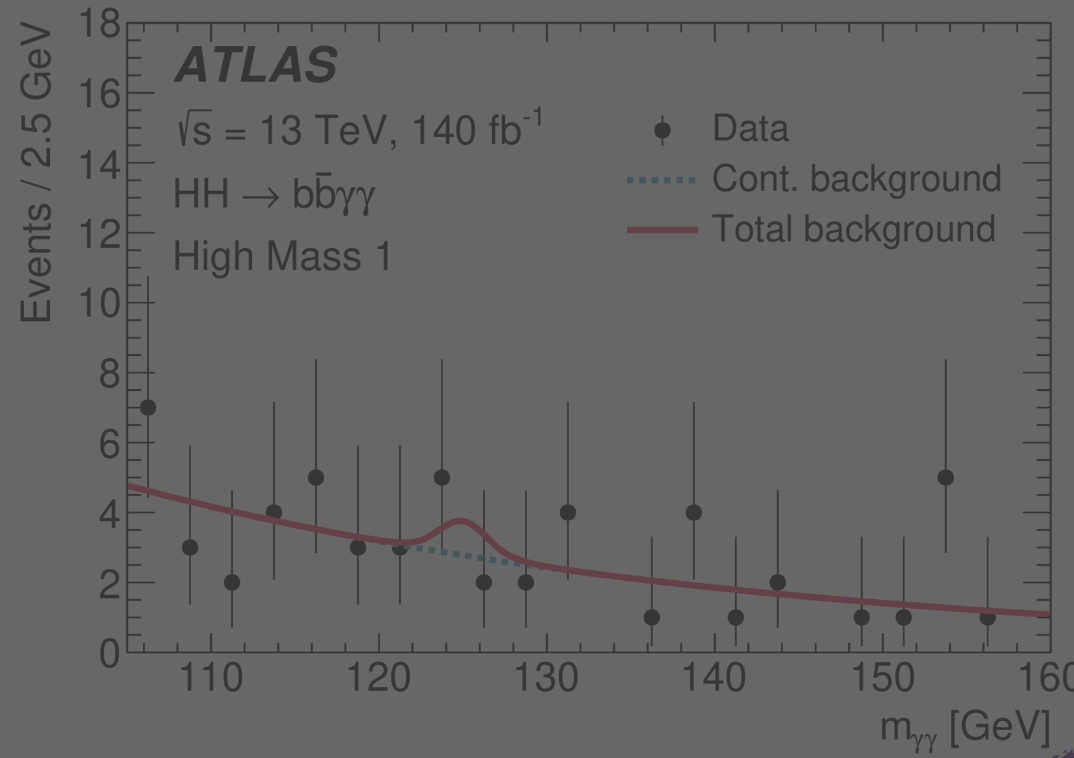

arXiv:2310.12301

$bb\tau\tau$

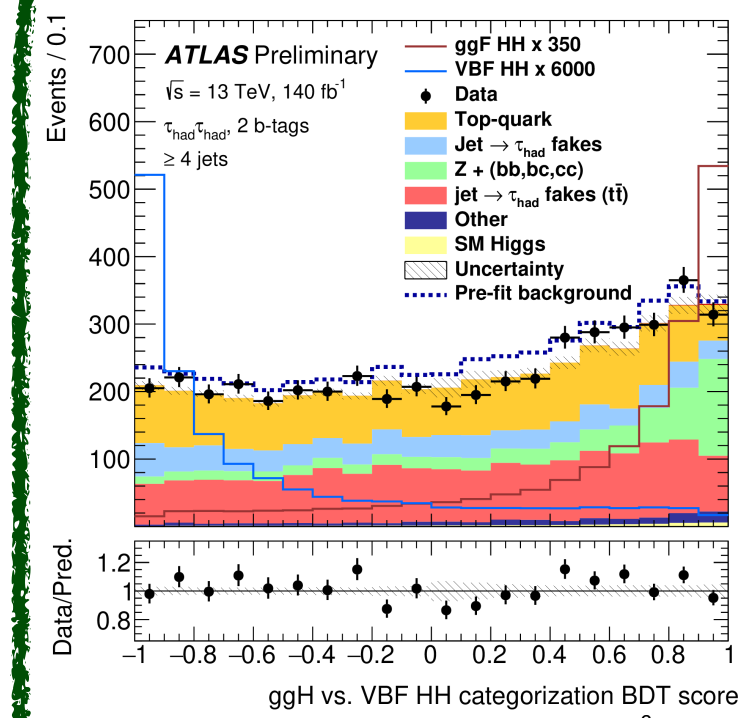

$m_{\tau\tau}$ (MMC) + $m_{bb} \Rightarrow m_{HH}$

+ other kine. variables

BDT

Signal extraction & categorisation

Fit MVA output distributions

Illustrated in merged bins of increasing signal significance

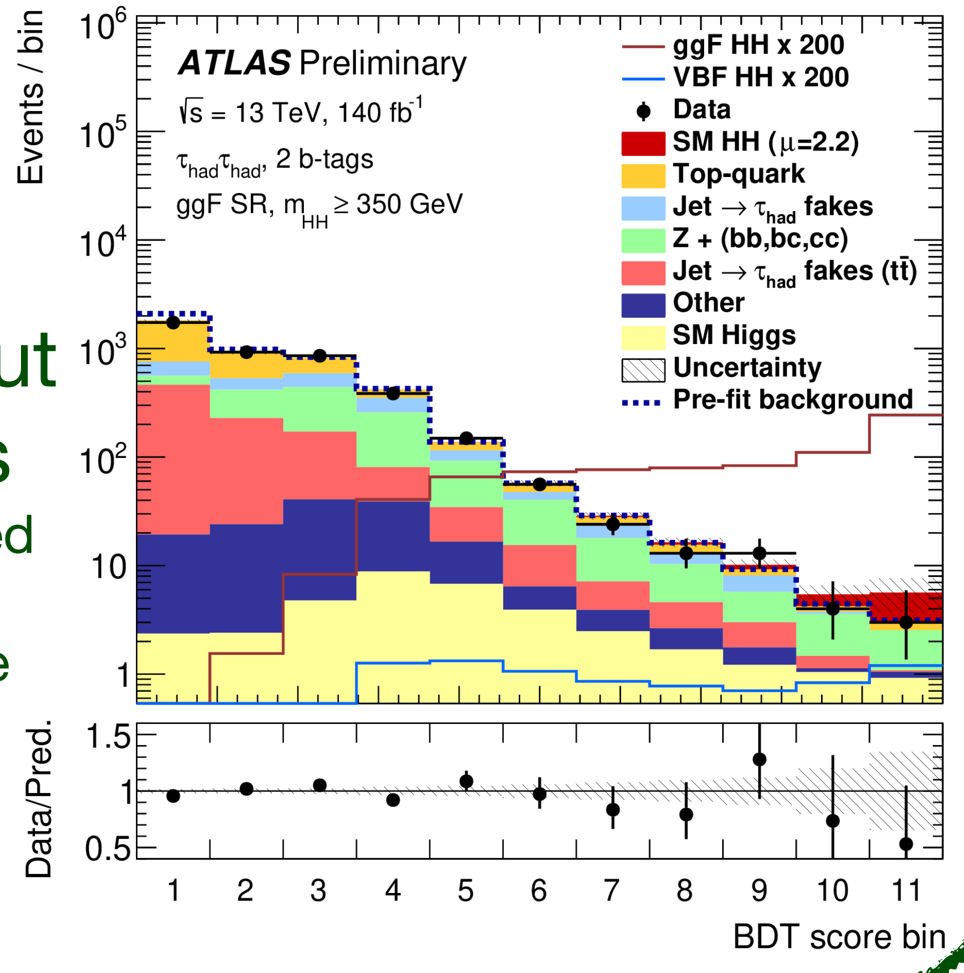

ATLAS-CONF-2023-071/

bbbb

Data-driven background estimate

Neural Network reweighting (2b → 4b)

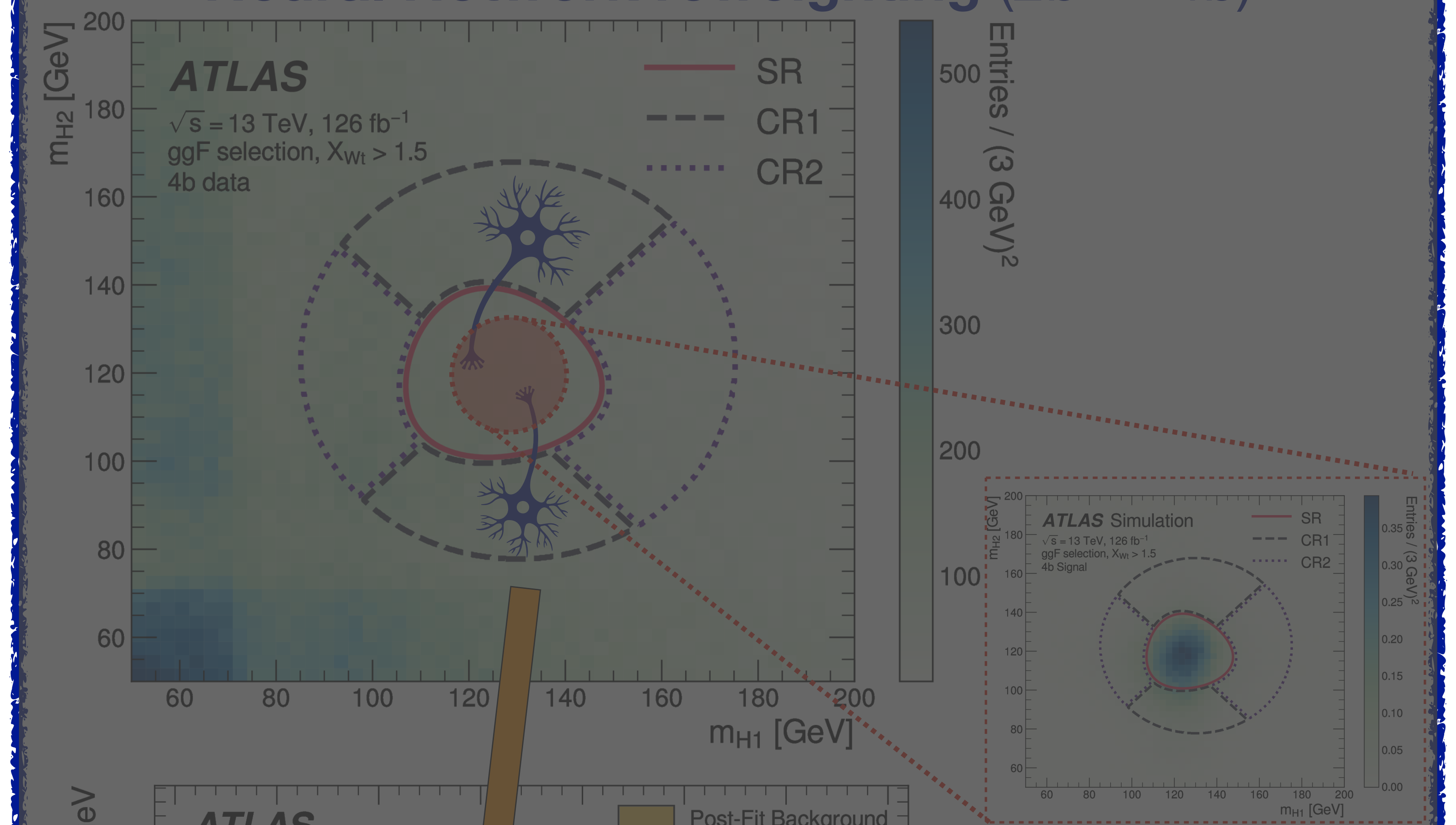

Signal centred in m_{H1}-m_{H2} plane

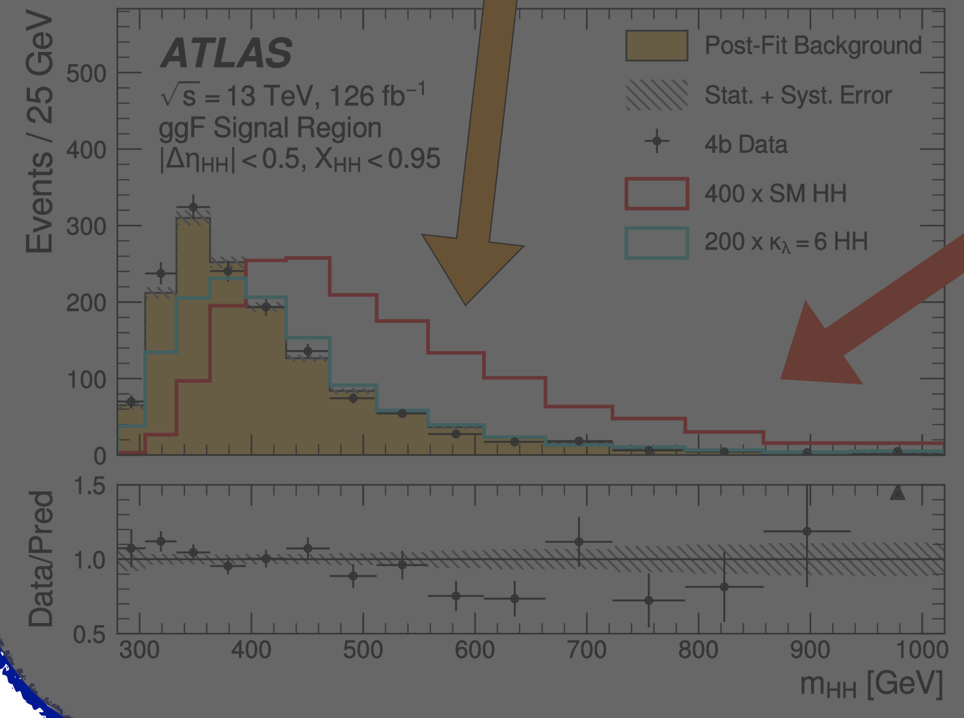

Fit signal in m_{HH} distribution

Phys. Rev. D 108 (2023) 052003

Full Run 2 (126-140 fb^{-1})

Analysis strategies

$bb\gamma\gamma$

BDT — distinguish HH($bb\gamma\gamma$) from continuum $\gamma\gamma$ (+tt/jets)

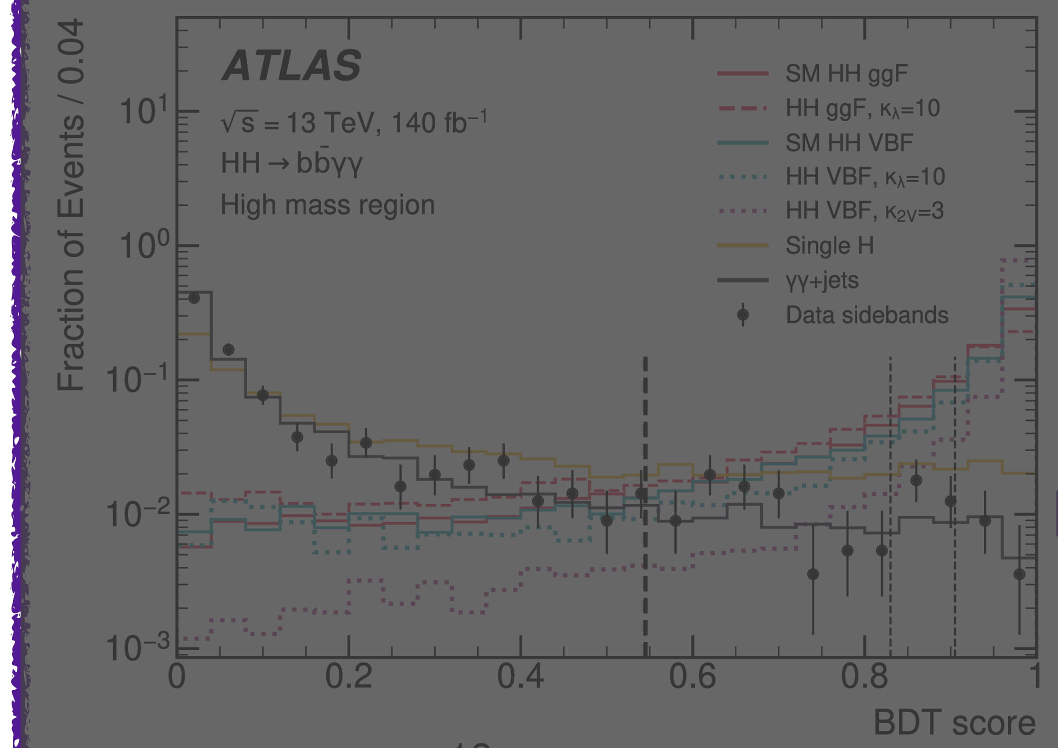

High/low m_{HH} categories

Fit $m_{\gamma\gamma}$ sidebands in BDT score categories

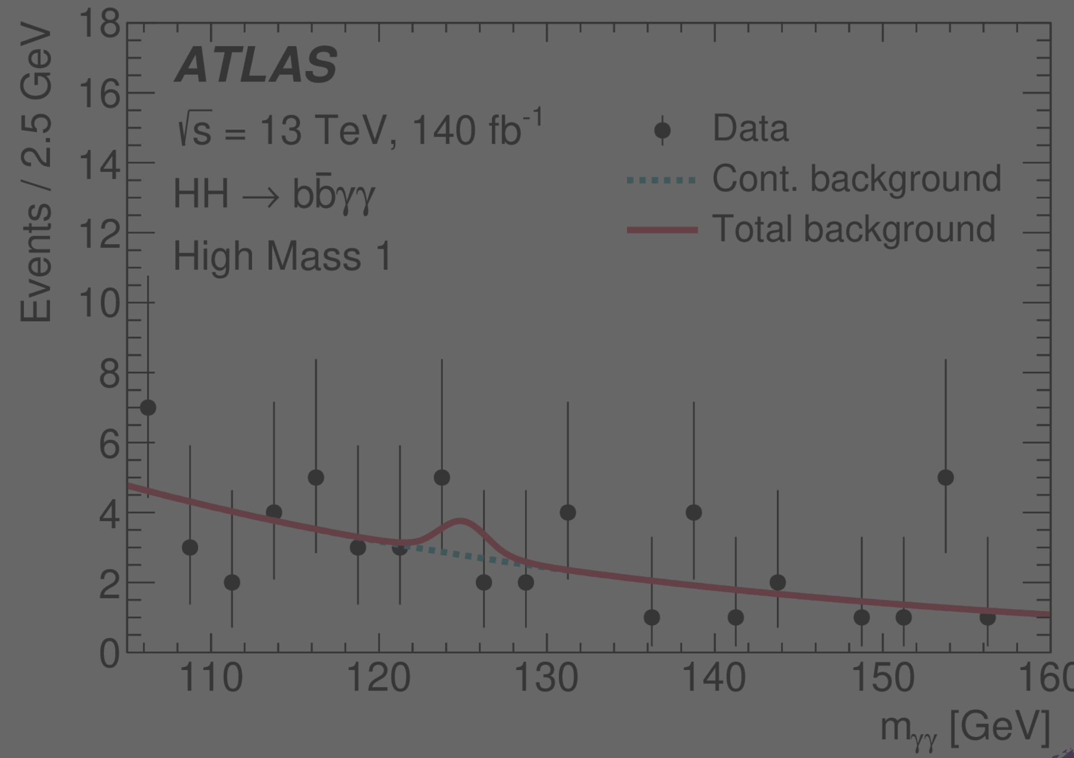

$bb\tau\tau$

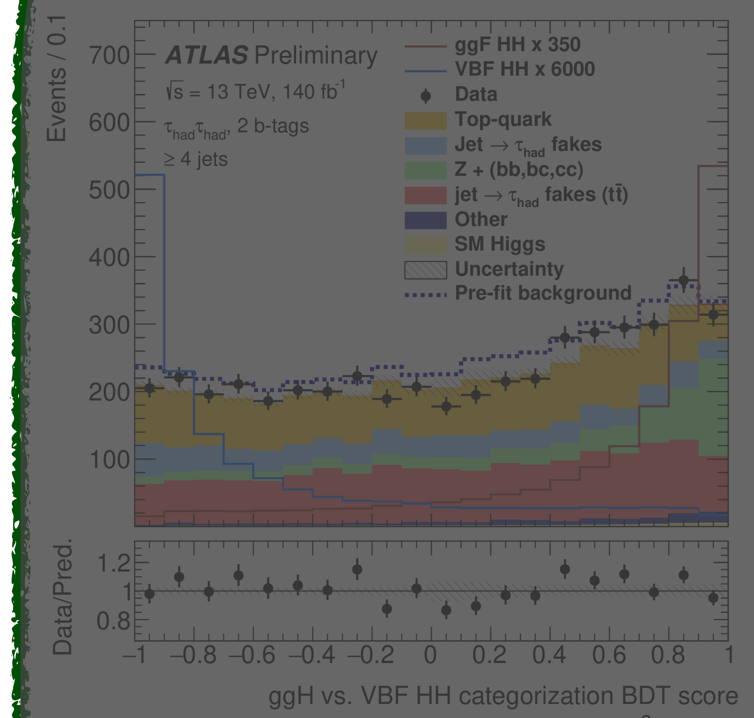

$m_{\tau\tau}$ (MMC) + m_{bb} ⇒ m_{HH}

+ other kine. variables

BDT

Signal extraction & categorisation

Fit MVA output distributions

Illustrated in merged bins of increasing signal significance

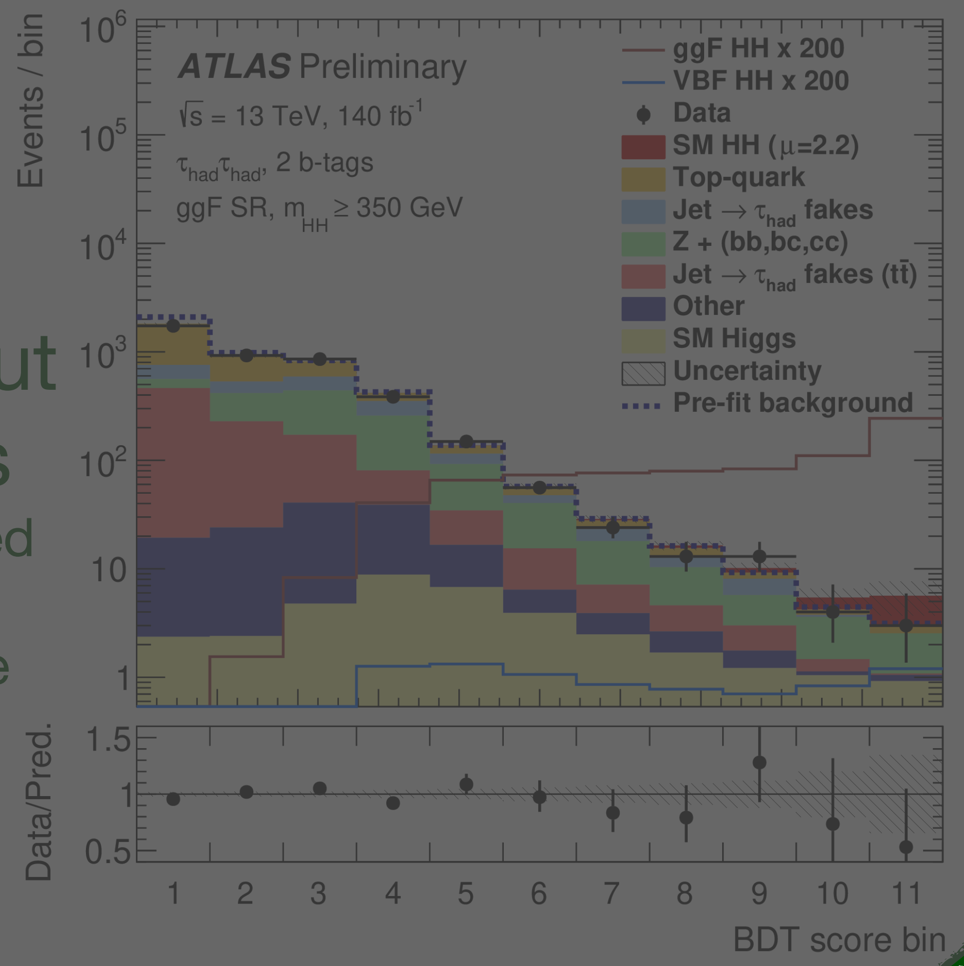

bbbb

Data-driven background estimate

Neural Network reweighting (2b → 4b)

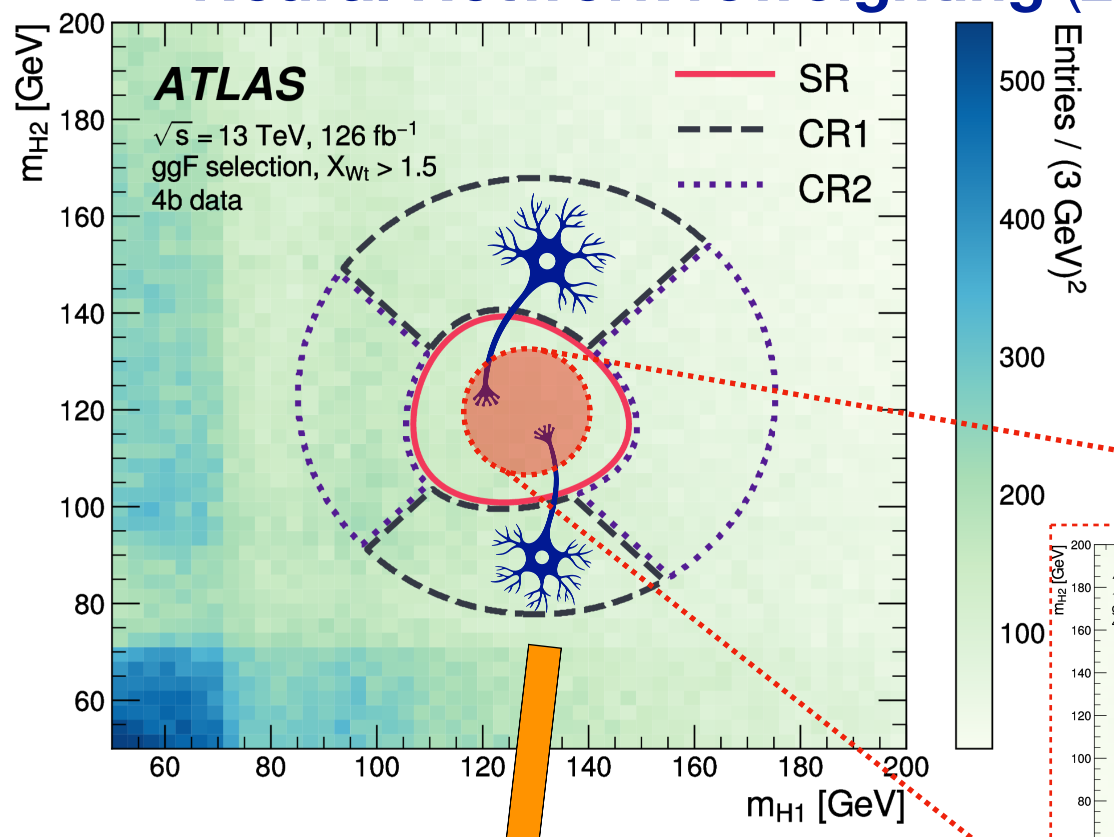

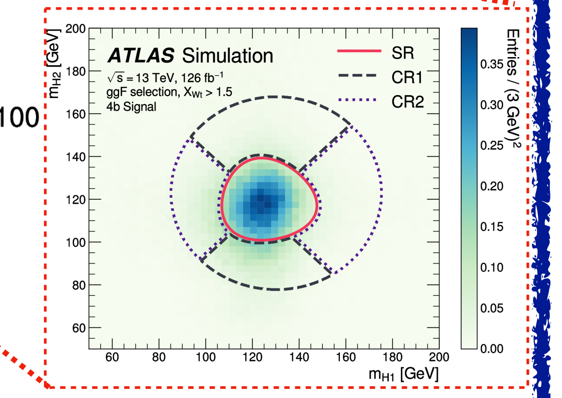

Signal centred in m_{H1}-m_{H2} plane

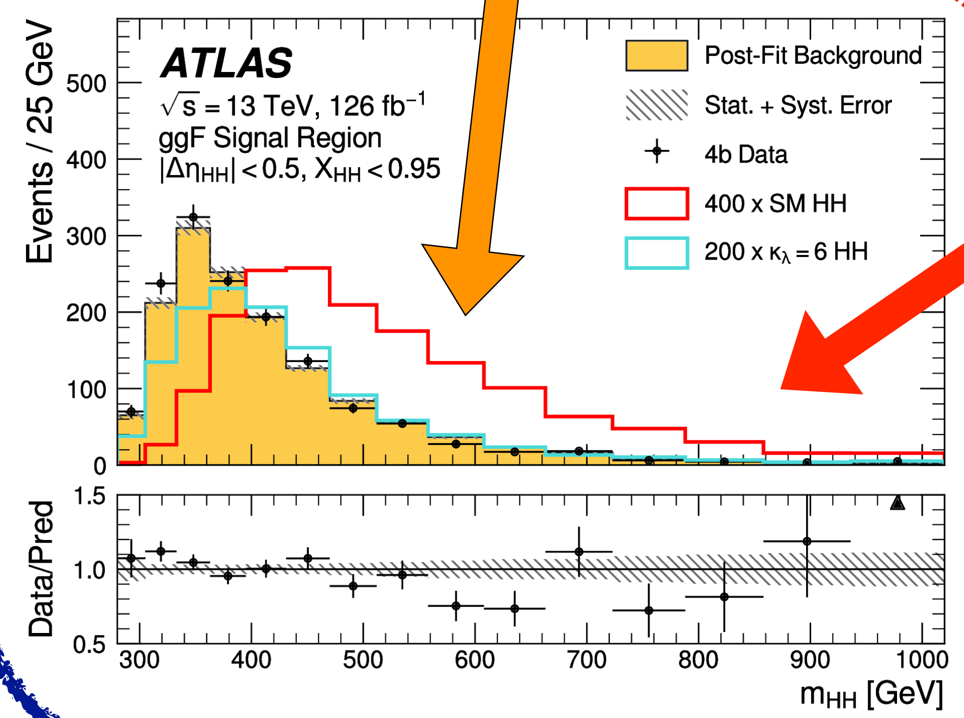

Fit signal in m_{HH} distribution

arXiv:2310.12301 | ATLAS-CONF-2023-071/ | Phys. Rev. D 108 (2023) 052003

Full Run 2 (140 fb^{-1})

NEW: $bb\ell\ell + E_T^{miss}$

Same/different flavour event categories

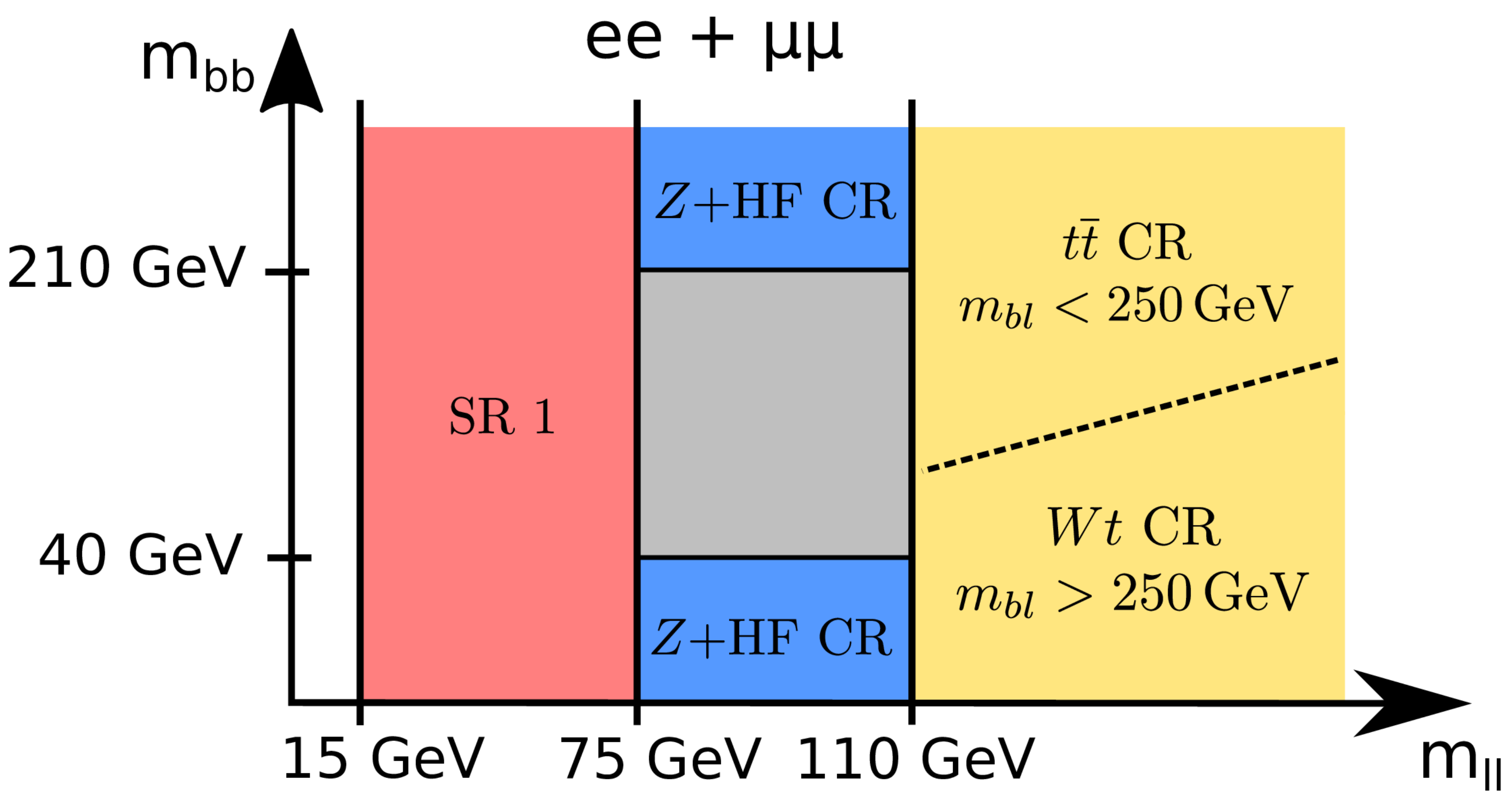

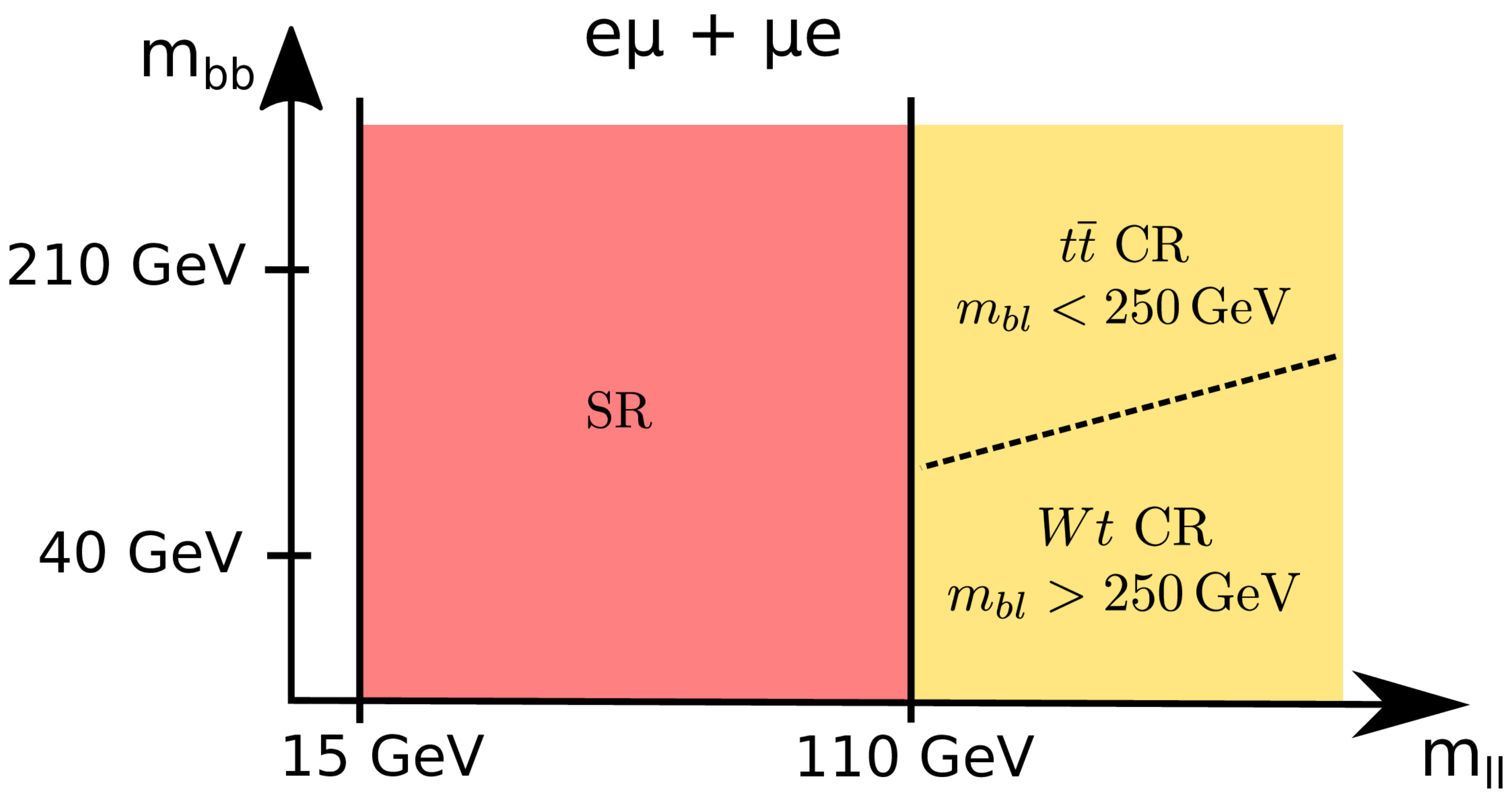

bb, $\ell\ell$ kine. variables (see backups)

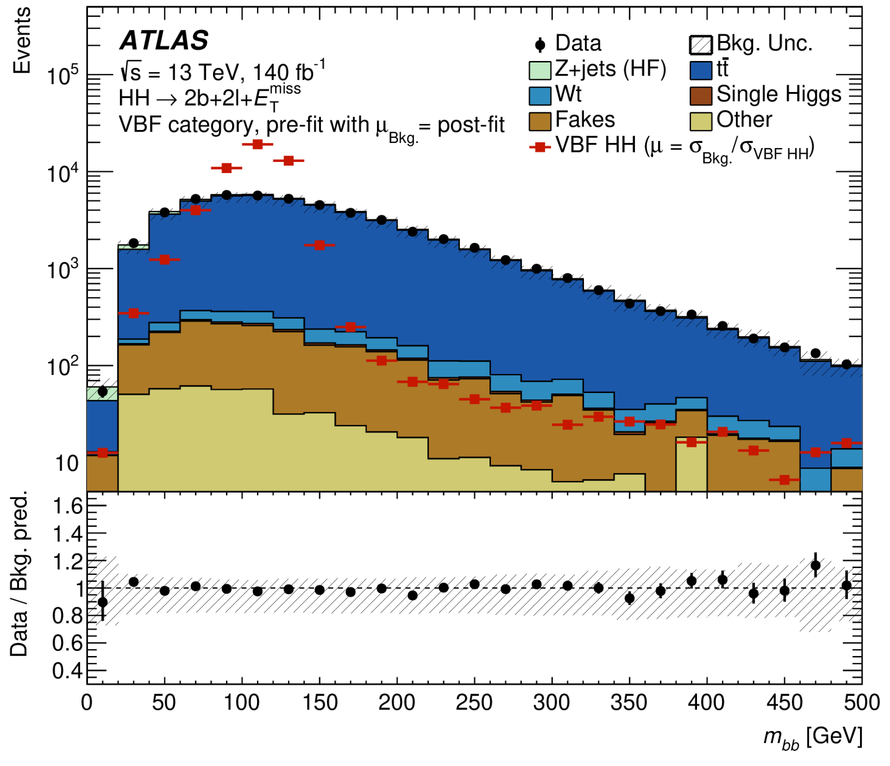

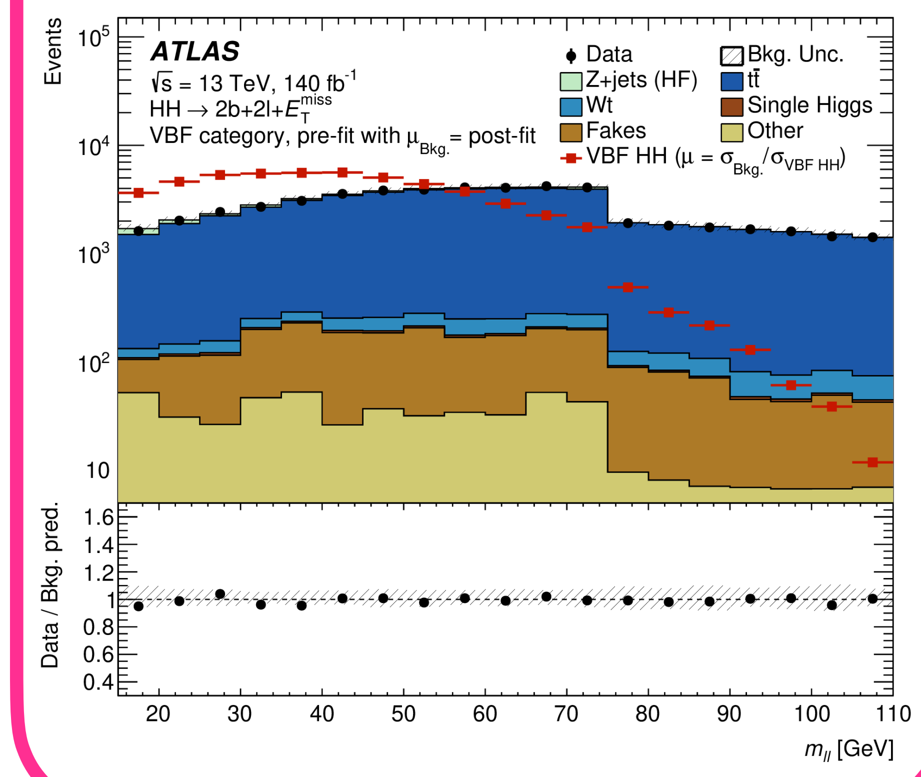

DNN (ggF)

BDT (VBF)

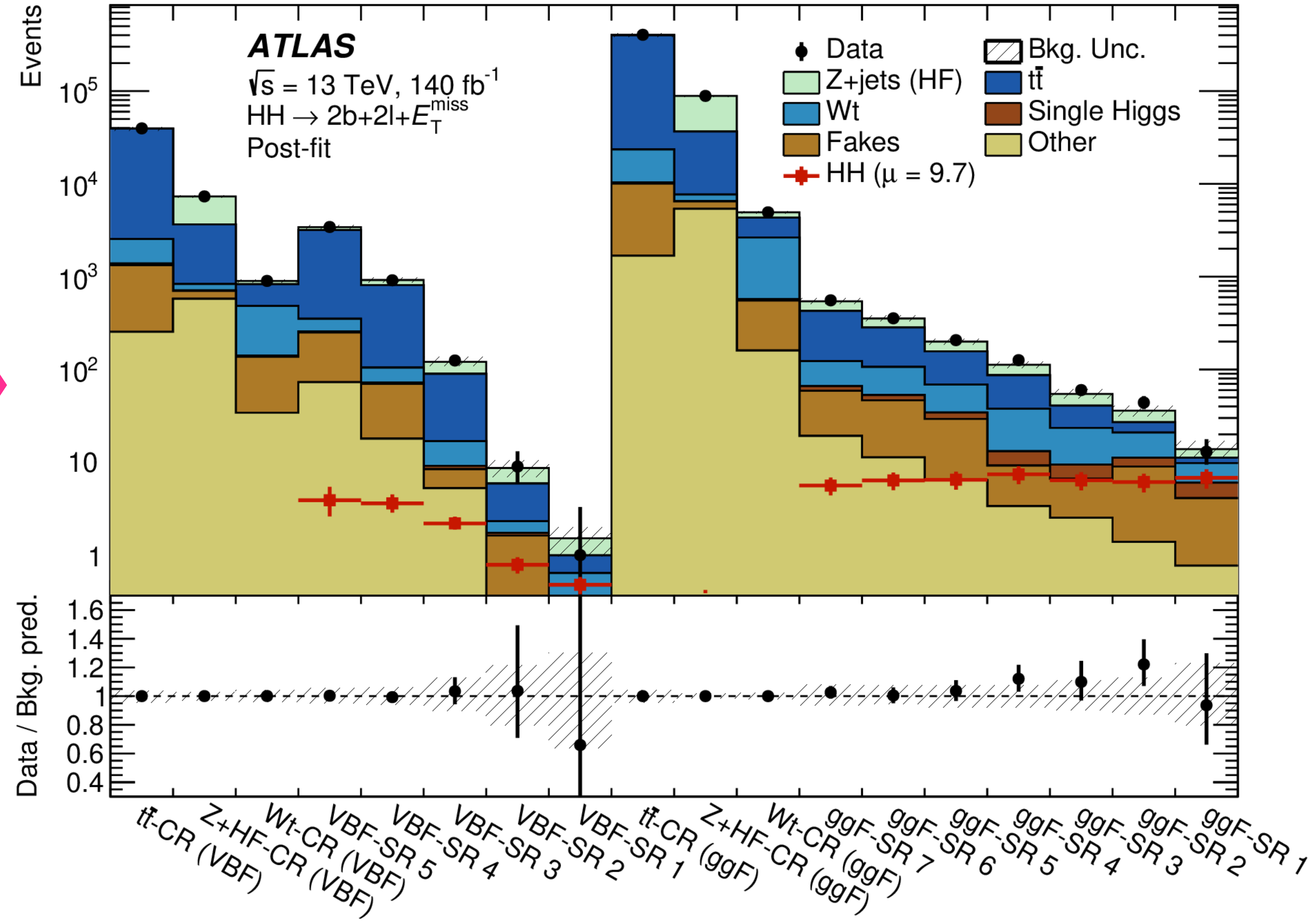

DNN (BDT) bins numbered 1-7(5) by decreasing signal purity

arXiv:2310.11286

Coupling limits

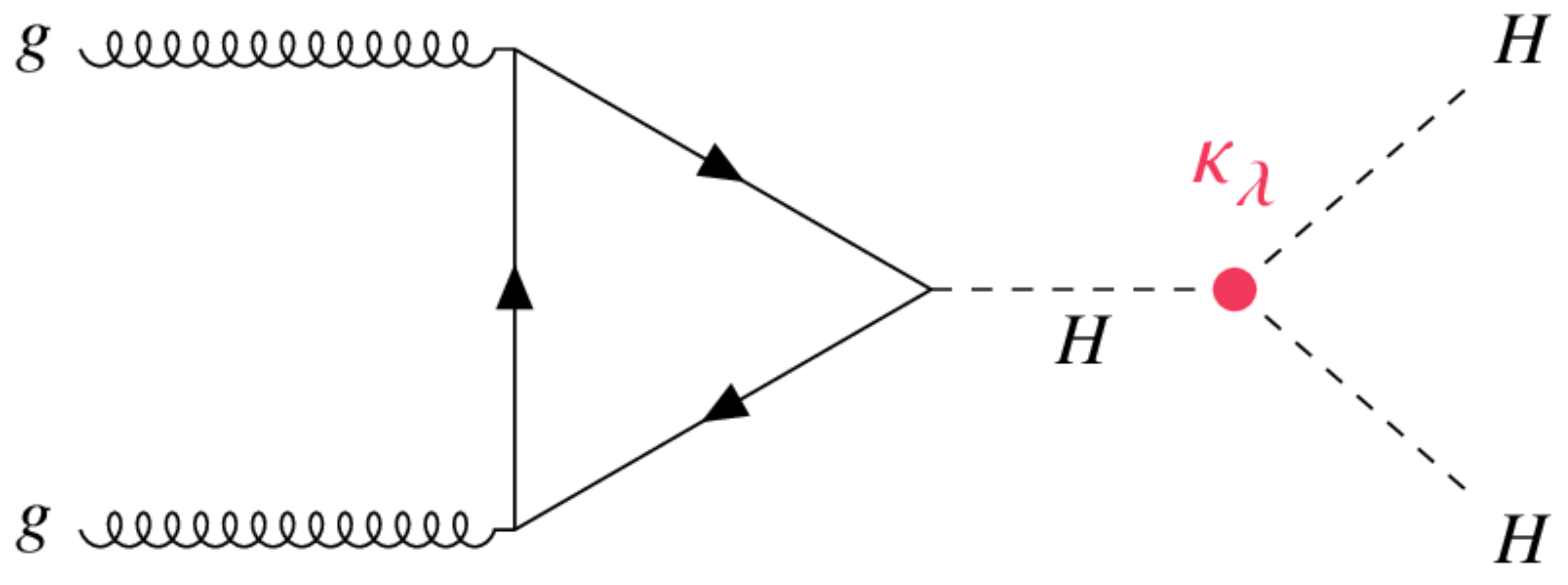

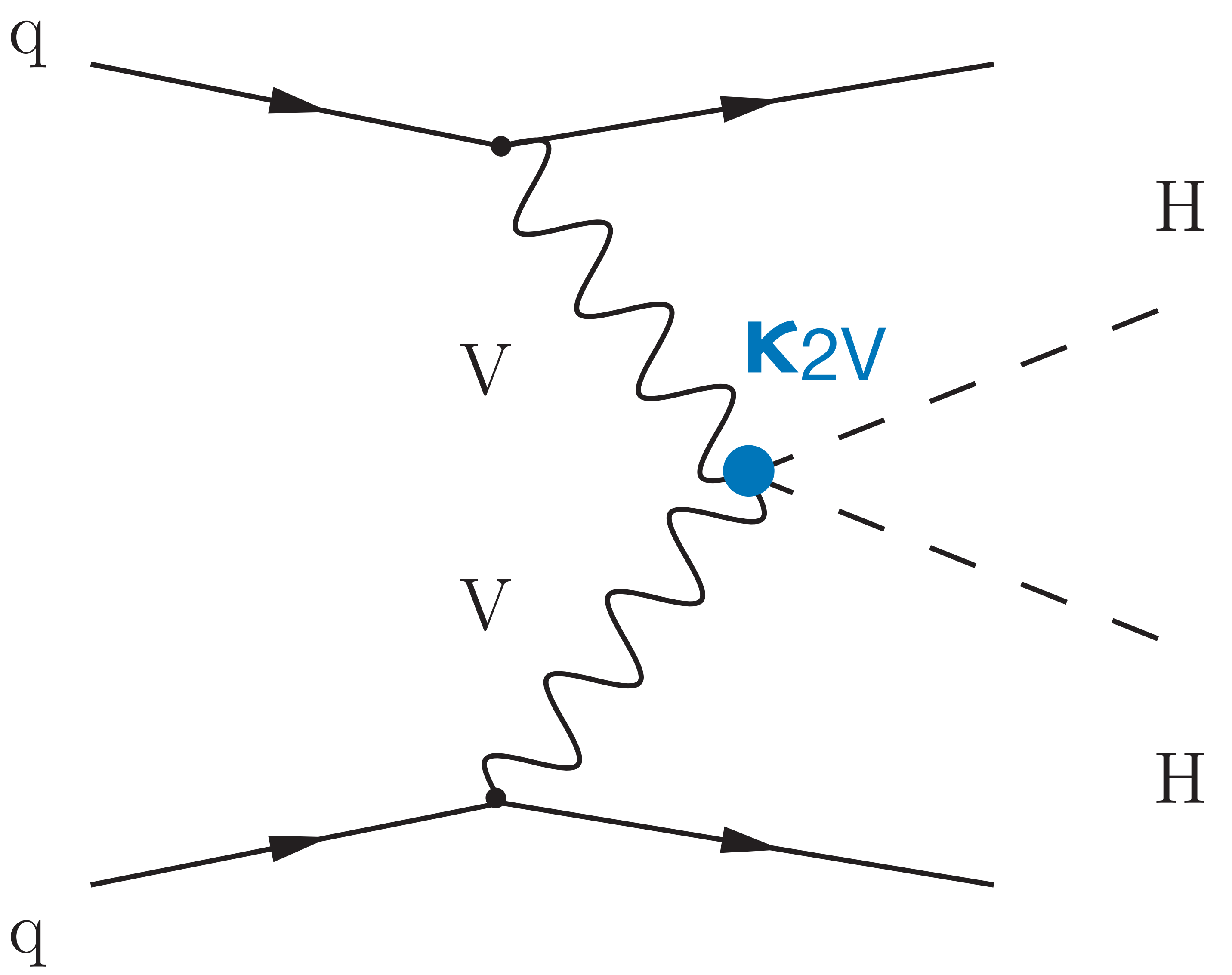

Anomalous enhancement of Higgs trilinear coupling: κ_λ
⇒ unique sensitivity in HH channels

Anomalous enhancement of HH to VV coupling: κ_{2V}
⇒ unique sensitivity in VBF HH

Coupling limits

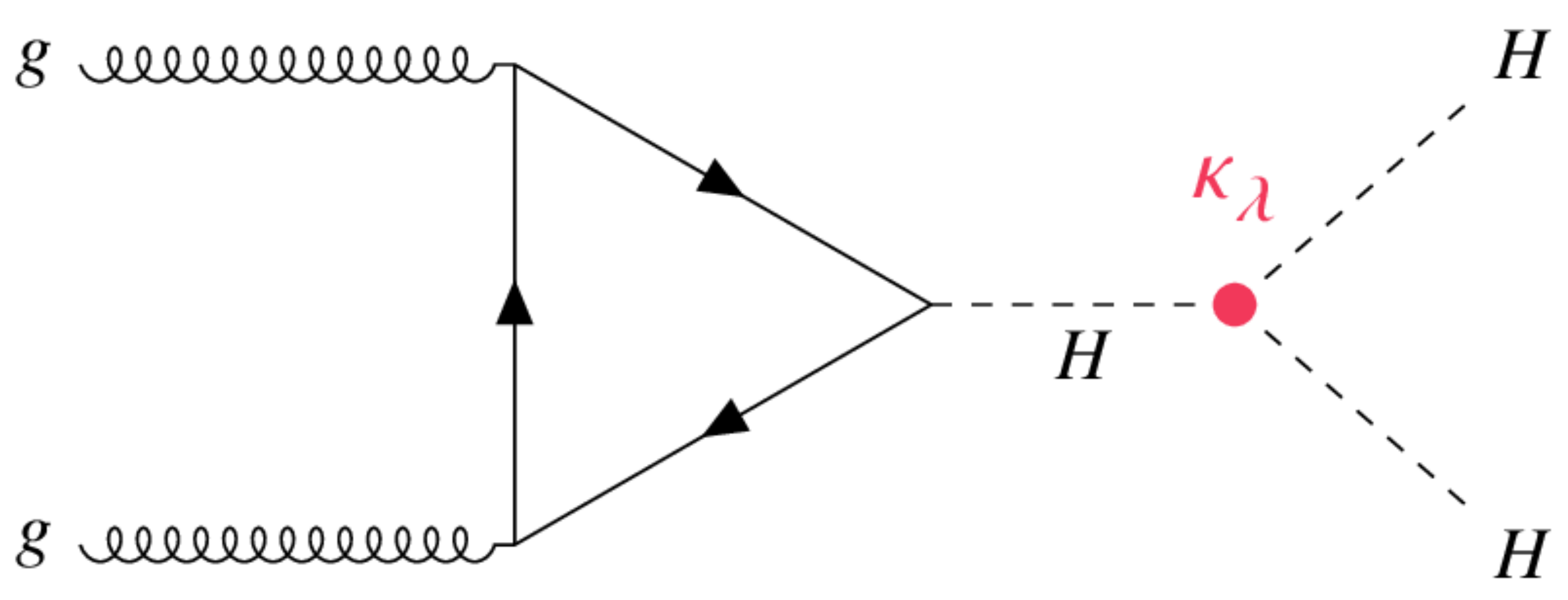

Anomalous enhancement of Higgs trilinear coupling: κ_λ
⇒ unique sensitivity in HH channels

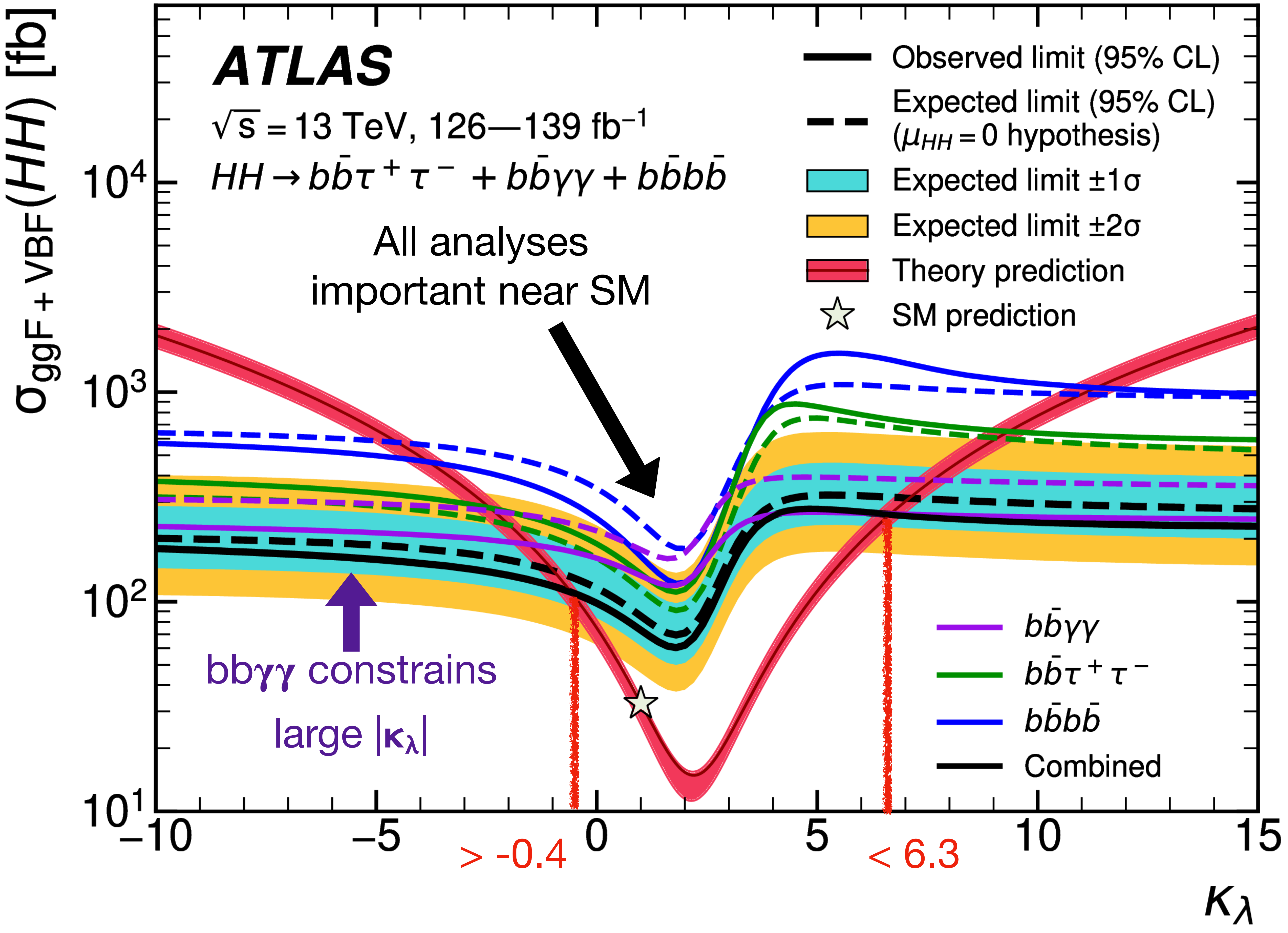

Phys. Lett. B 843 (2023) 137745

Coupling limits

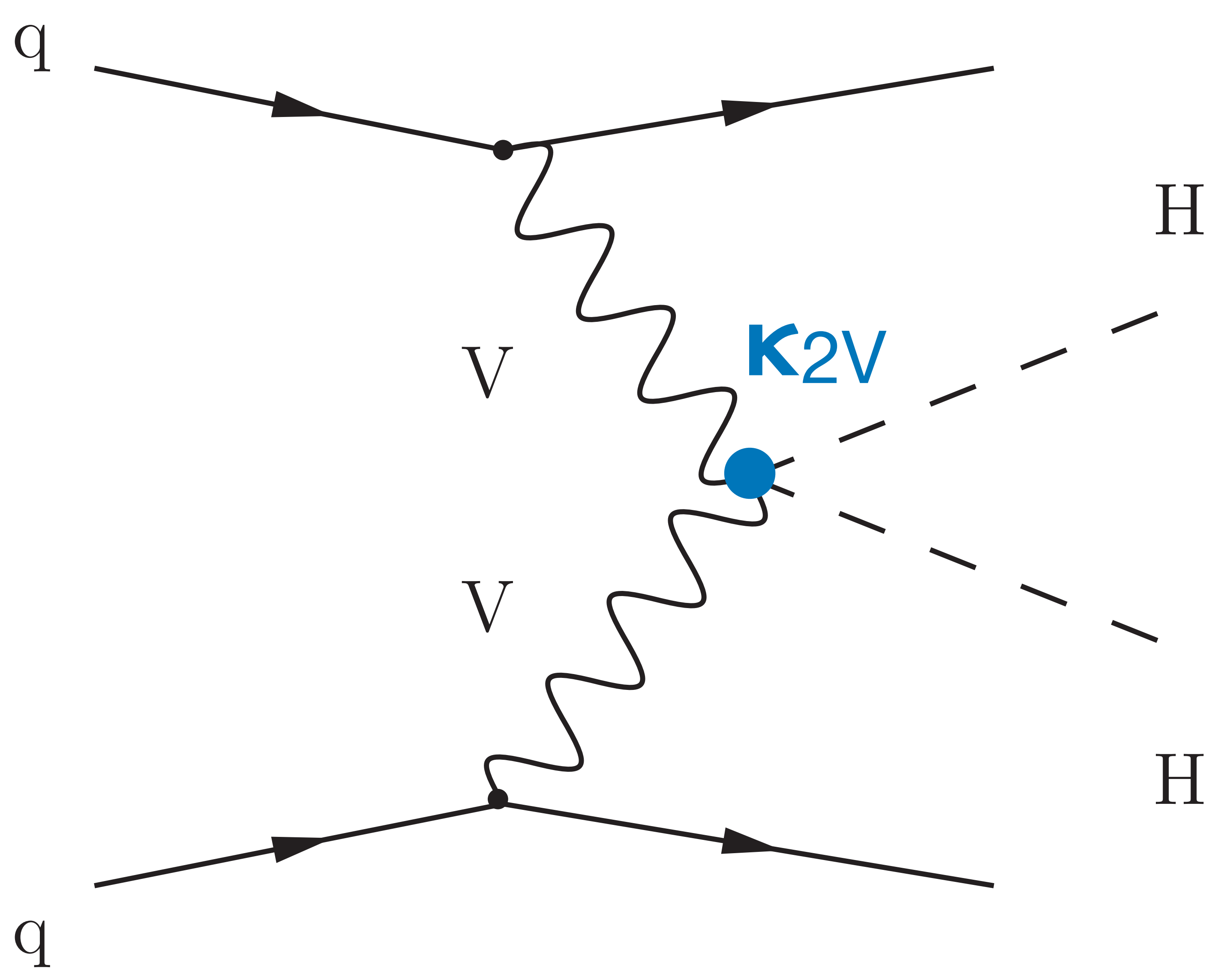

Anomalous enhancement of HH to VV coupling: κ_{2V}

⇒ unique sensitivity in VBF HH

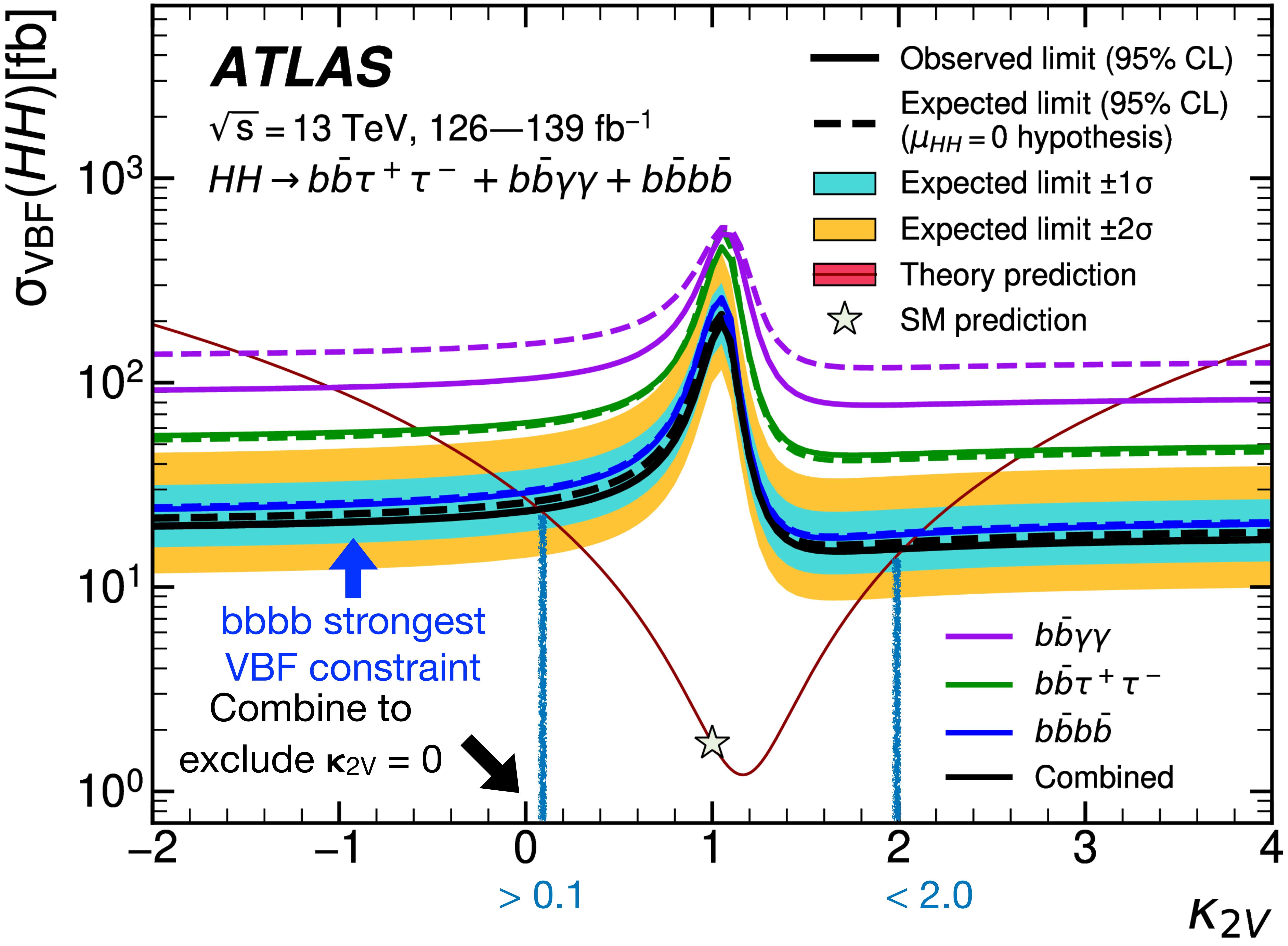

Phys. Lett. B 843 (2023) 137745

Limits from $bb\ell\ell + E_T^{miss}$

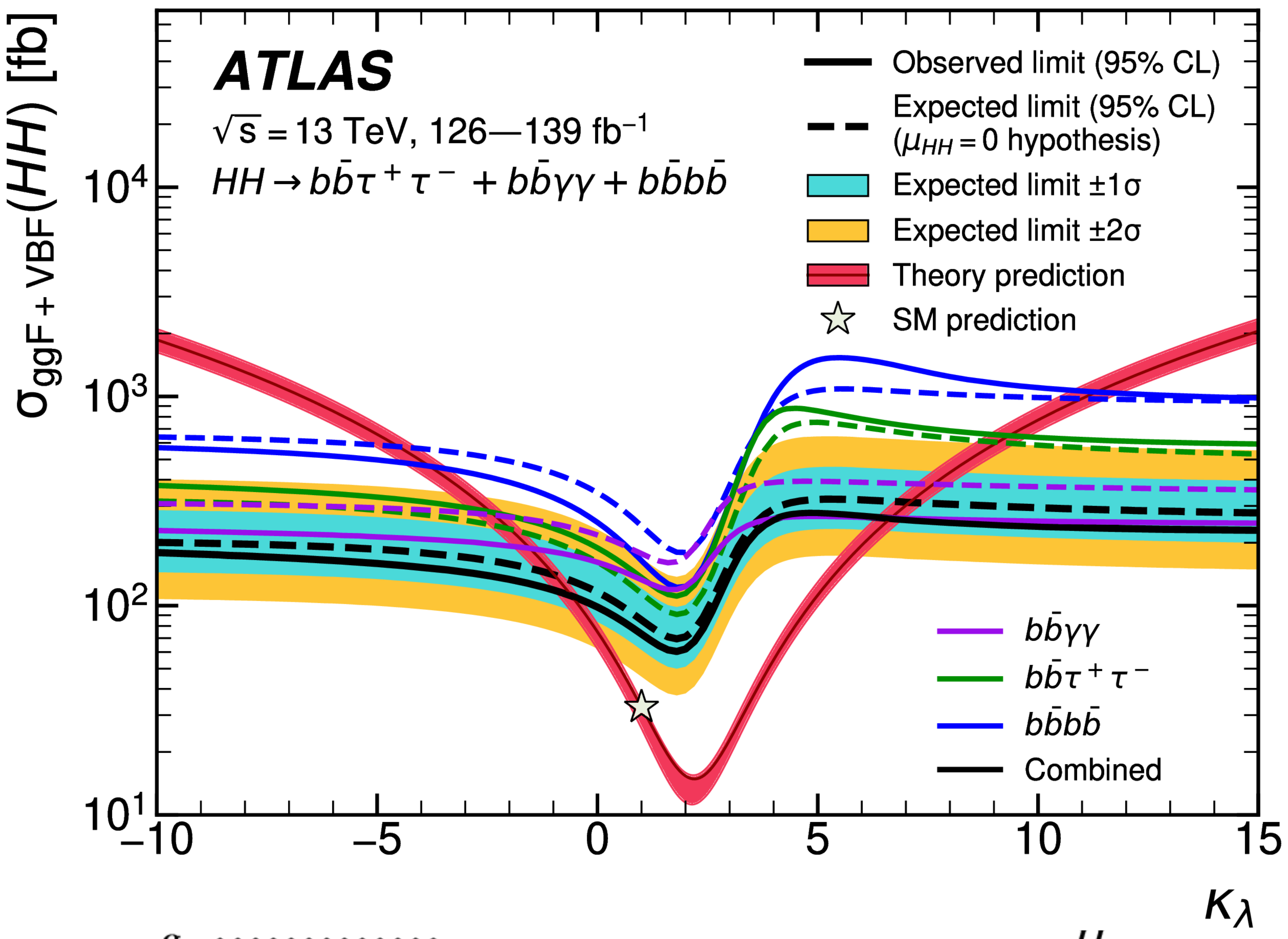

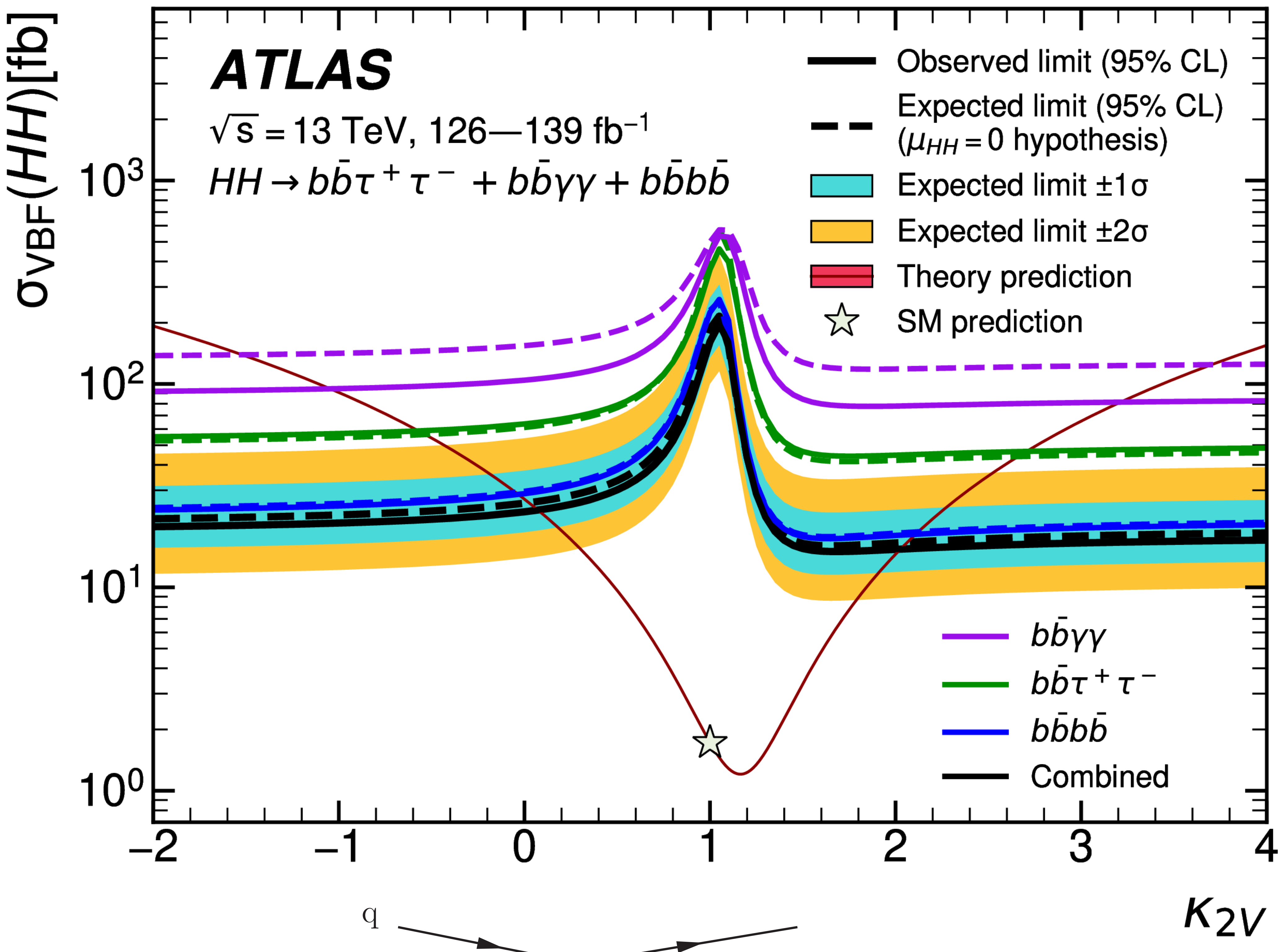

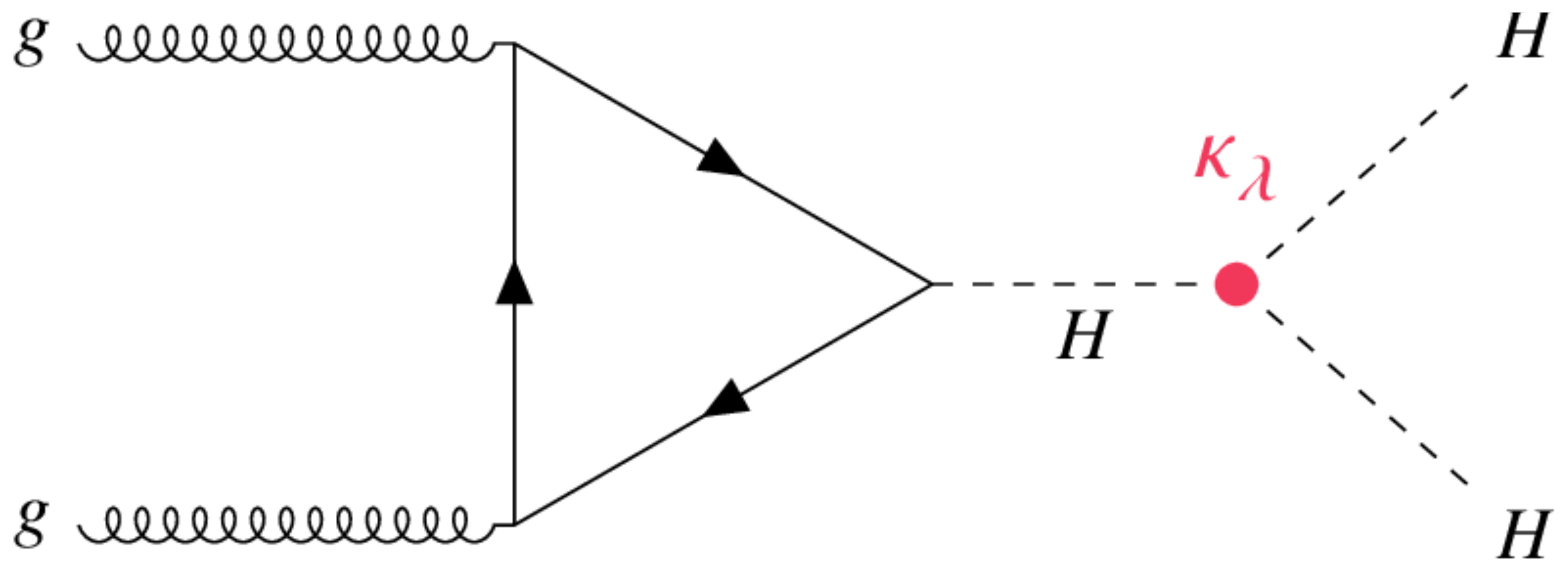

[More limits including EFT in backups]

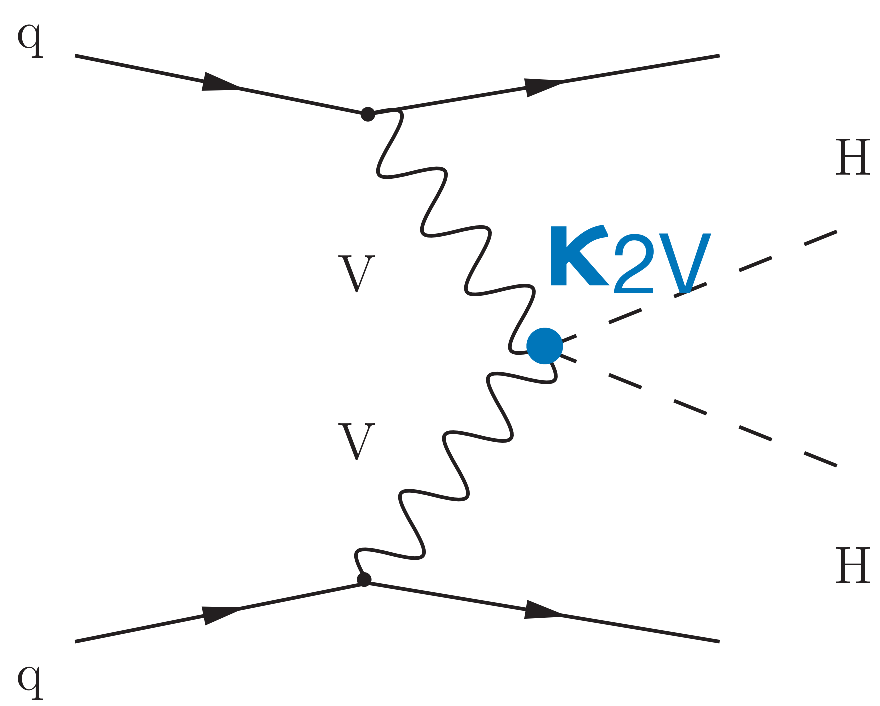

Limits from $bb\ell\ell + E_T^{miss}$

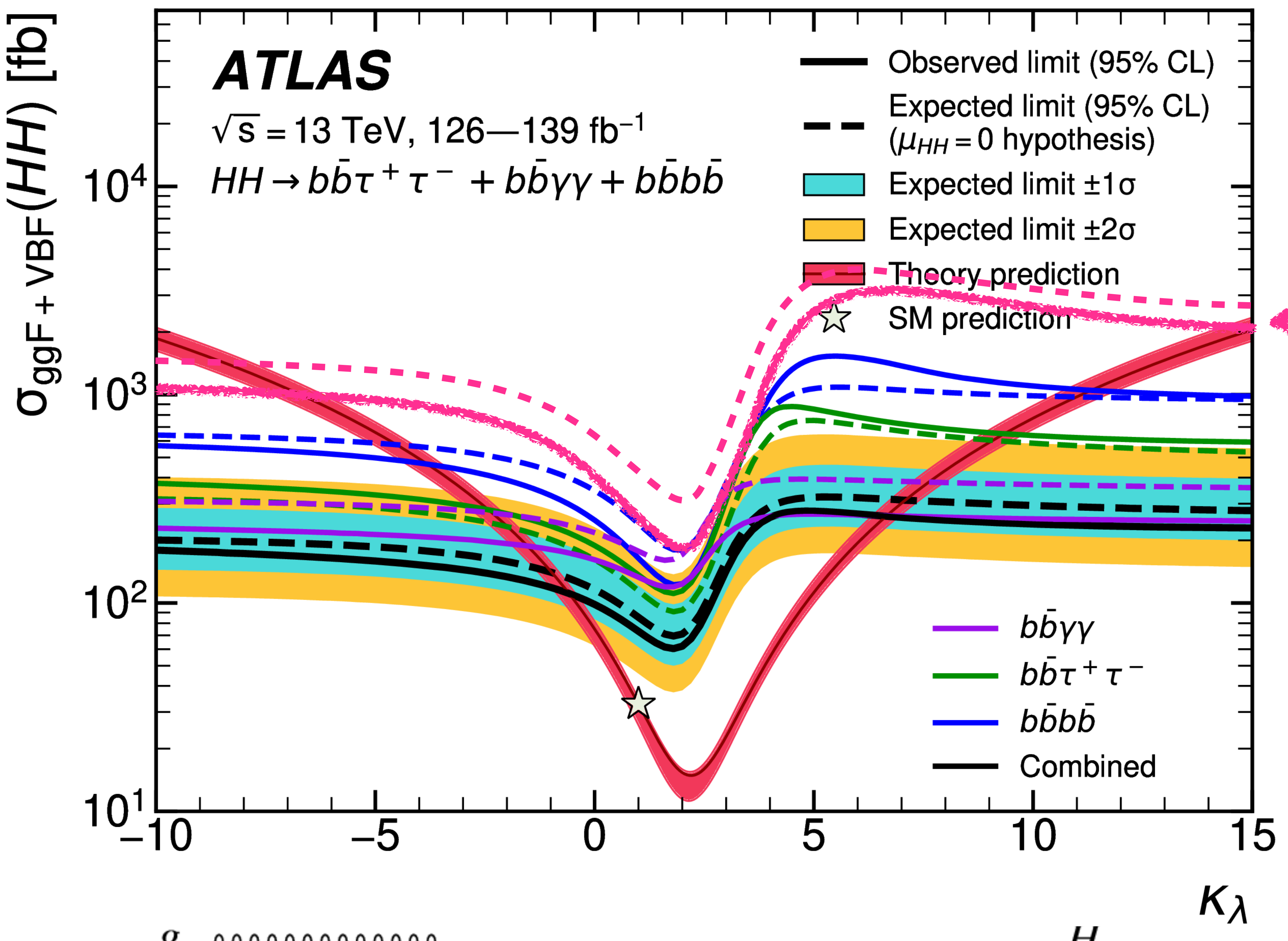

$bb\ell\ell\nu\nu$

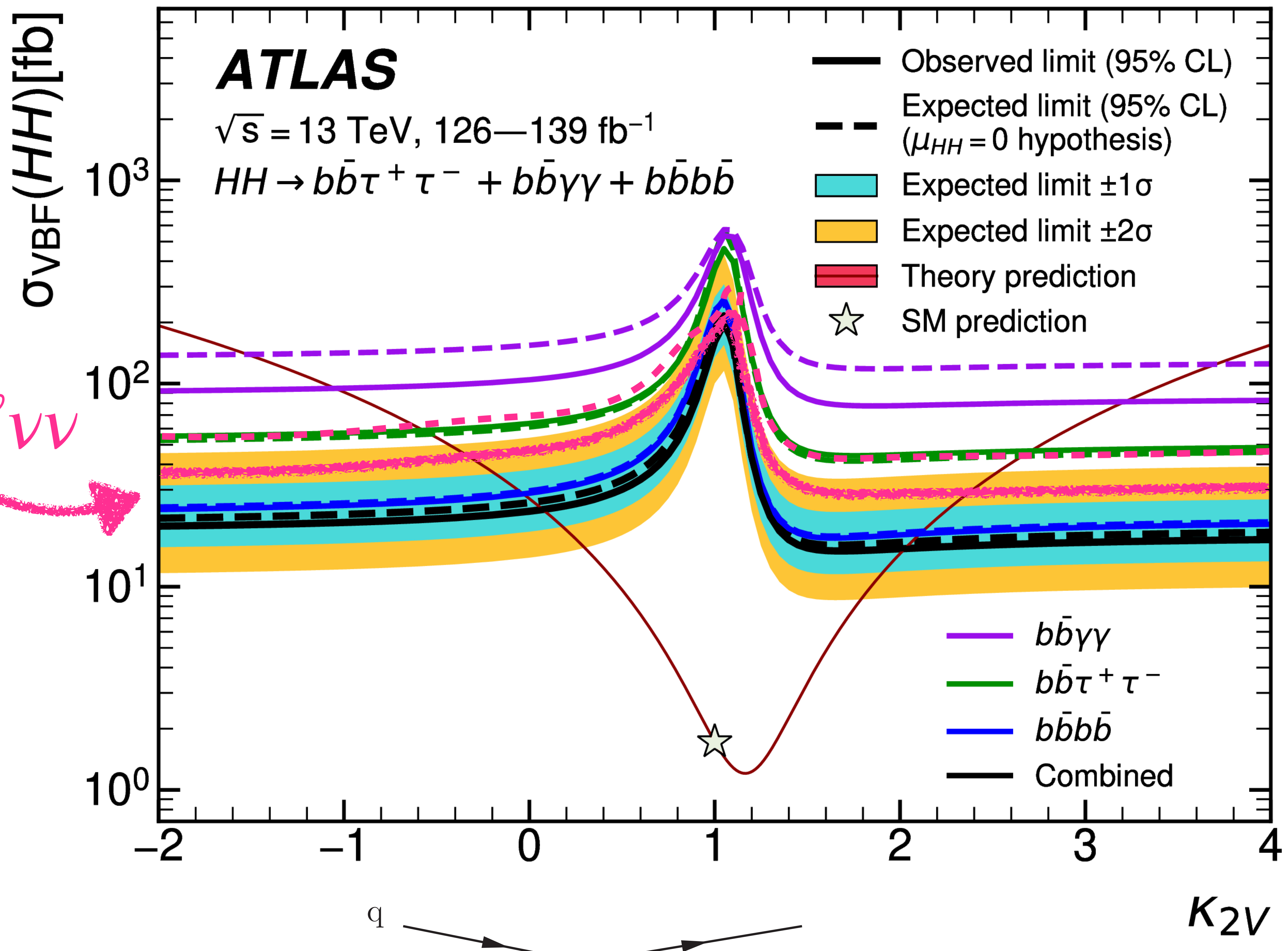

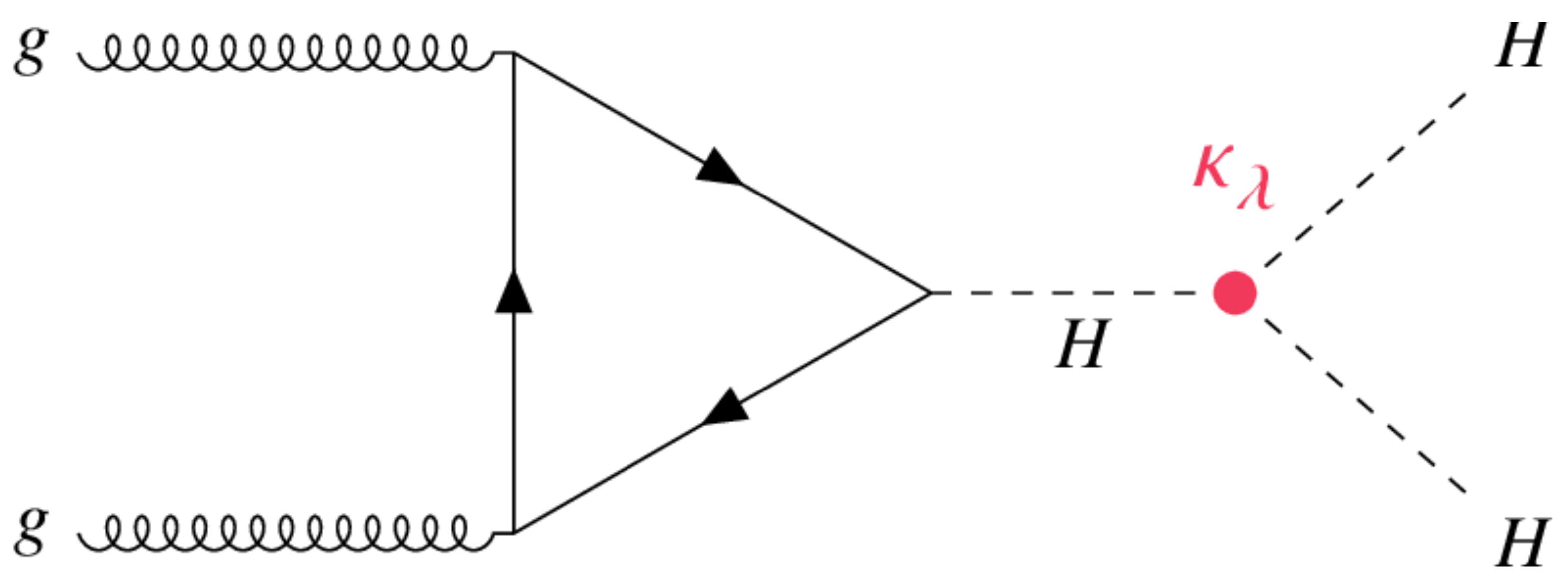

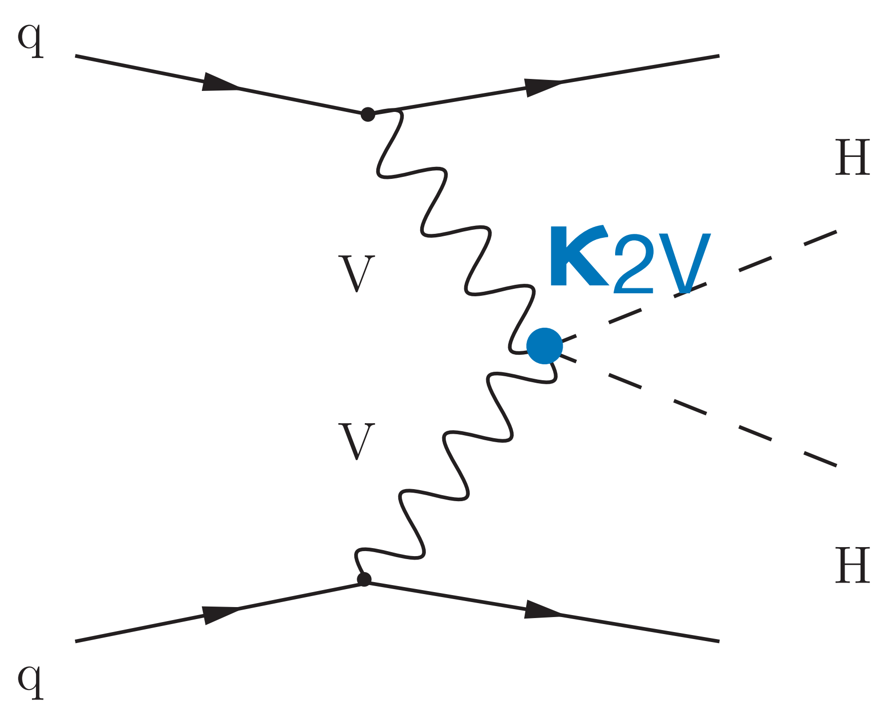

[*More limits including EFT in backups*]

Limits from $bb\ell\ell + E_T^{miss}$

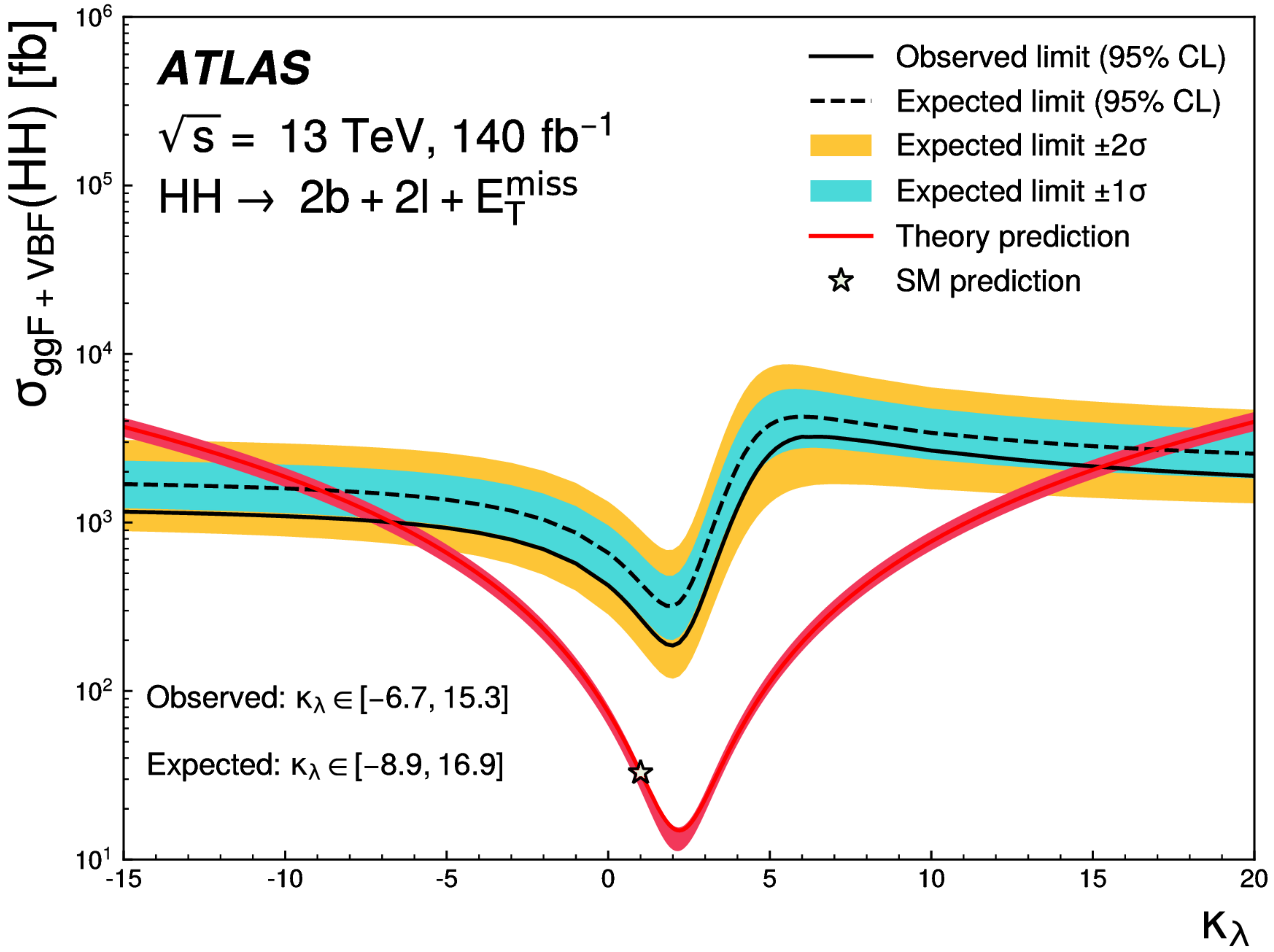

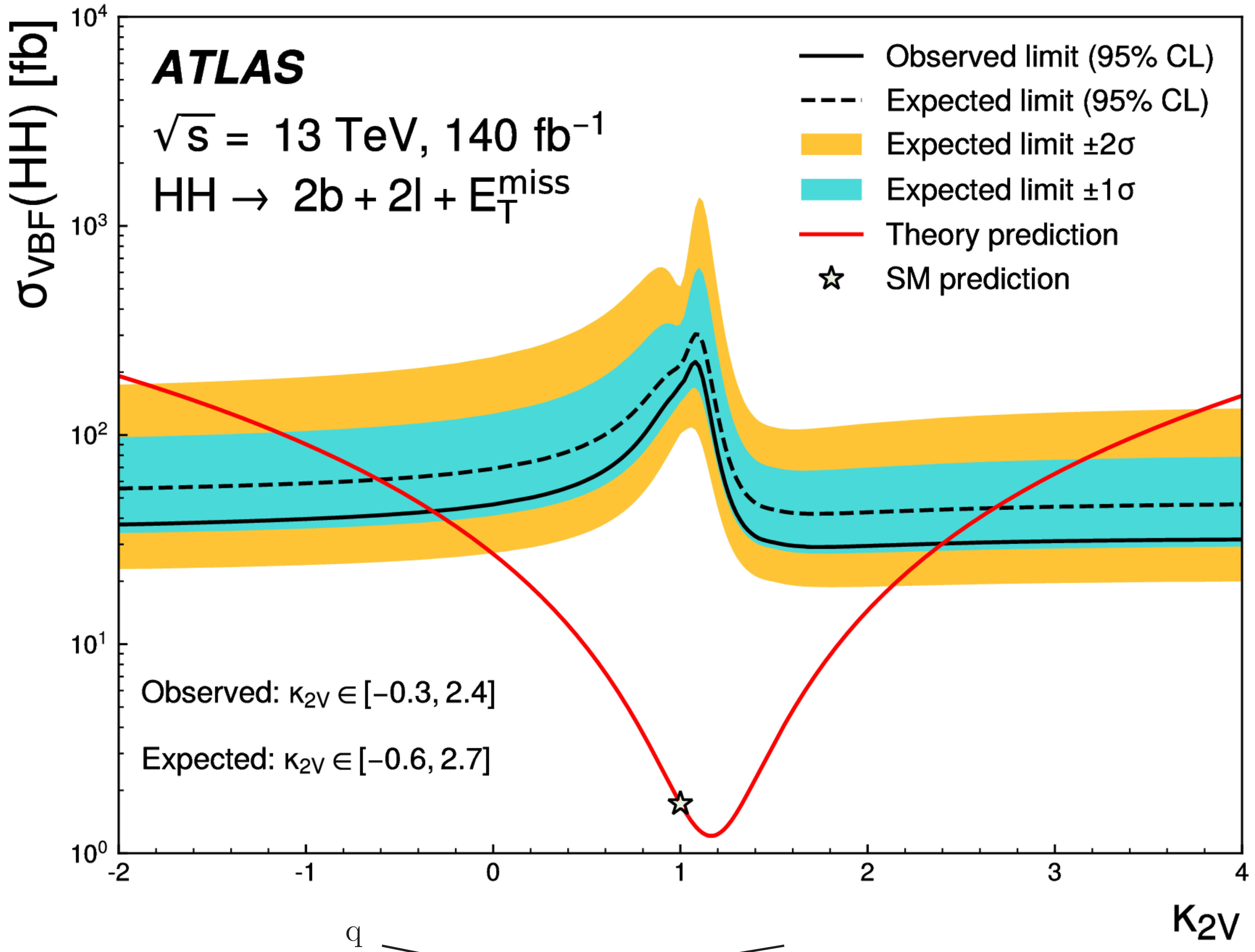

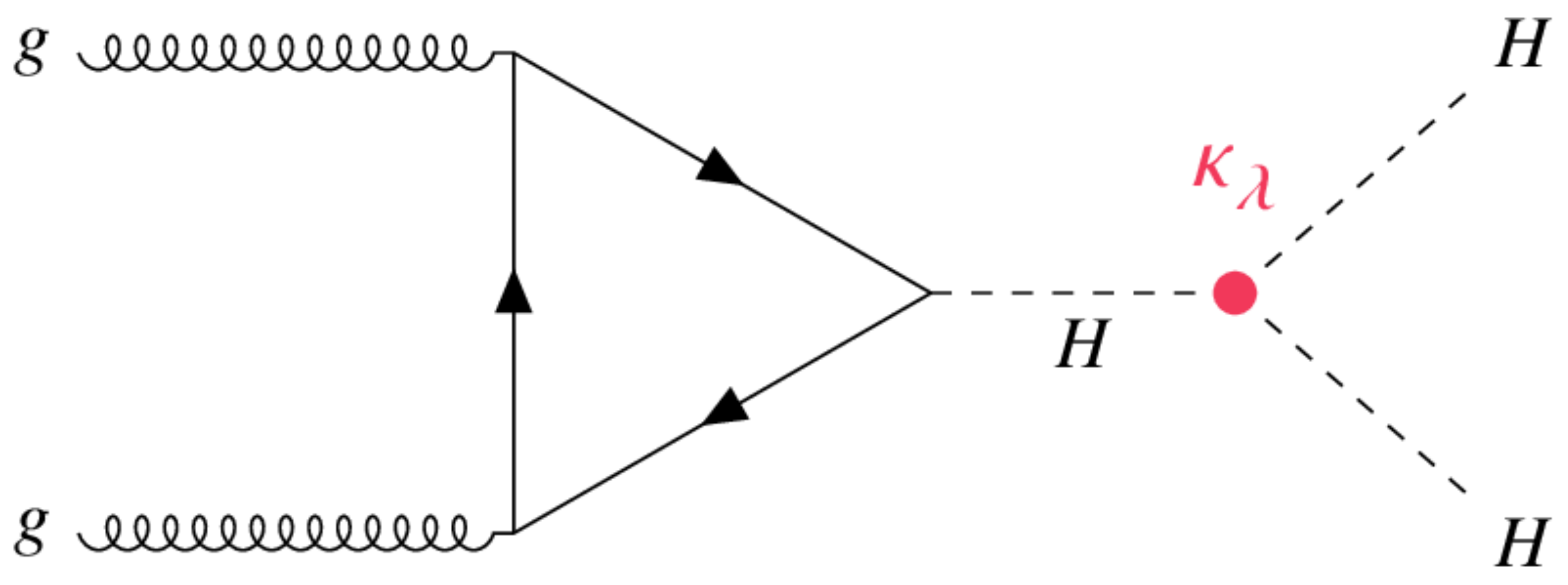

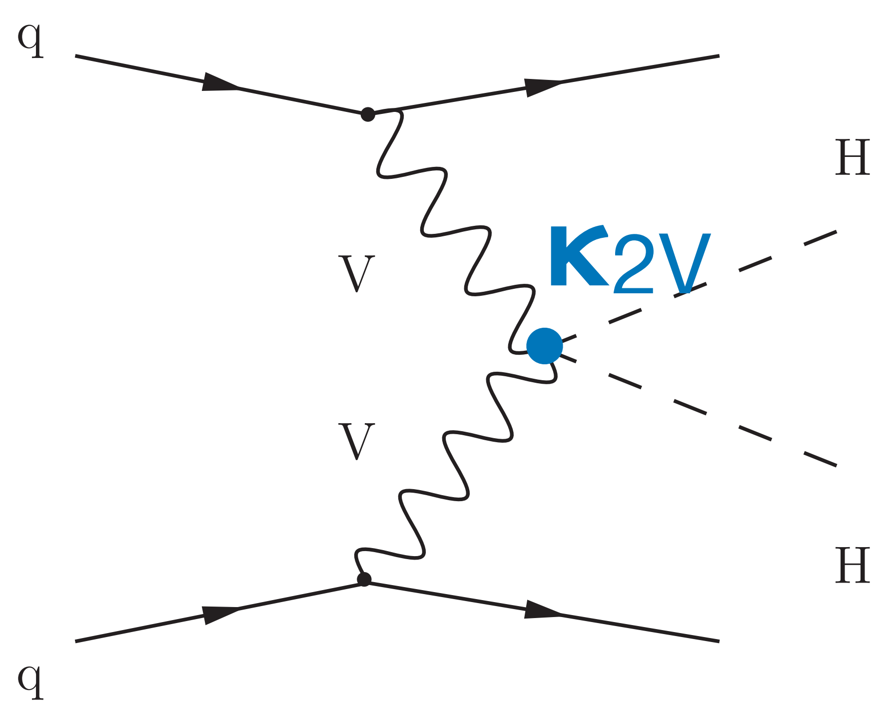

More limits including EFT in backups

Cross-section limits

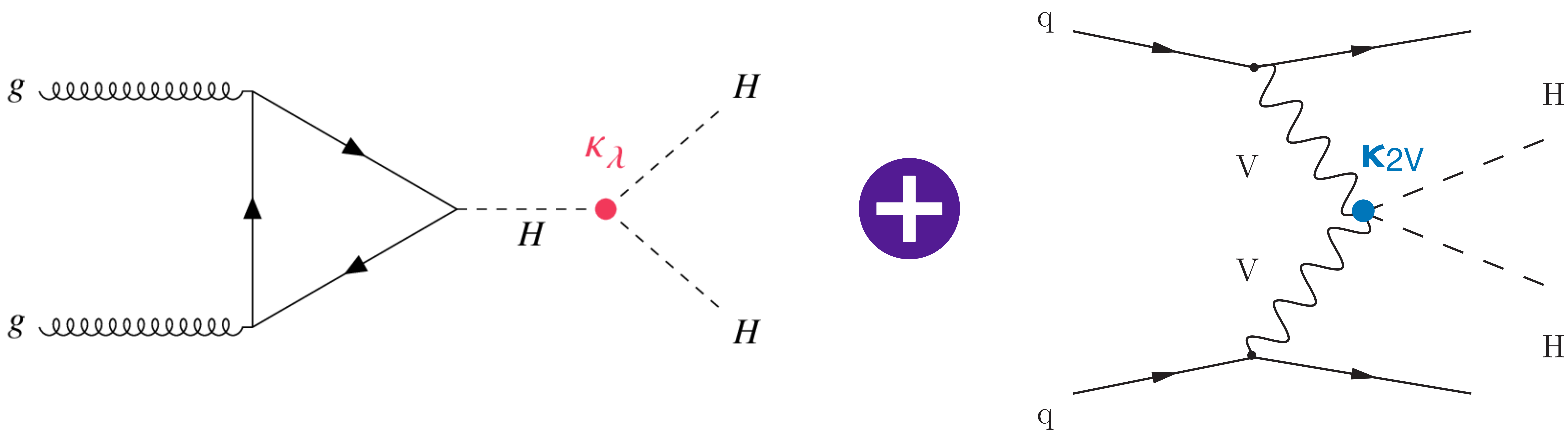

Total SM HH cross-section dominated by ggF + VBF

Cross-section limits

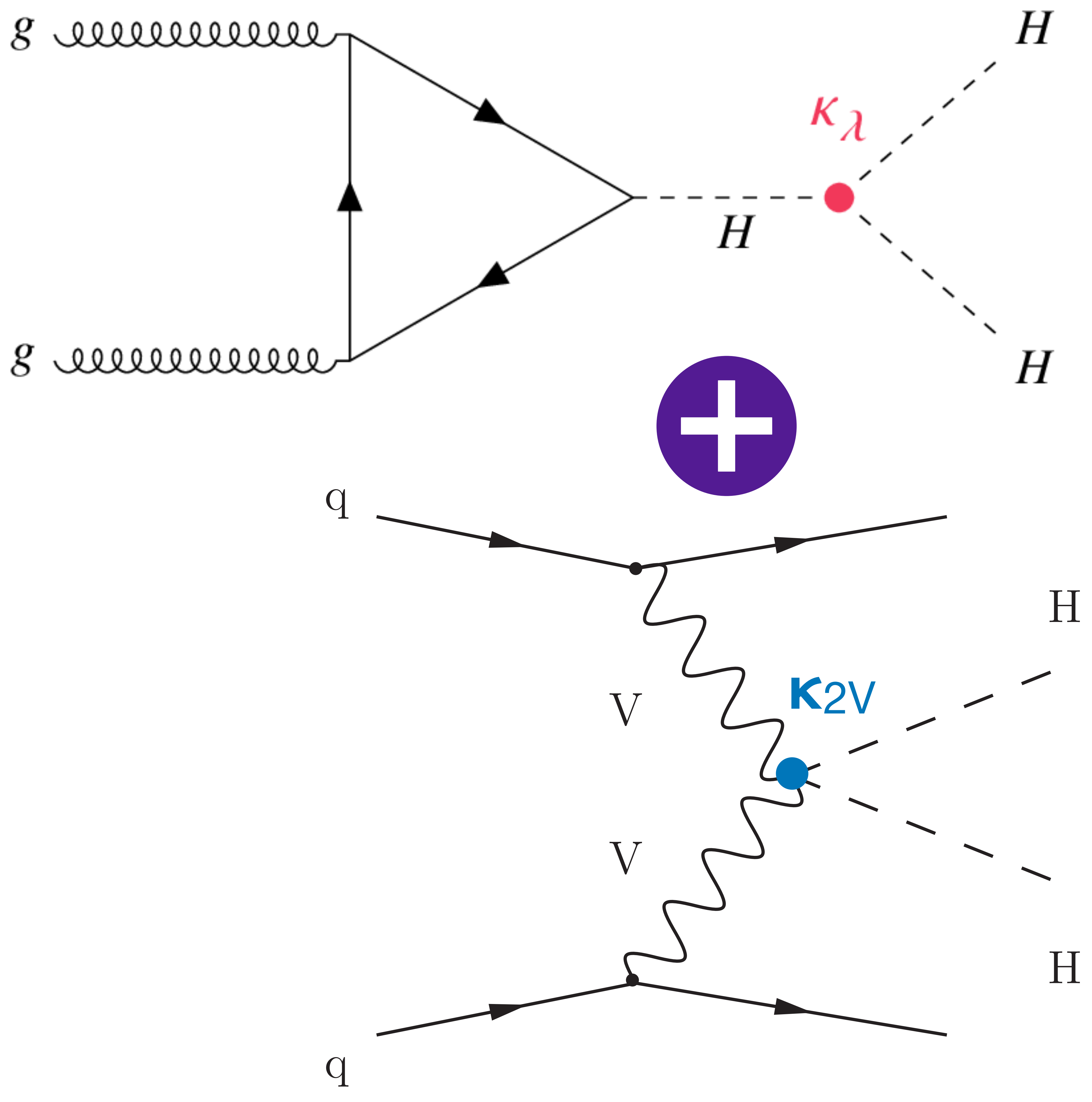

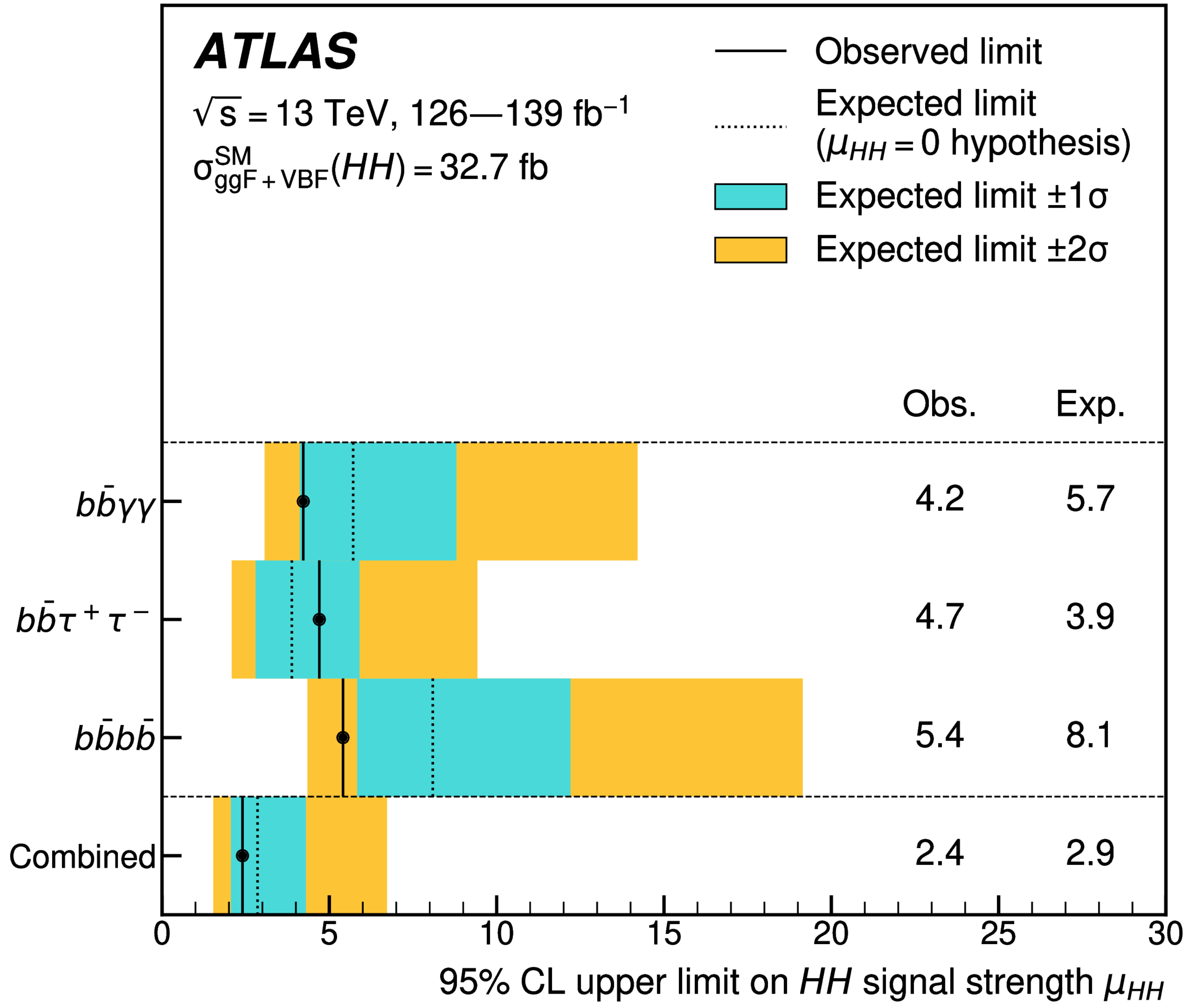

Phys. Lett. B 843 (2023) 137745

Cross-section limits

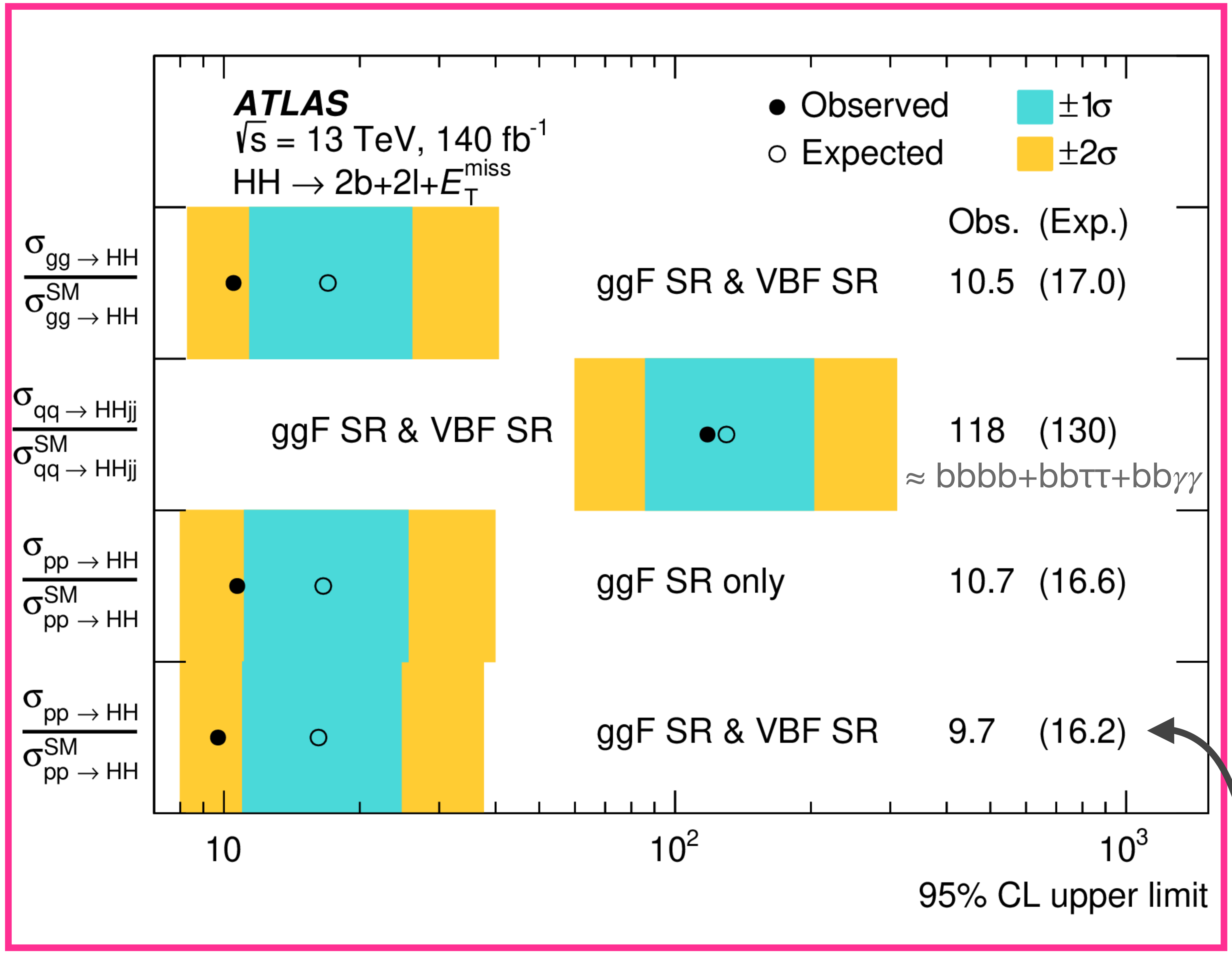

bbℓℓ + ETmiss

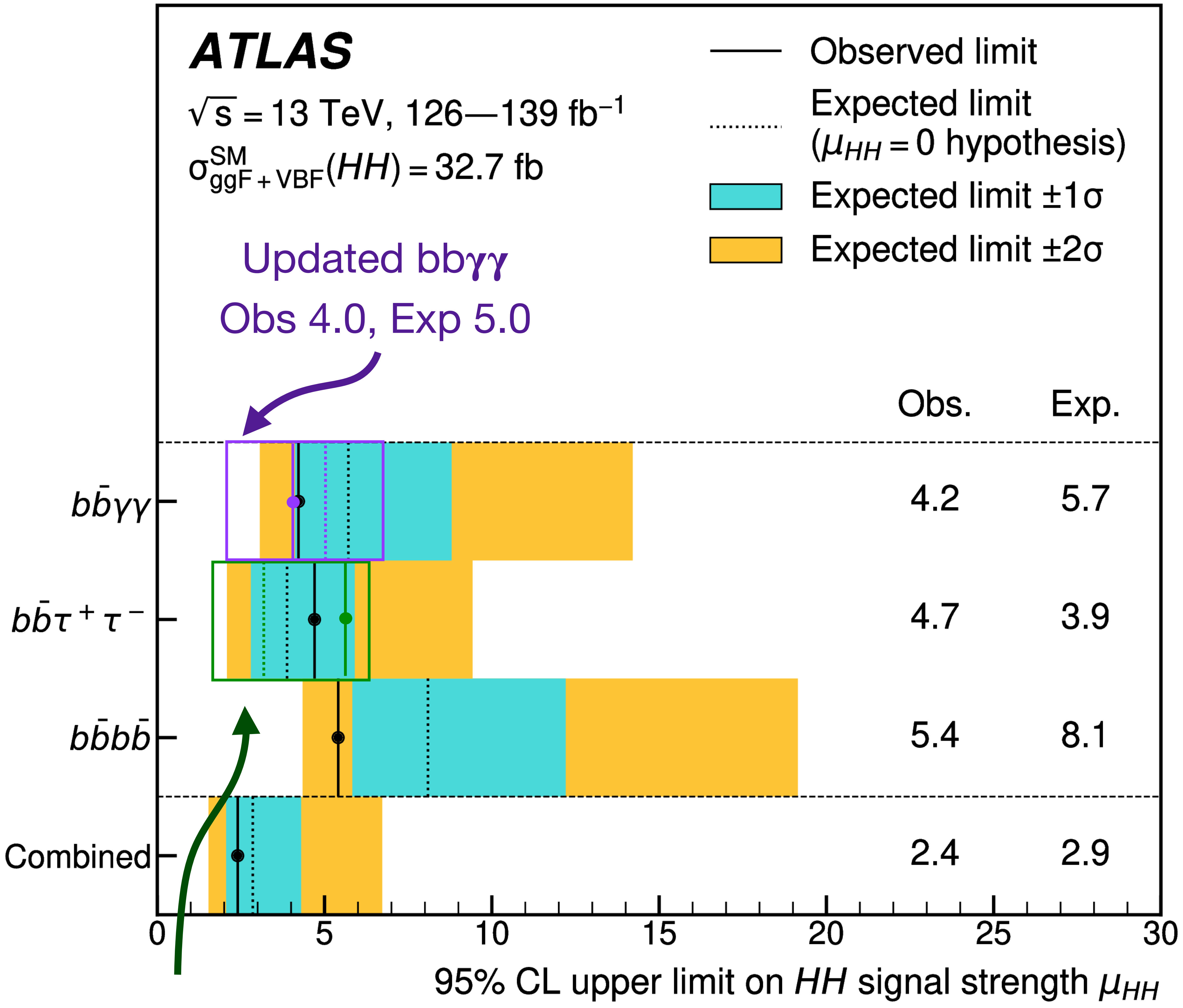

Updated bbττ
Obs 5.9, Exp 3.2

Phys. Lett. B 843 (2023) 137745

H + HH combination

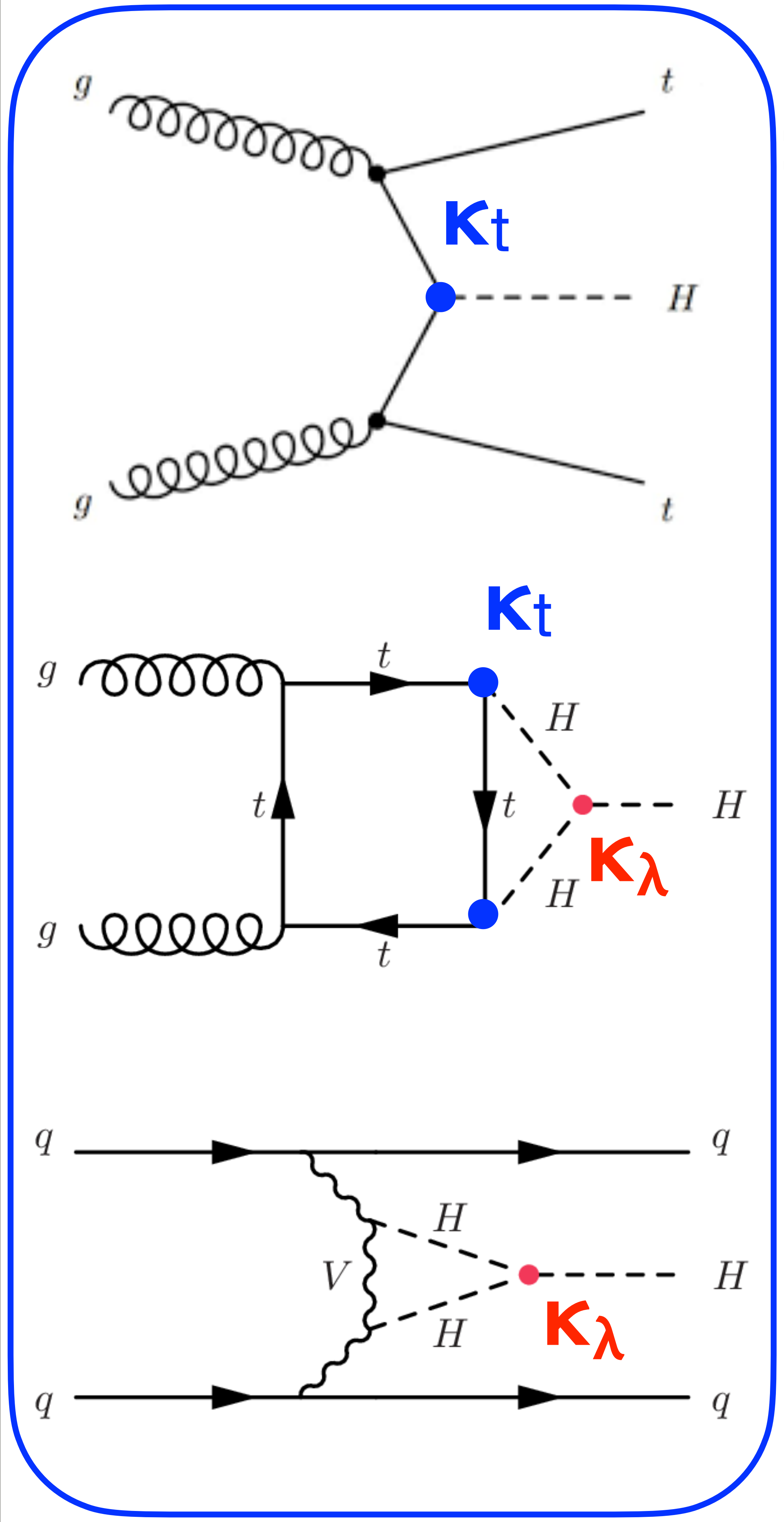

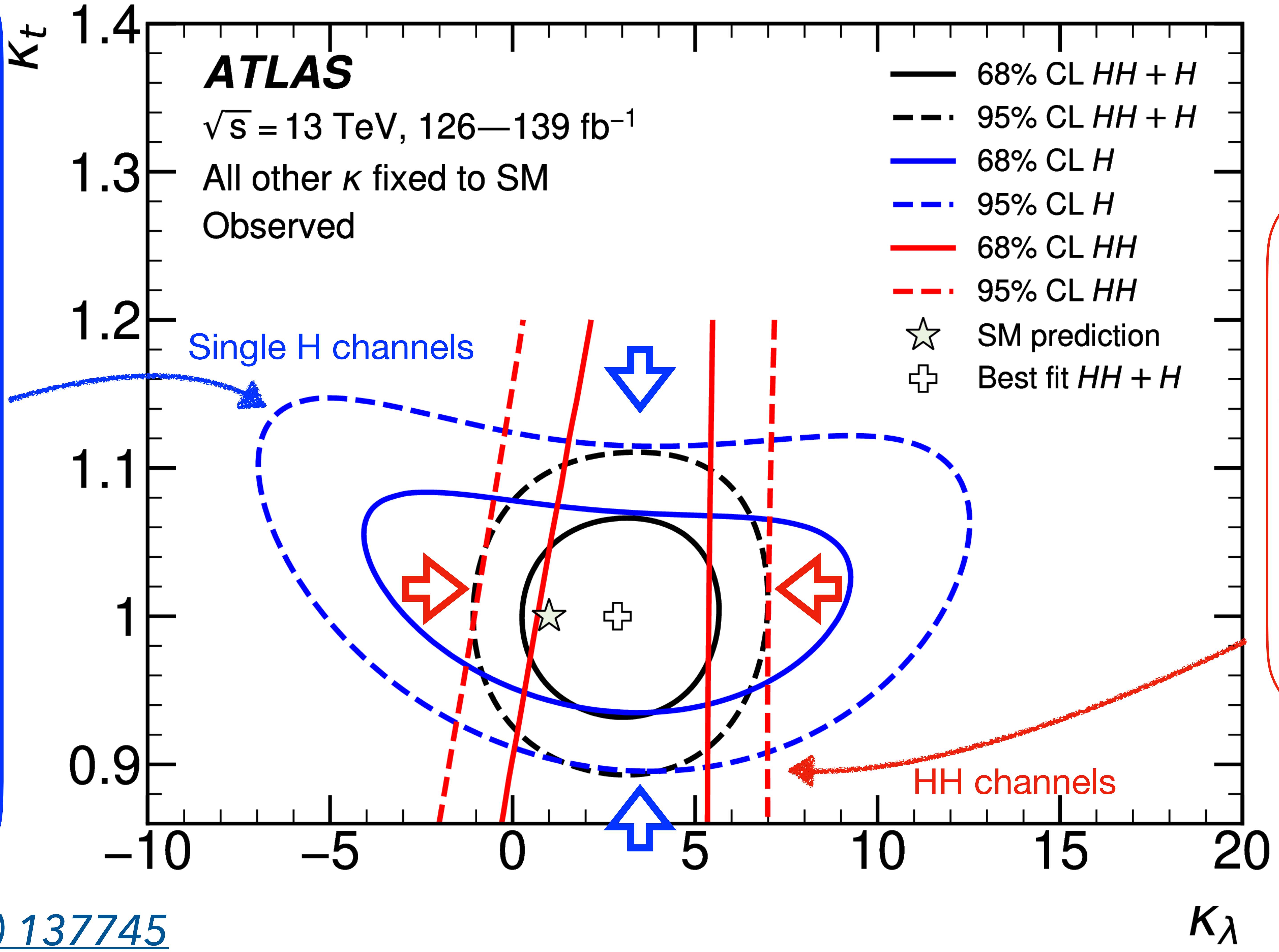

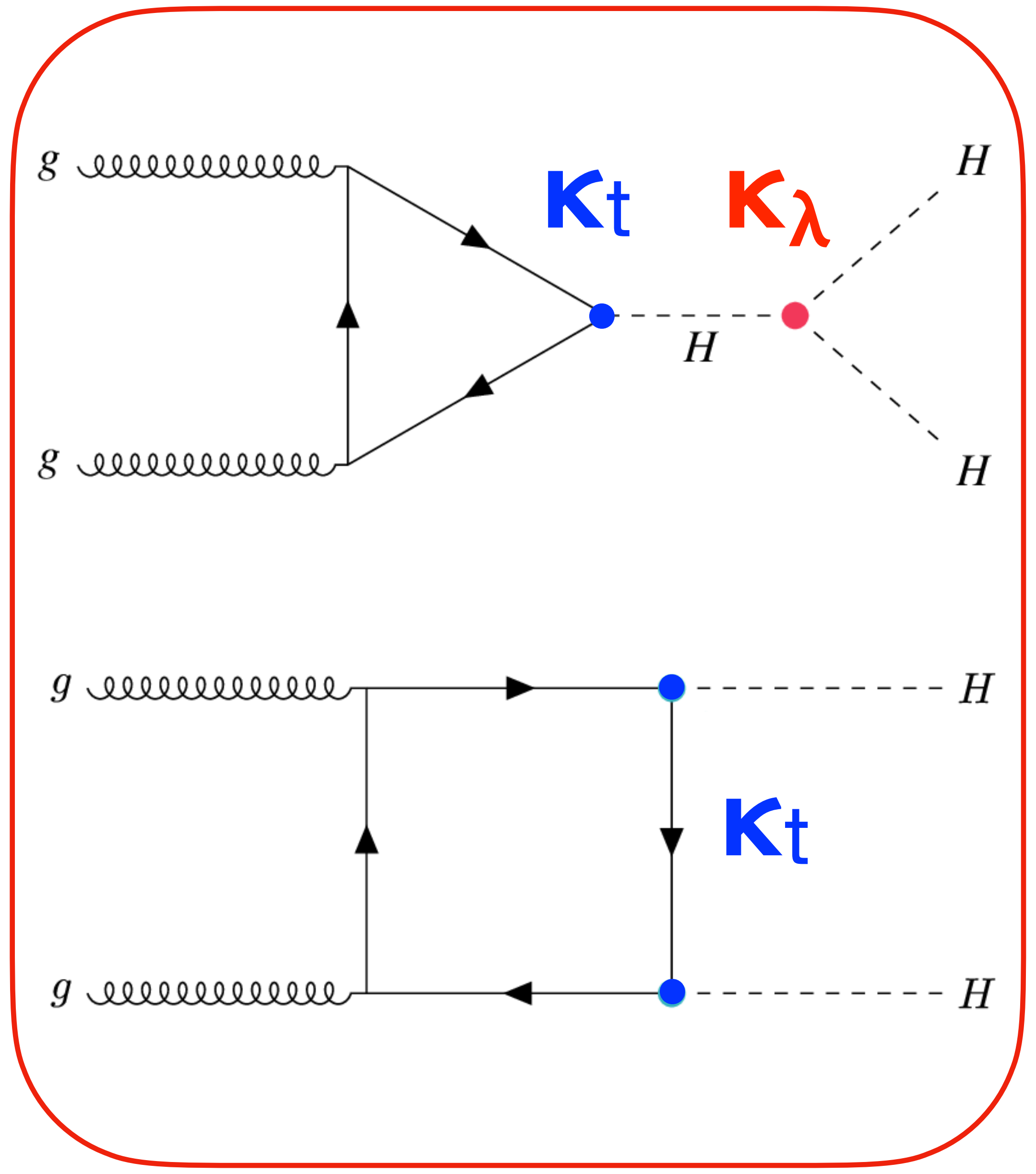

Phys. Lett. B 843 (2023) 137745

Resonant HH production

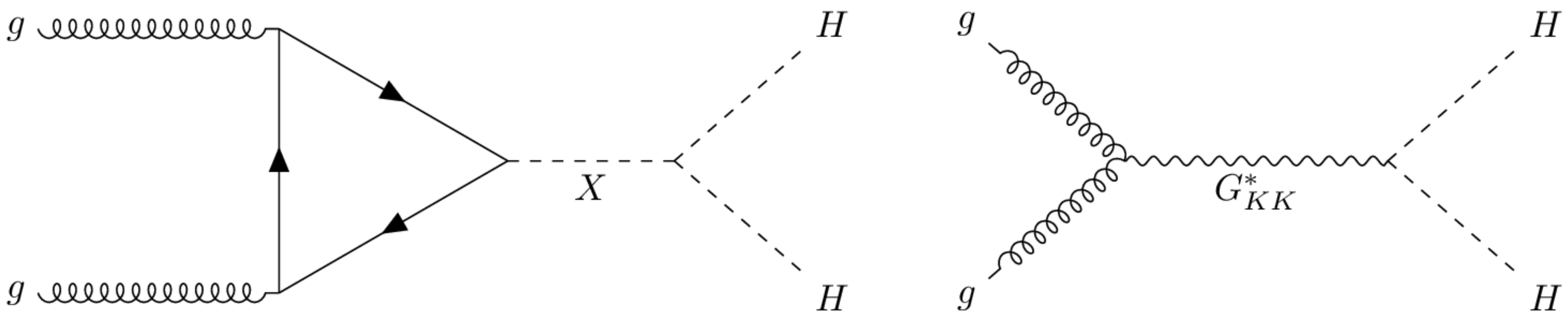

- Enhancement of HH production could originate from a resonance
- Heavy particle coupling (decaying) to HH
- E.g. scalar particle (extended H sector, Higgs portal to dark sector)

Other results:
HH → bb$\tau\tau$/bb$\gamma\gamma$ vs HEFT [ATL-PHYS-PUB-2022-021]
Resonant searches with additional BSM scalar (X SH) [O. Lundberg, tomorrow]

Resonant HH production

Also: MSSM limits!

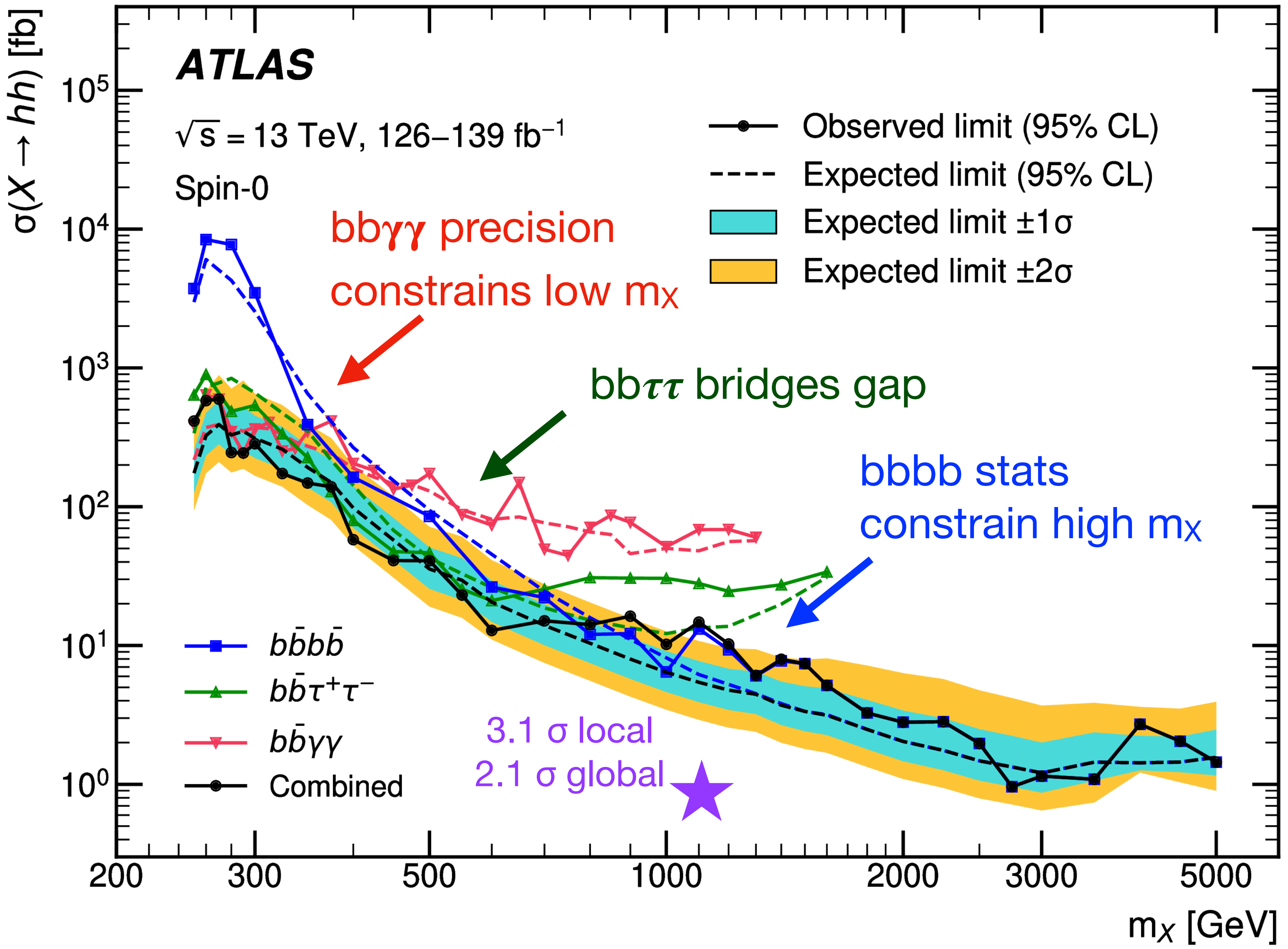

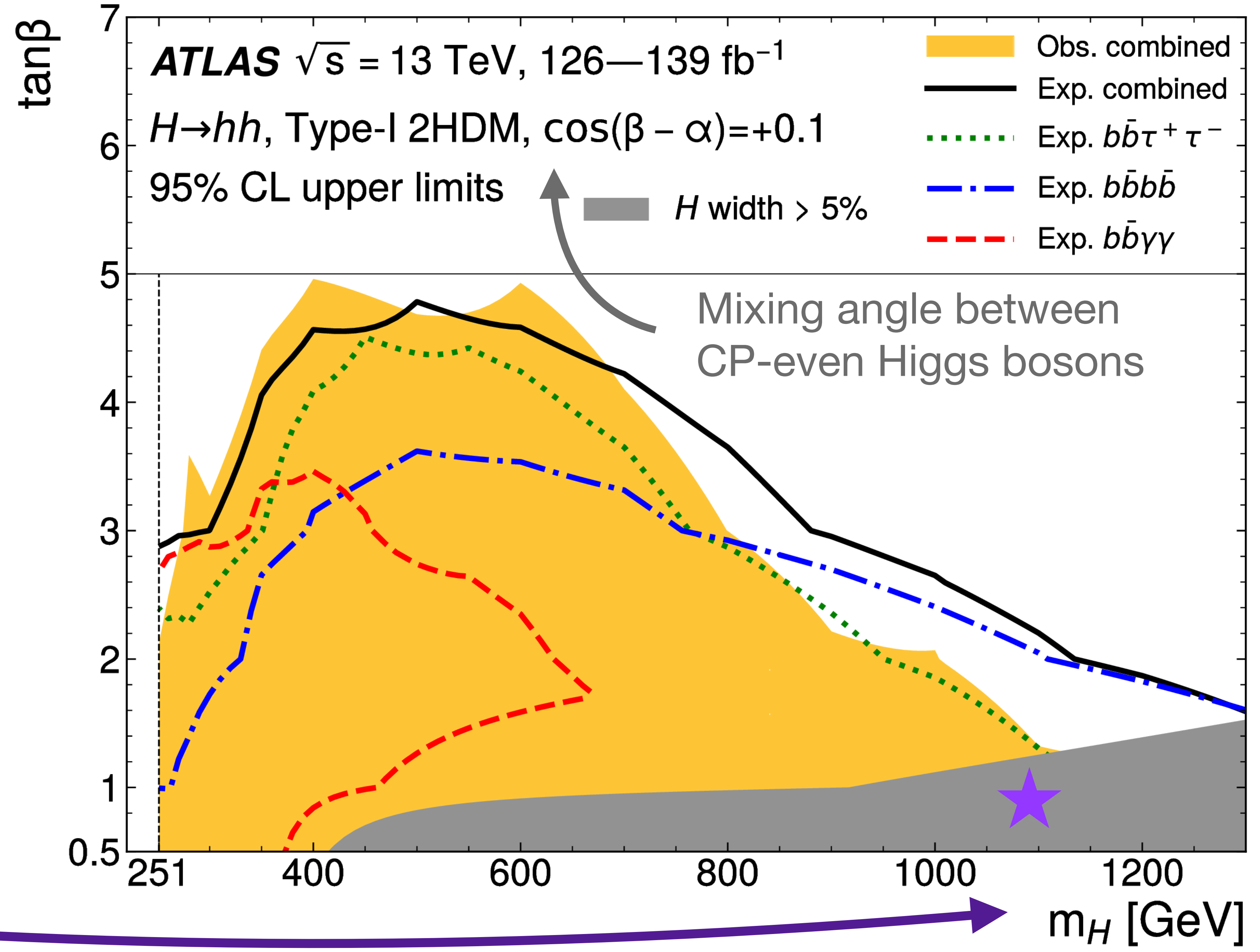

- Combine resonant searches in three channels:
  - bb$\gamma\gamma$ [Phys. Rev. D 106 (2022) 052001]
  - bb$\tau\tau$ [JHEP 07 (2023) 040]
  - bbbb [Phys. Rev. D 105 (2022) 092002]

- Interpret in 2-Higgs-doublet model
- Limits from heavy CP-even scalar H decaying to *hh* interpreted as SM Higgs
- Parameterise in ratio of up/down-quark coupling boson VEVs, tan(β)

HDBS-2023-17 -- arXiv:2311.ComingSoon

Where do we go from here?

And how do we get there?

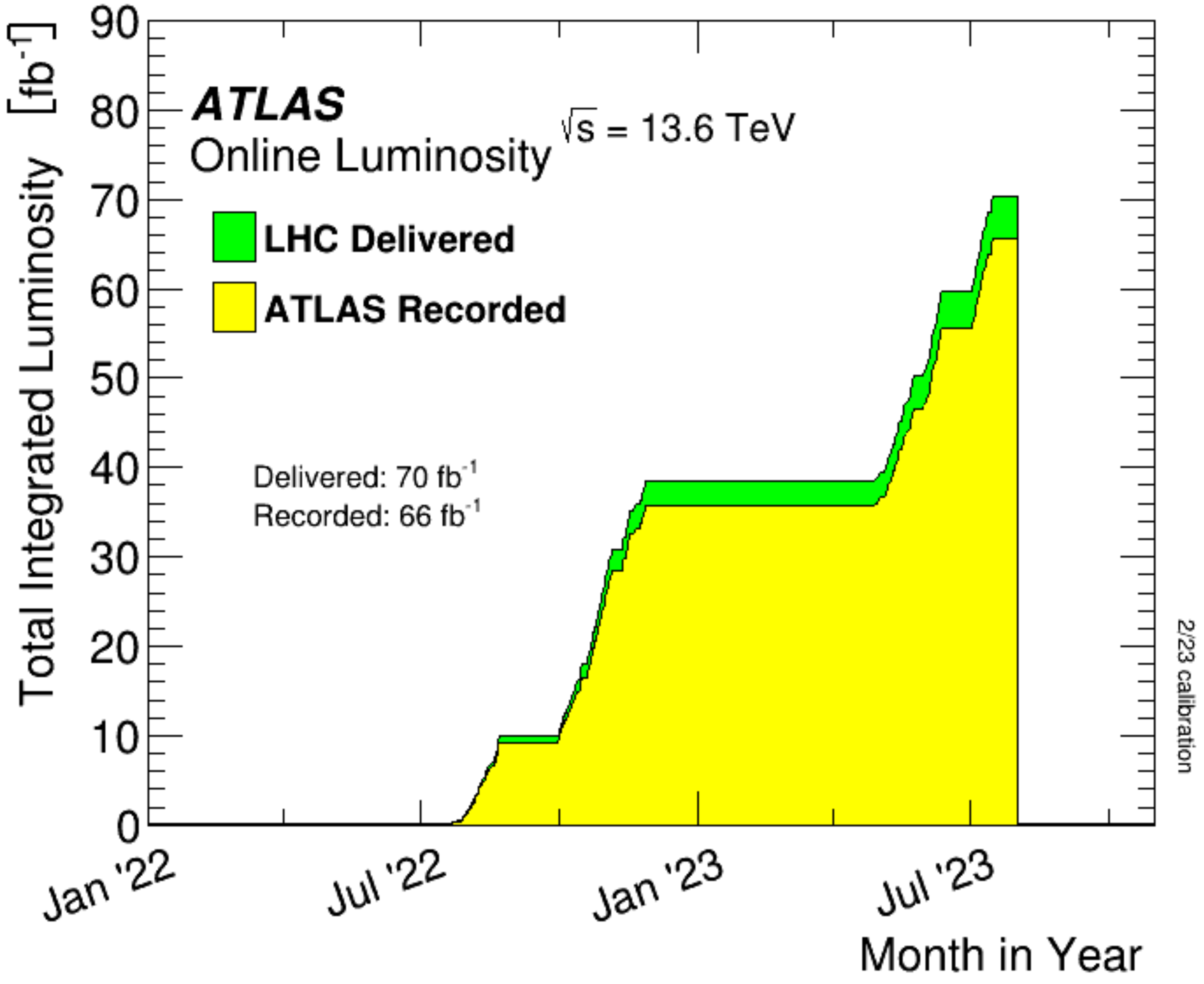

Run 3 dataset

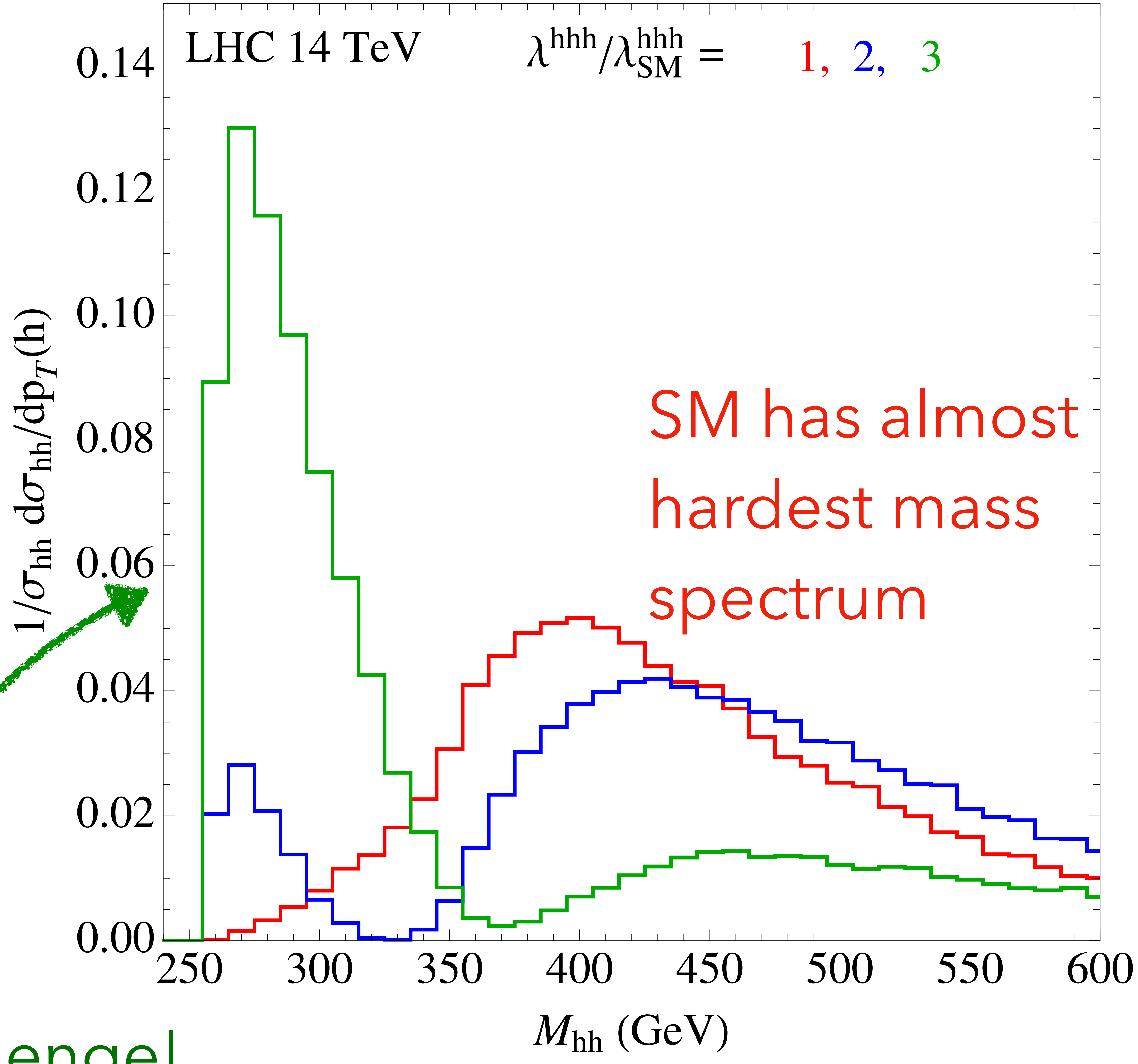

SM has almost hardest mass spectrum

Trigger challenge!

arXiv: 1311.2931 / PLB 728 (2014) 433-436

Where do we go from here?

And how do we get there?

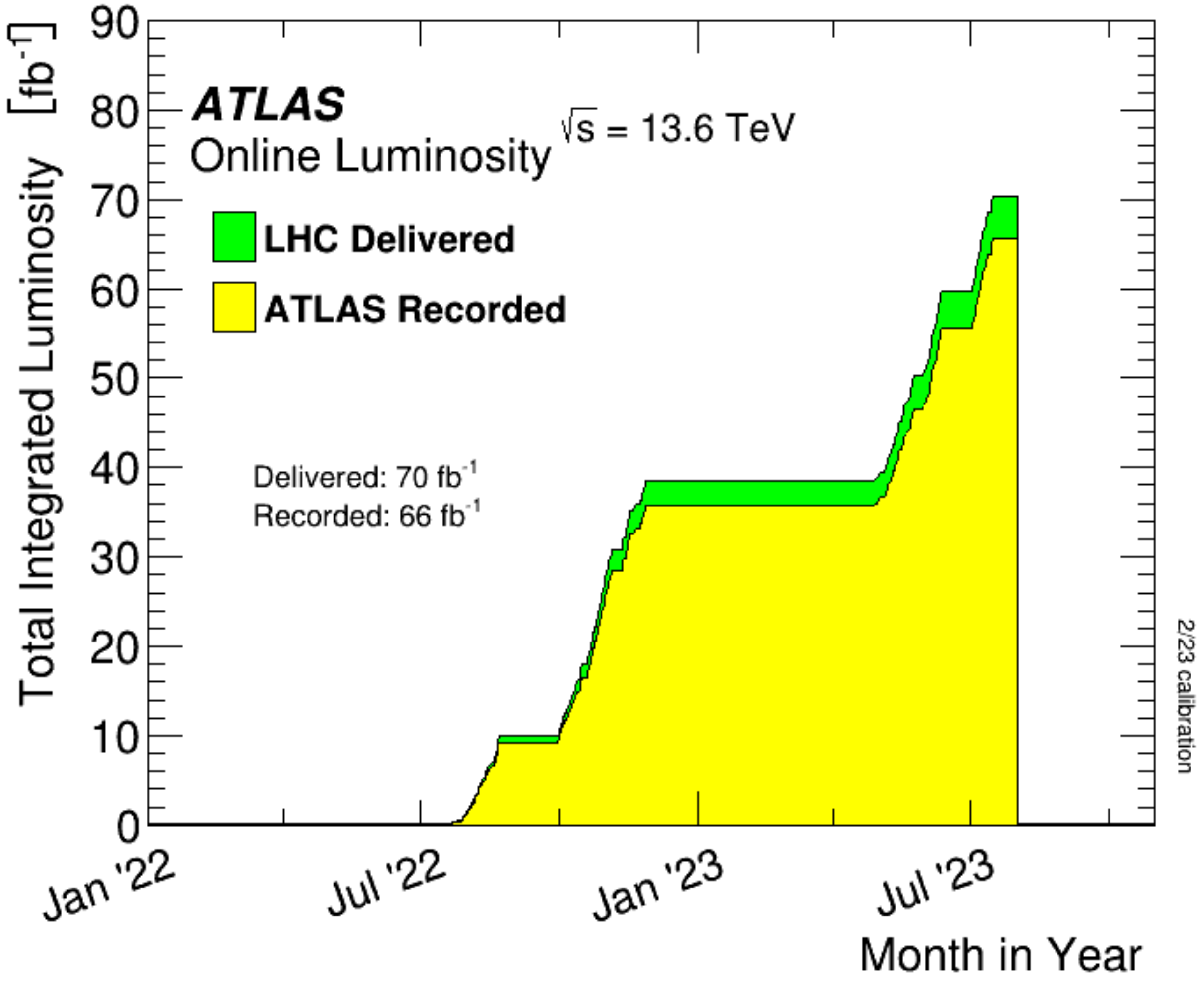

Run 3 dataset

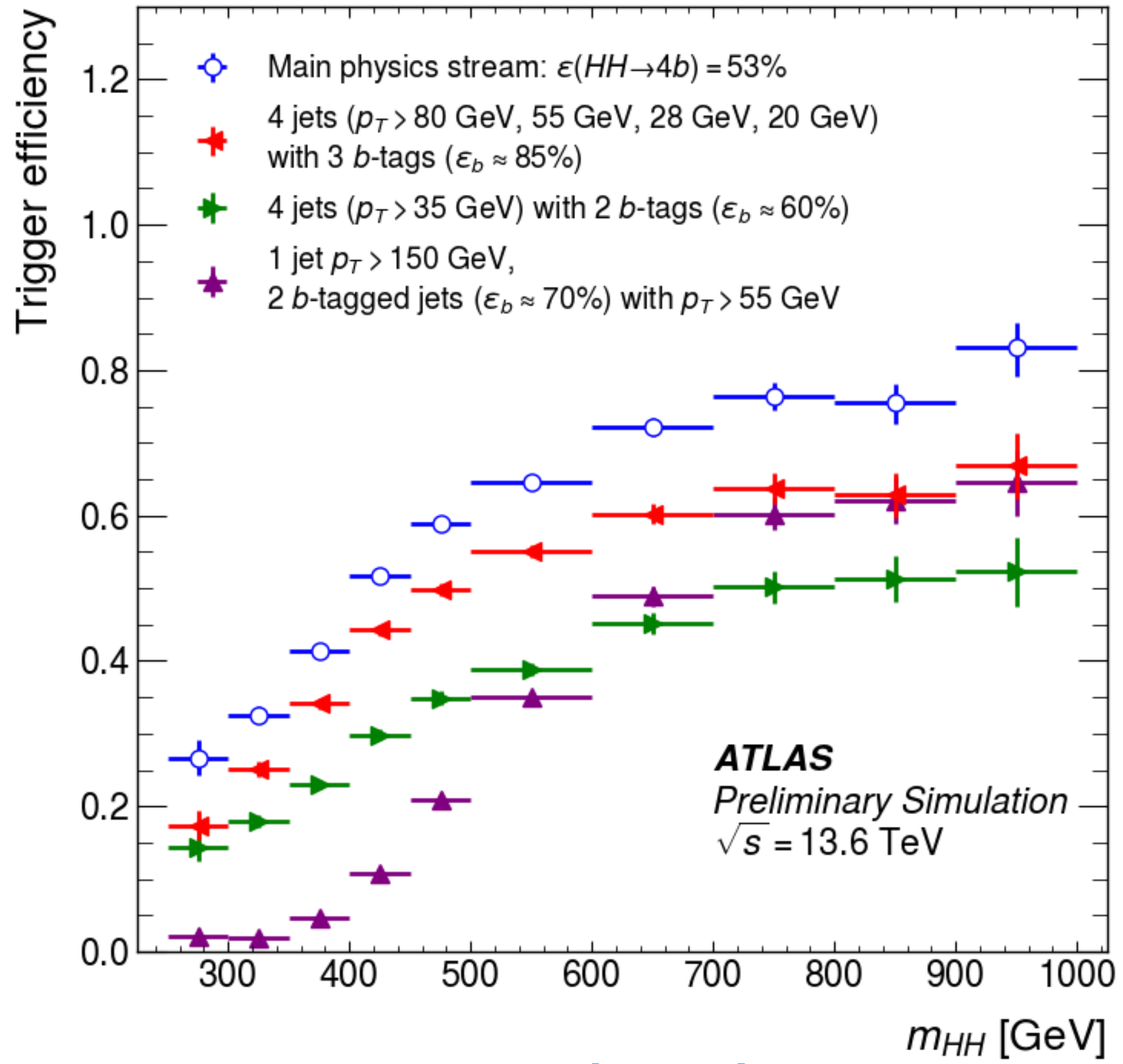

[More details]

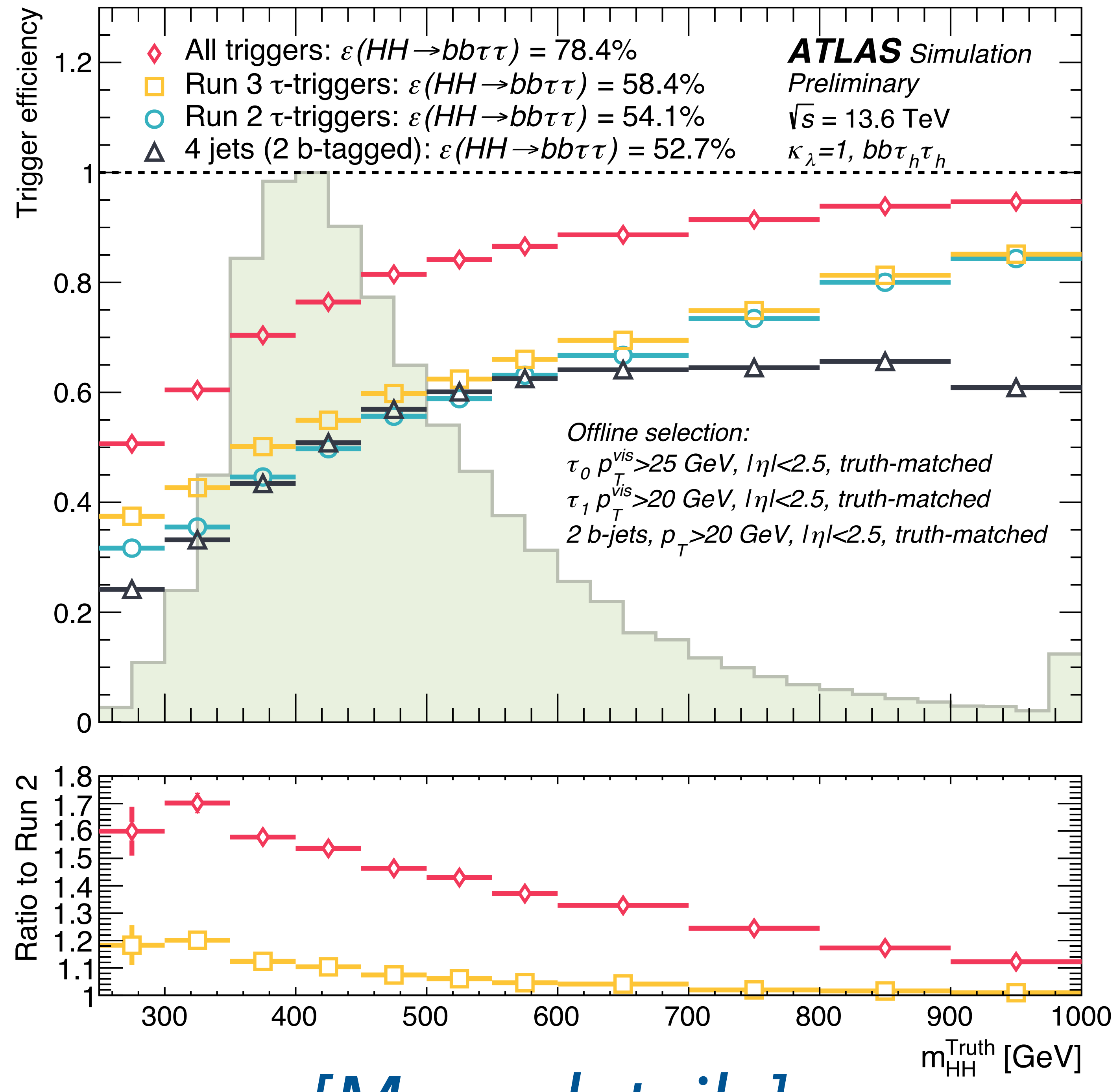

[More details]

Trigger improvements in bbbb, bb$\tau\tau$: 50% more efficient than Run 2

- Tracking for hadronic signatures ⇒ Particle Flow jets
- Deep/Graph Neural Net b-taggers
- Optimised event selections, increased bandwidth

Where do we go from here?

Even further down the line — assume SM signal

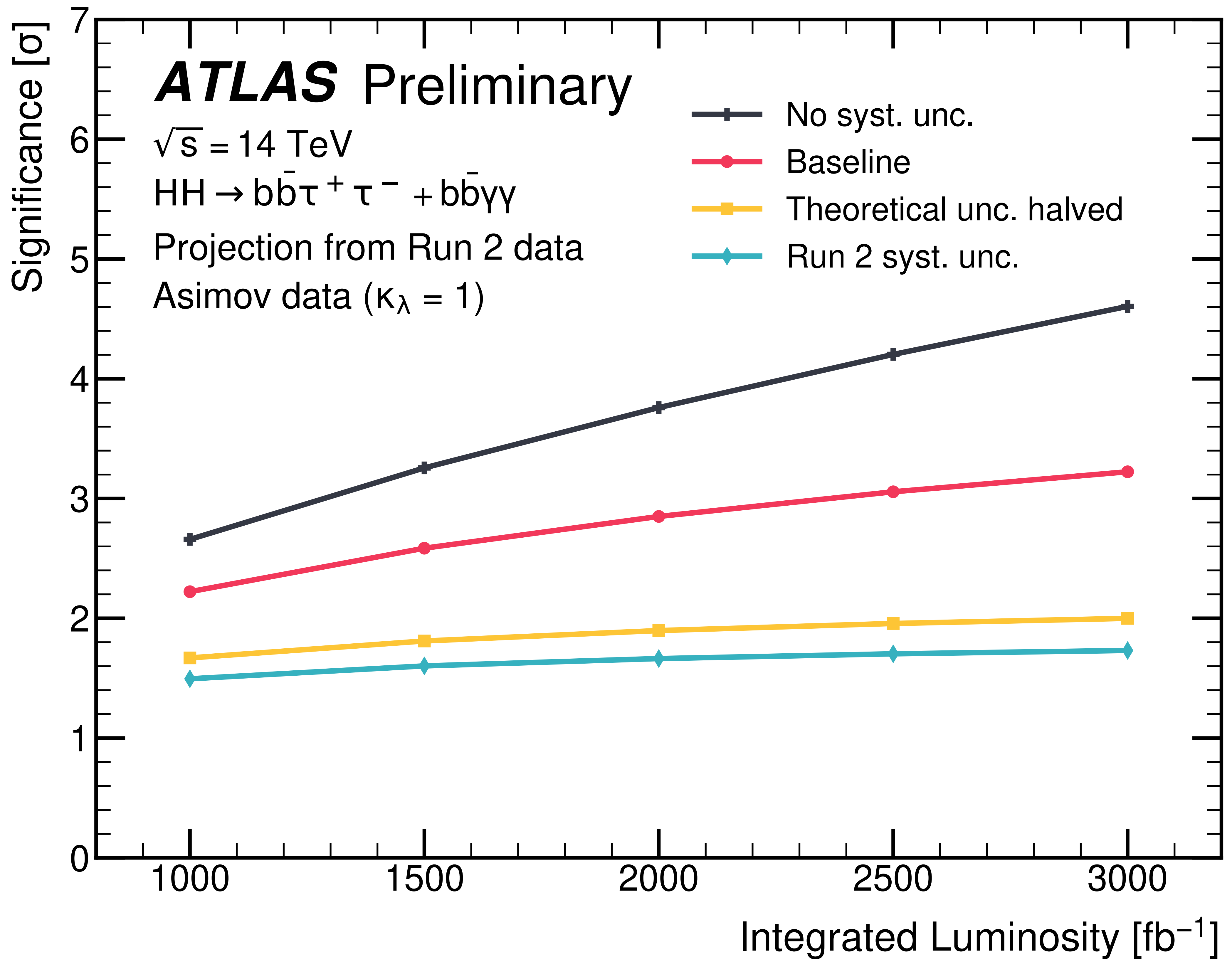

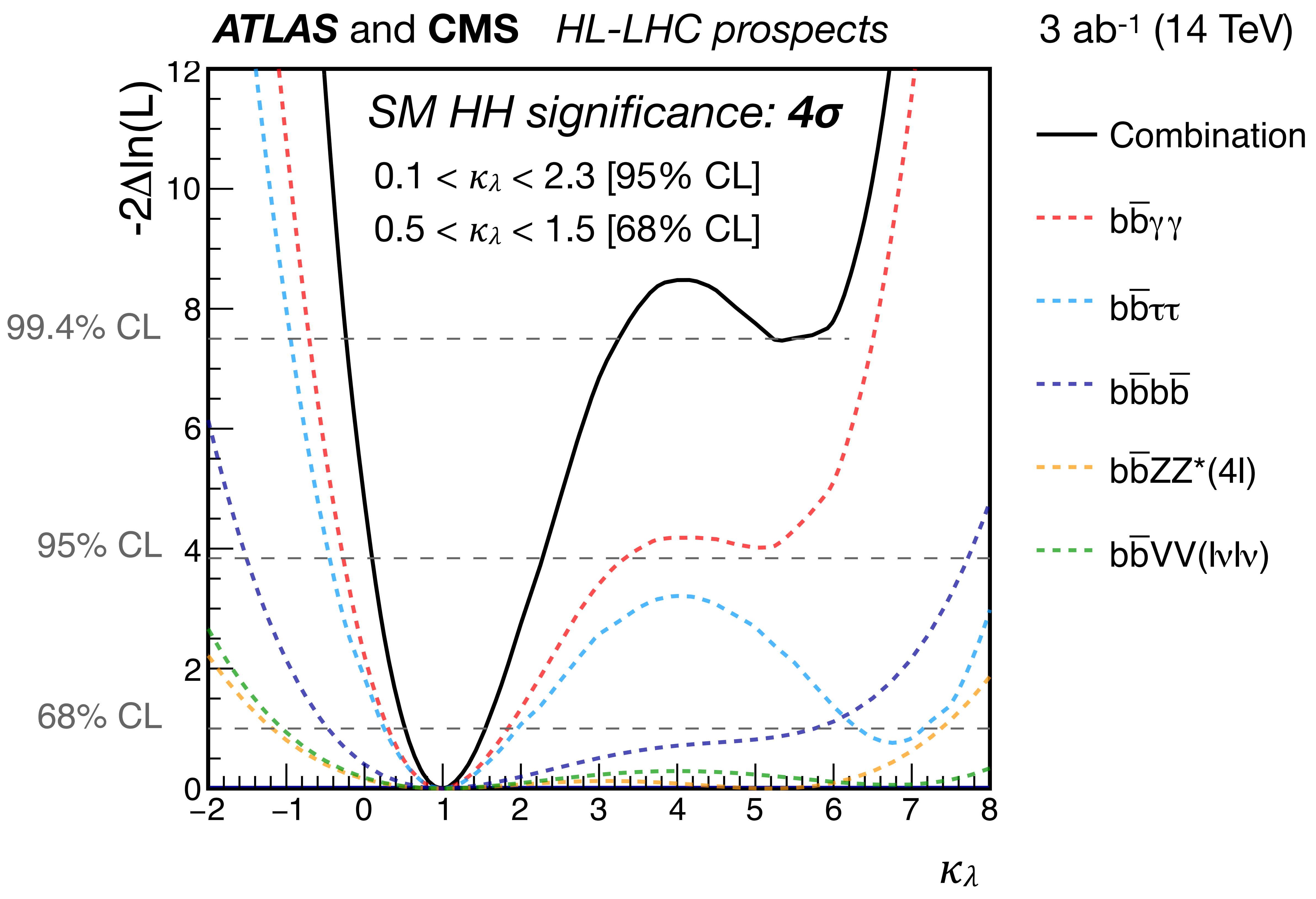

New ATLAS HL-LHC projections
(bbττ, bbγγ)

Snowmass White Paper: Physics with ATLAS/CMS Phase-II
ATL-PHYS-PUB-2022-018/CMS-PAS-FTR-22-001

Wrapping up

- Active ATLAS programme in DiHiggs searches
  - Key to deeper understanding of ElectroWeak Symmetry Breaking
- Latest searches have exclusion sensitivity at O(1 x σ_{SM})
  - Advances in reconstruction, trigger, analysis strategy necessary
- Potential for major gains with a large Run 3 dataset — keep pushing!

双希双喜

Backups

HH in translation

- 希: Hope (xī), also used as an abbreviation for the Higgs boson (希格斯玻色子)
- 喜: Joy (xǐ)
- 双喜临门: Double joy arrives at the door (shūang xī lín mén)
  - Two happy events in coincidence
- 双希: Double(di-) Higgs (shūang xī)

Coupling limits

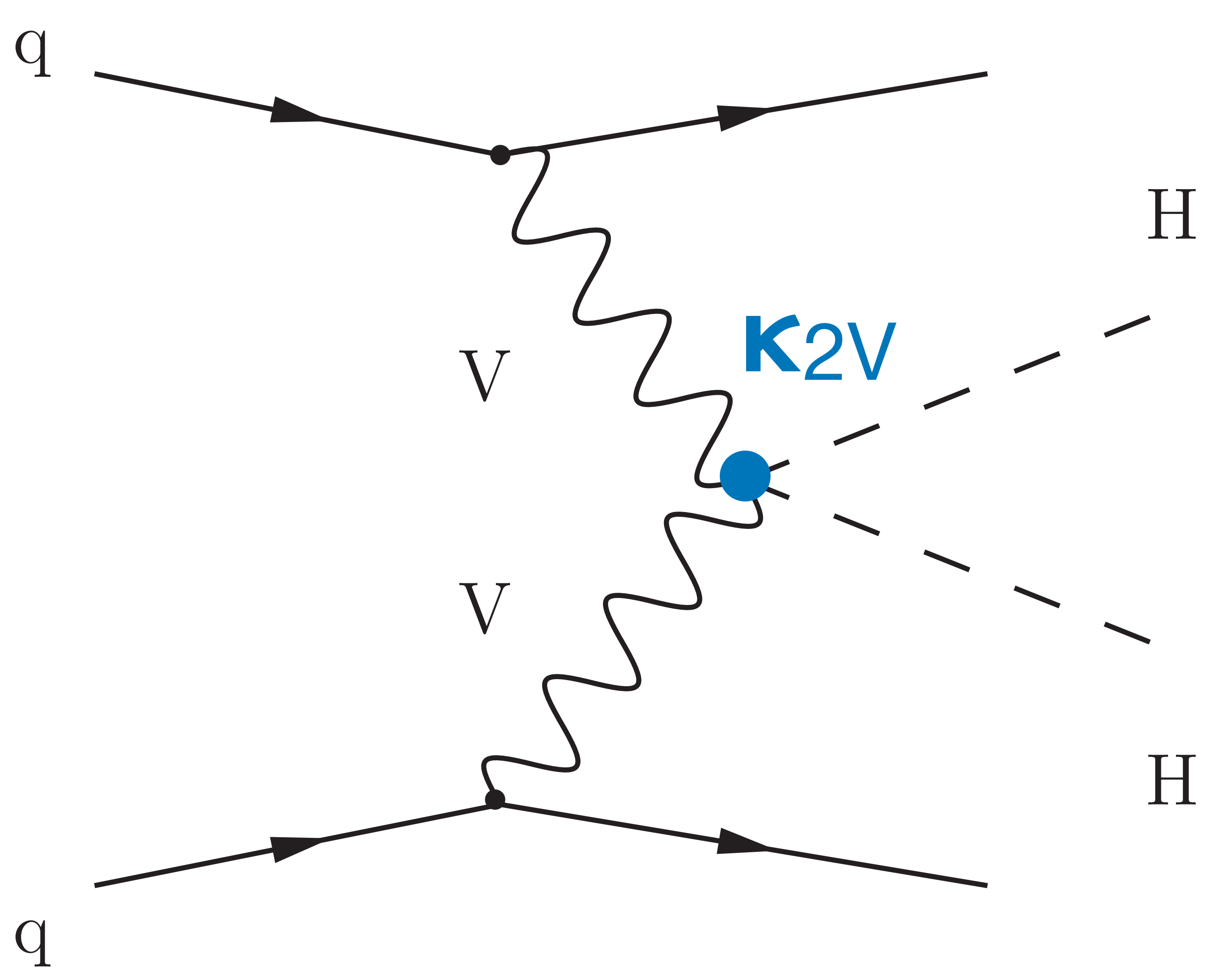

Anomalous enhancement of HH to VV coupling: κ_{2V}

⇒ unique sensitivity in VBF HH

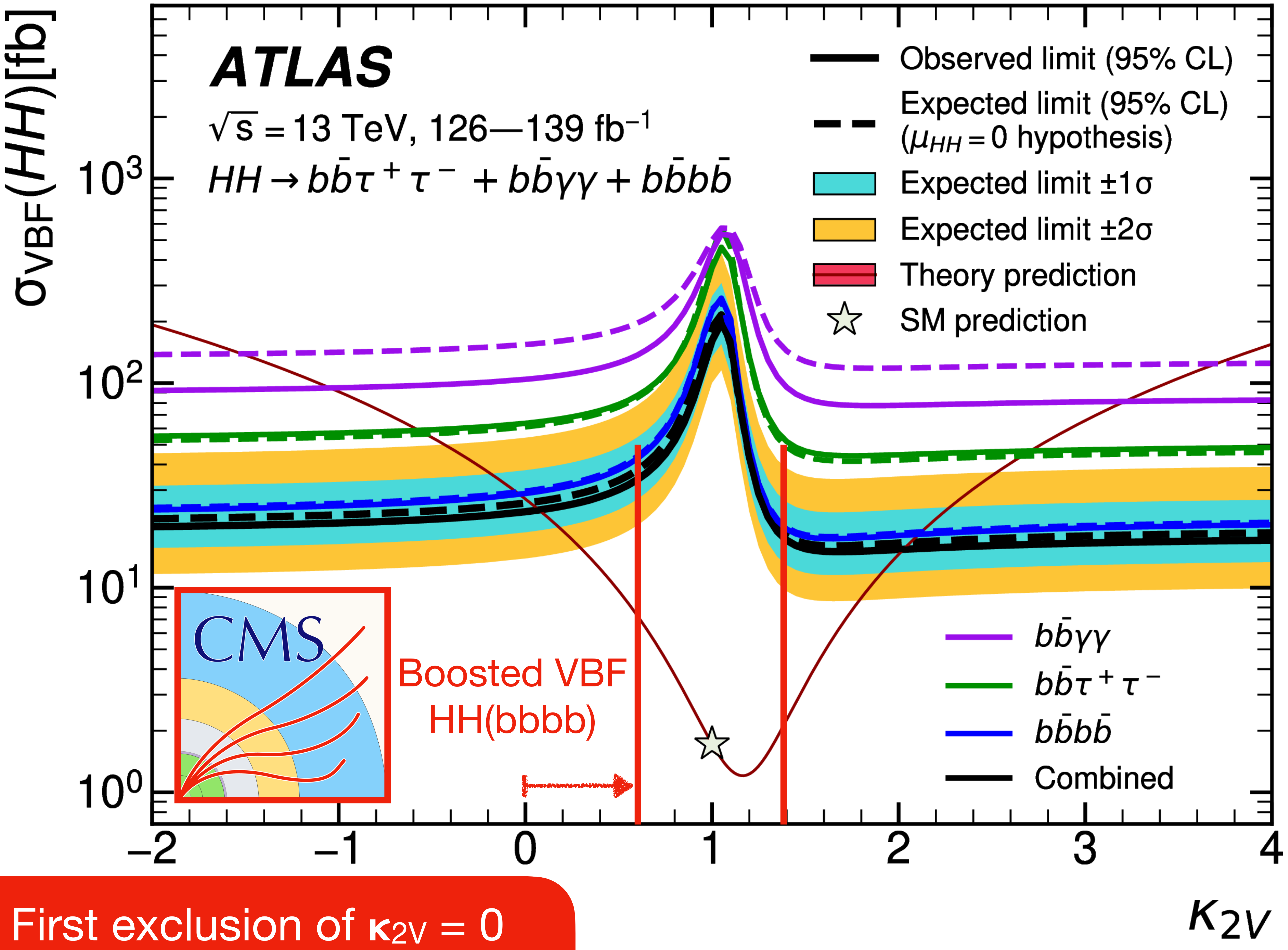

First exclusion of $\kappa_{2V} = 0$

PRL 131 (2023) 041803

Phys. Lett. B 843 (2023) 137745

$bb\tau\tau$ BDT — ggF vs VBF

τ_{had} + τ_{had} trigger

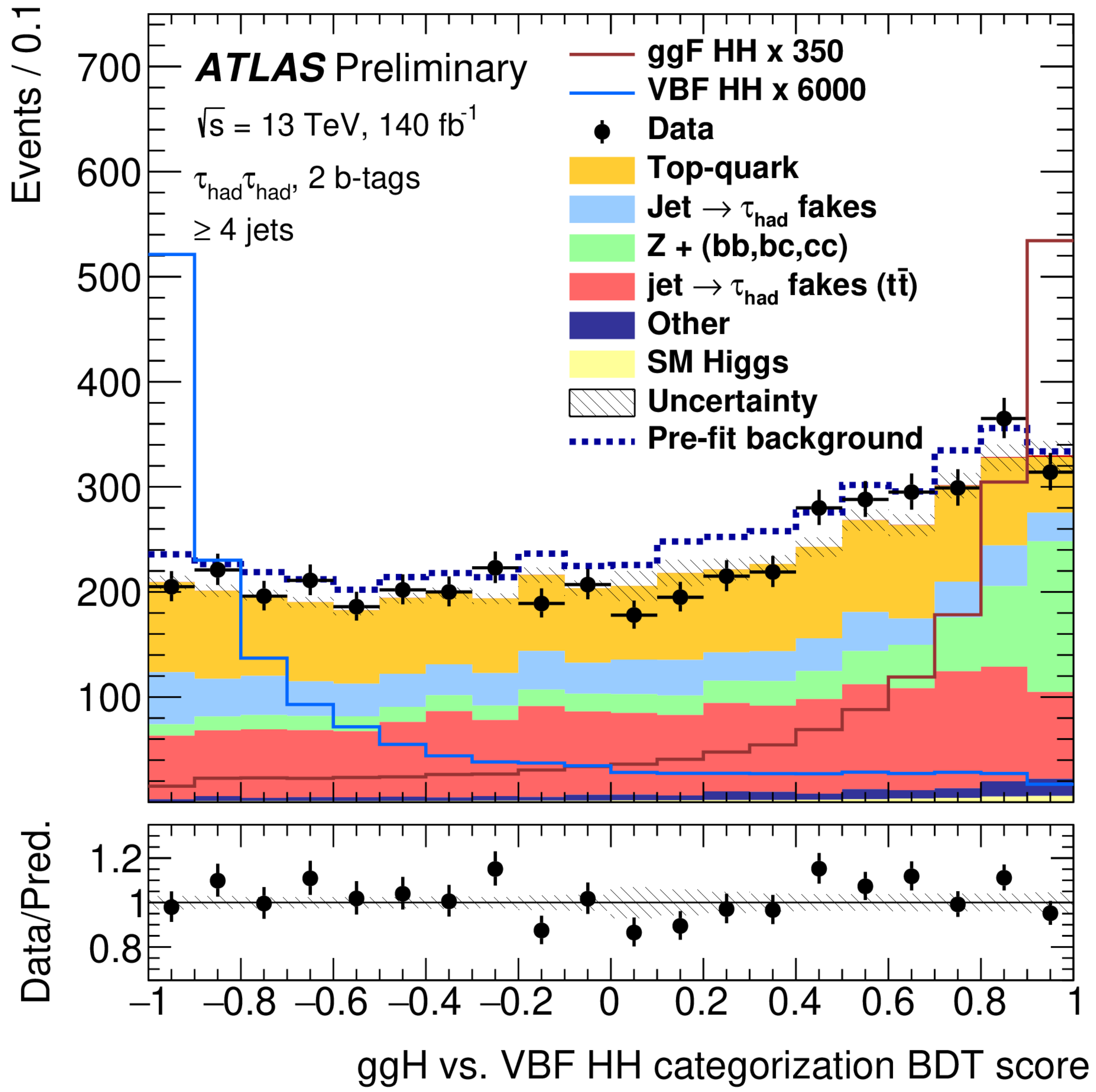

Single lepton trigger

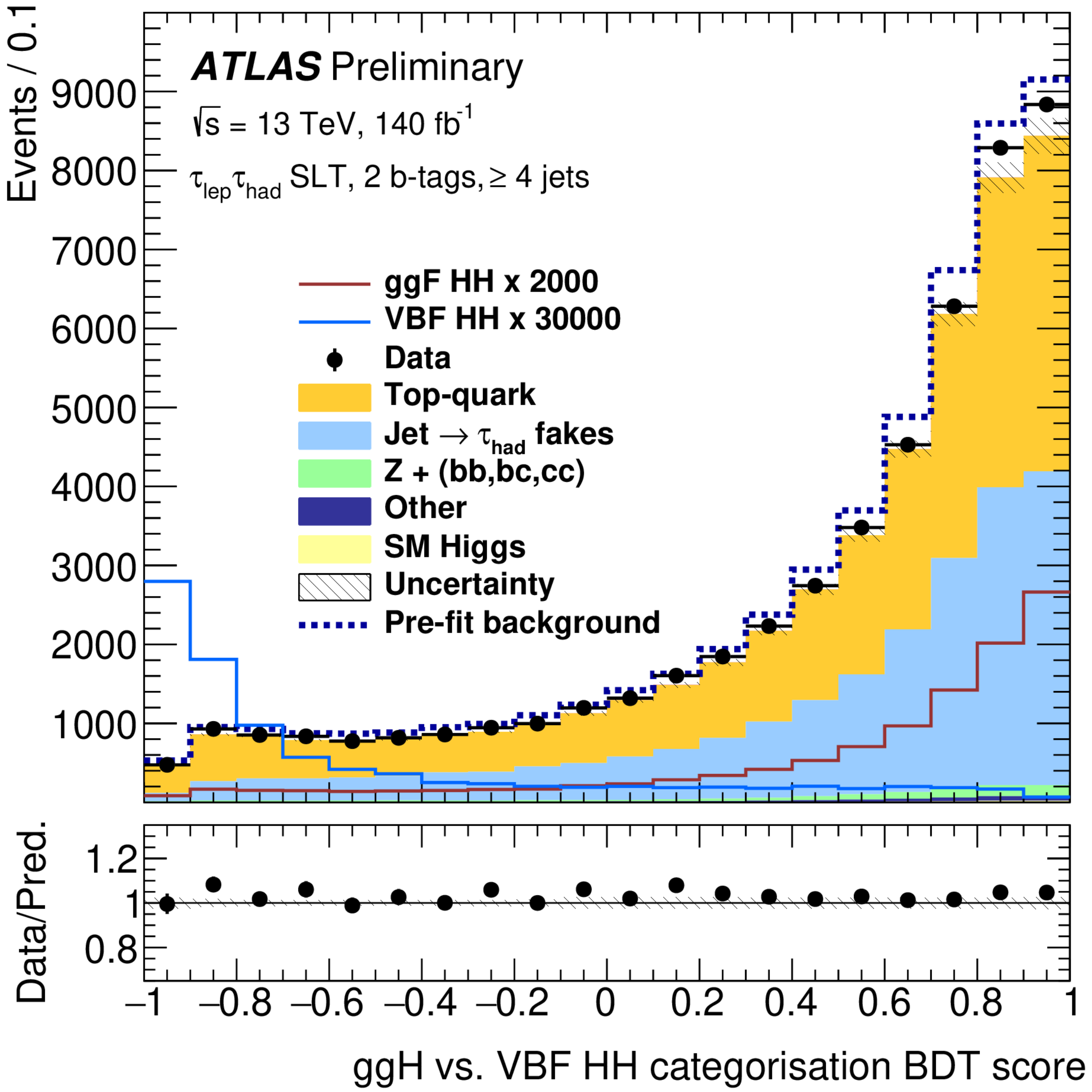

Lepton + τ_{had} trigger

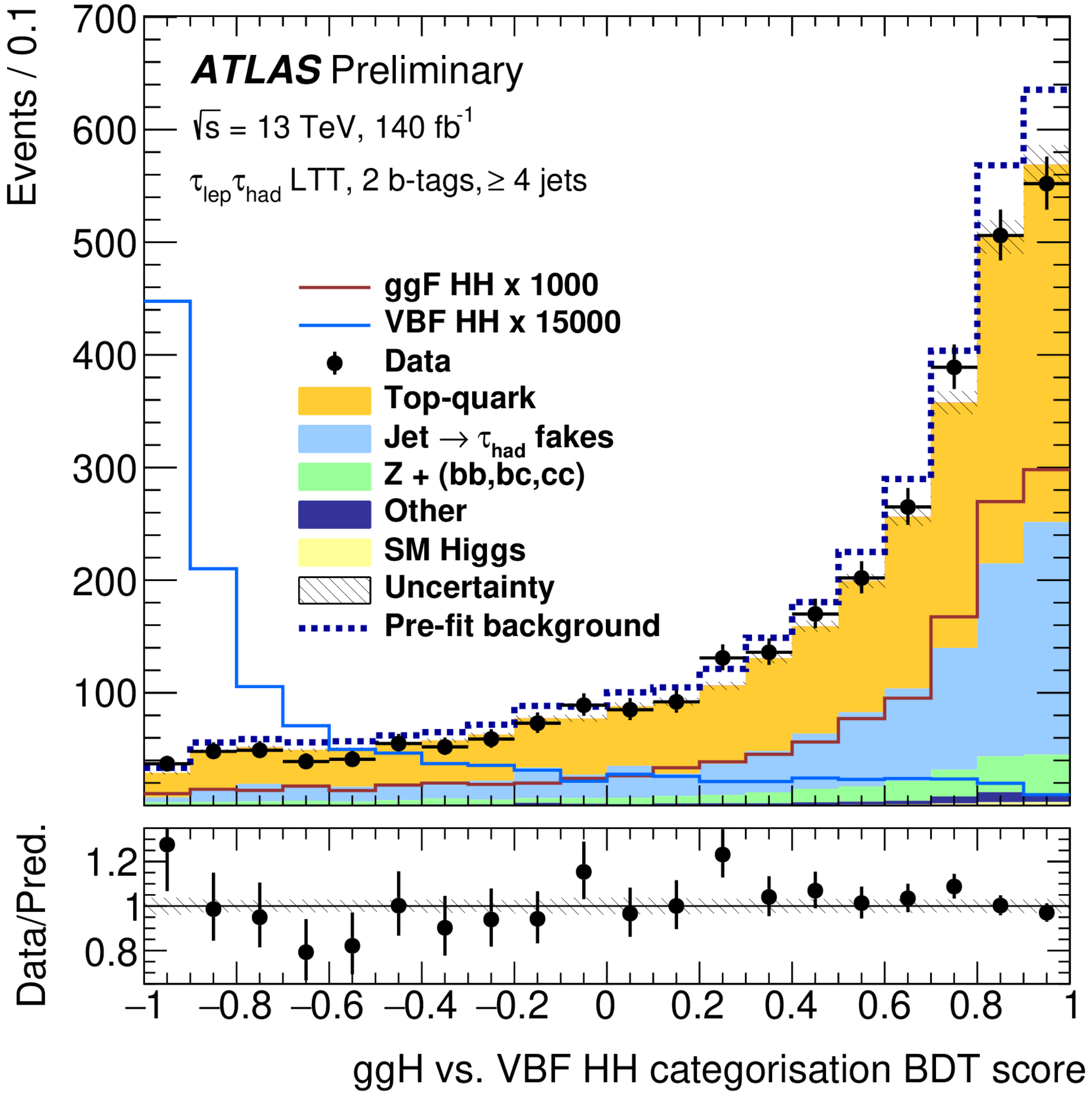

bb$\tau\tau$ BDT (mass bins)

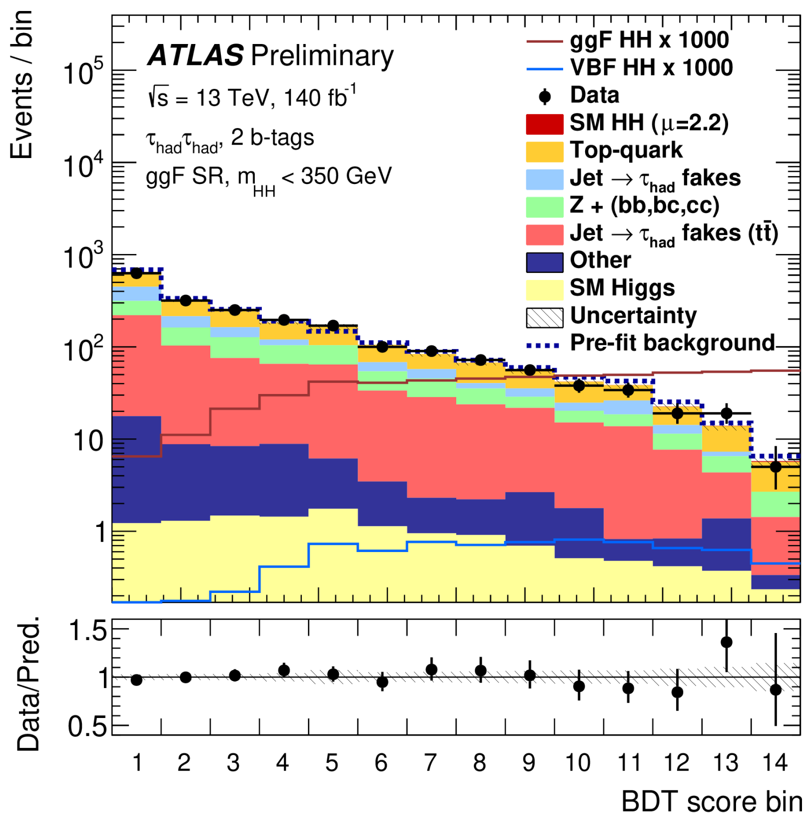

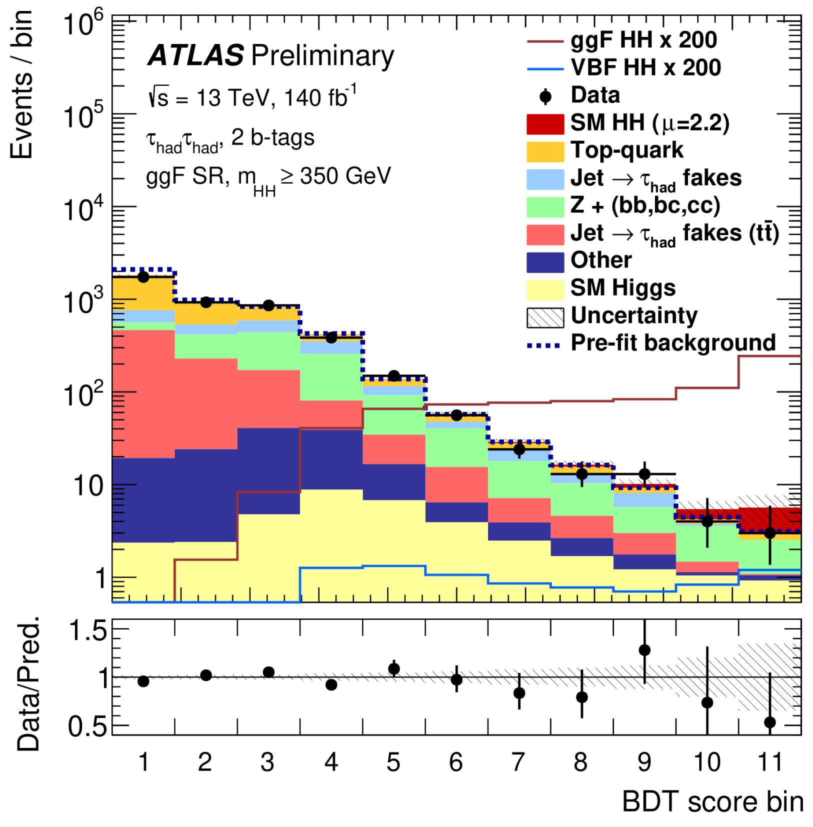

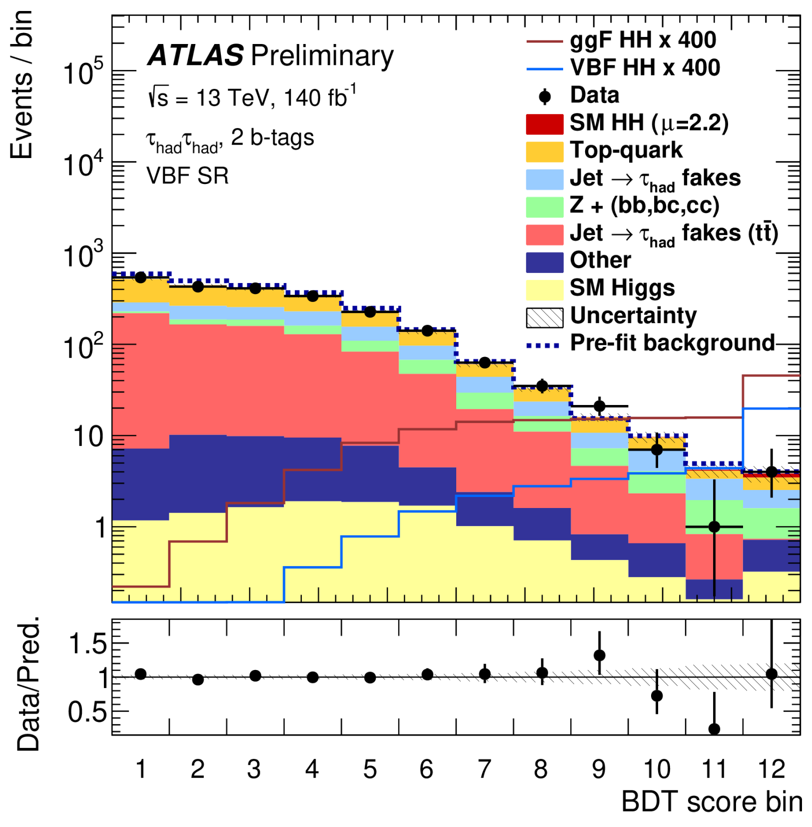

$\tau_{had} + \tau_{had}$ trigger

Single lepton trigger

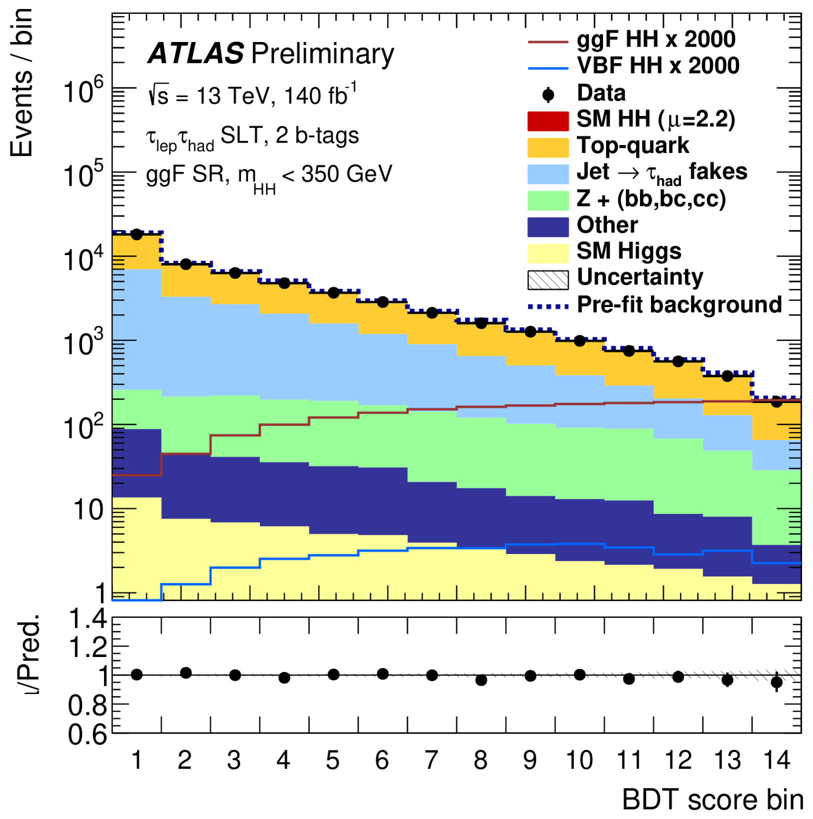

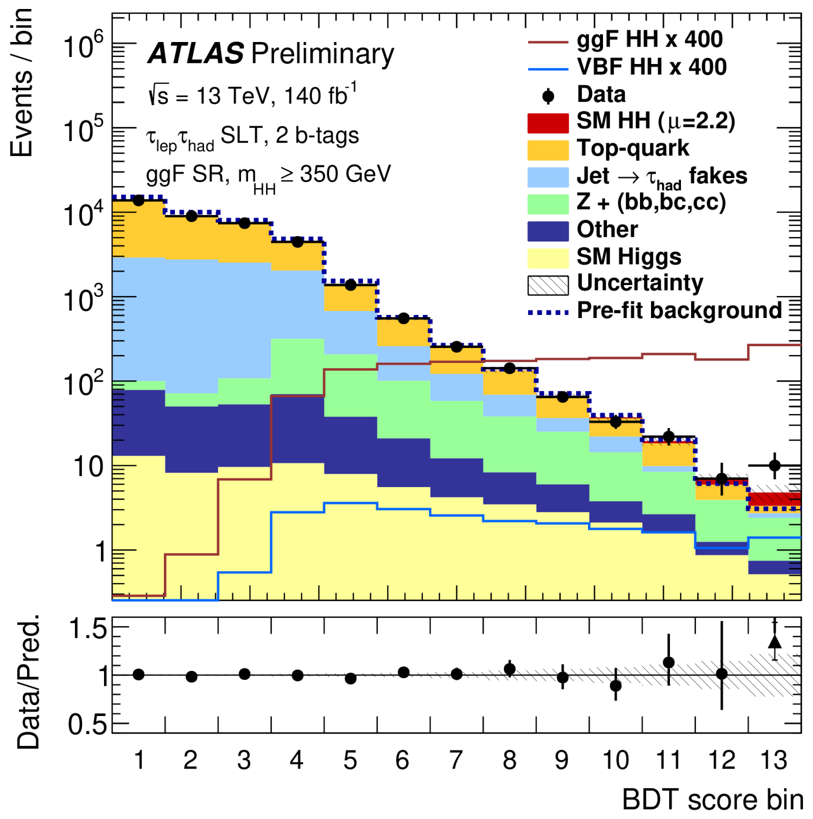

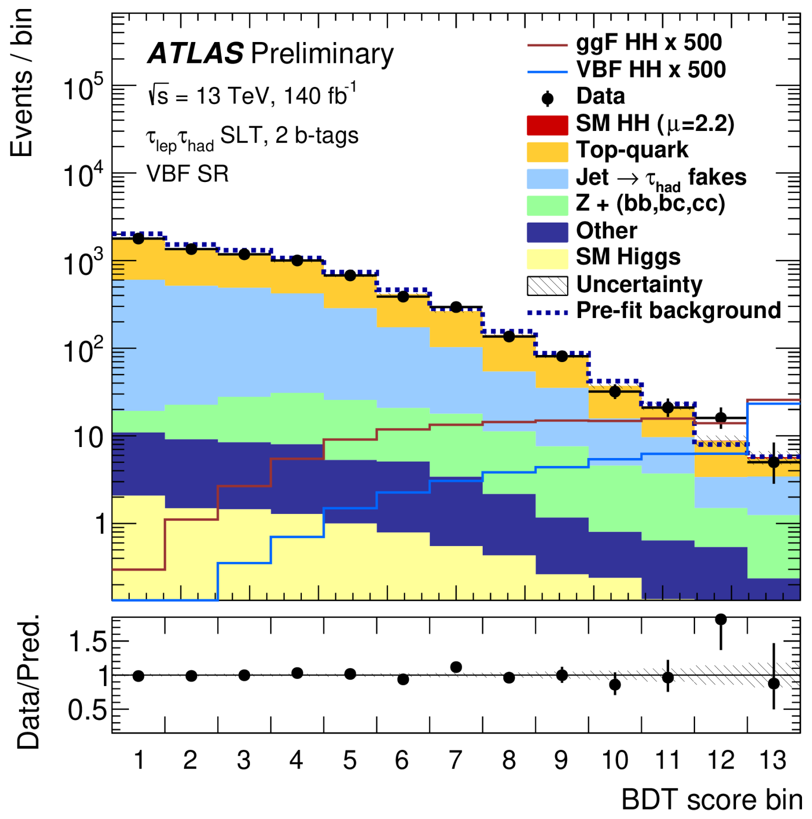

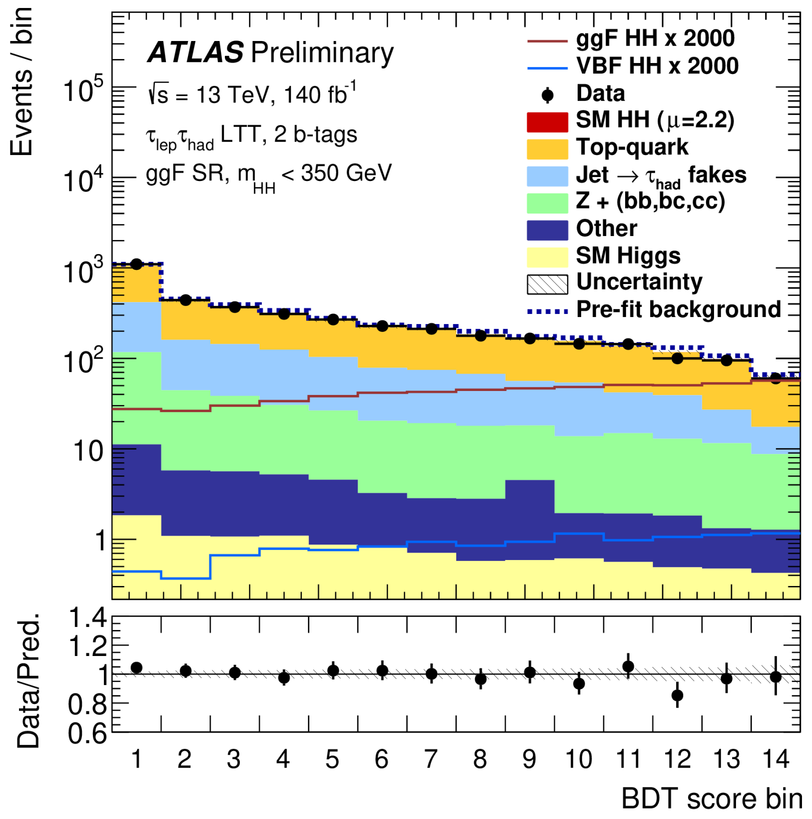

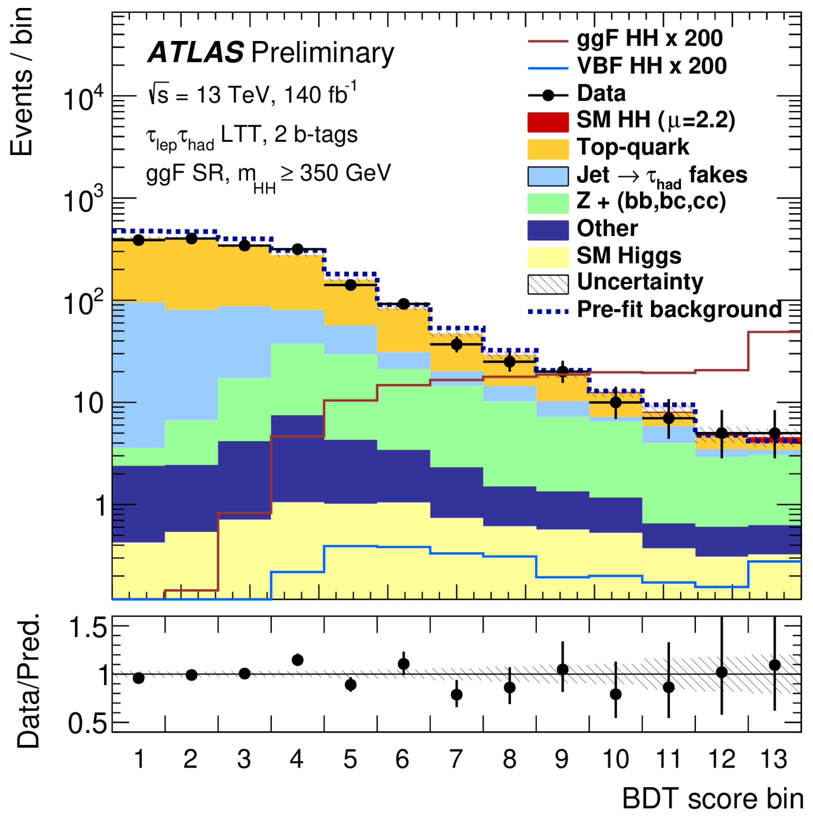

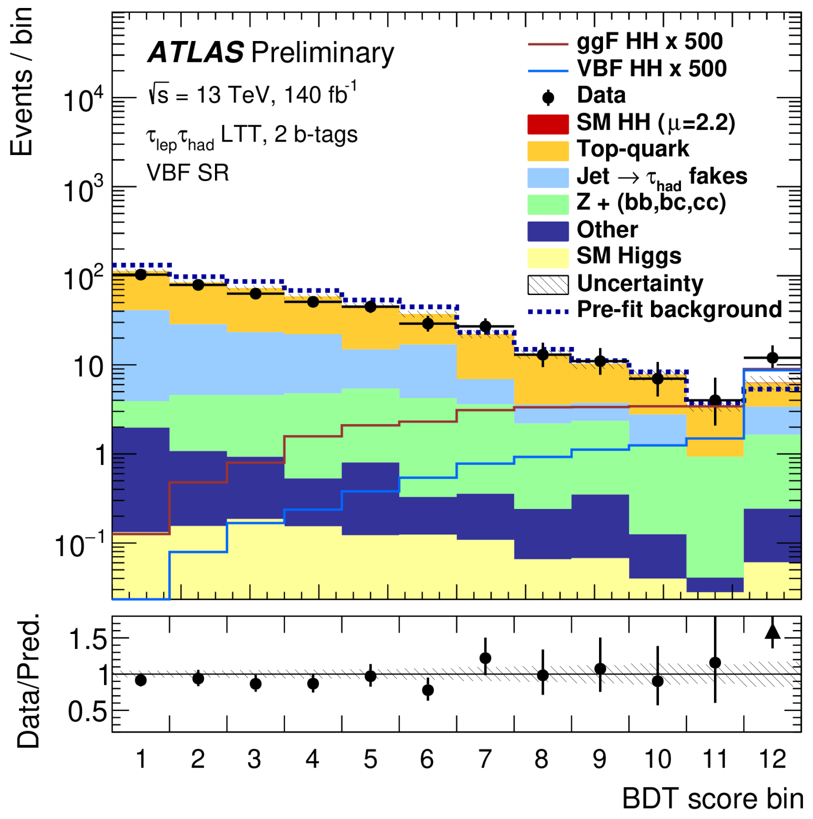

Lepton + τ_{had} trigger

bb$\tau\tau$ kinematic variables

Table 2: Input variables for the categorisation BDTs in each of the three SRs. The superscripts a and c specify the selection of jets that are taken into account for the calculation in addition to the two τ-lepton candidates and $\vec{p}_T^{\text{miss}}$. For variables with a c, only the four-momenta of central jets, i.e. jets with $|\eta| < 2.5$, are included, while an a indicates that all available jets are included.

Variable	$\tau_{\text{had}}\tau_{\text{had}}$	$\tau_{\text{lep}}\tau_{\text{had}}$ SLT	$\tau_{\text{lep}}\tau_{\text{had}}$ LTT
m_{jj}^{VBF}	✓	✓	✓
$\Delta\eta_{jj}^{\text{VBF}}$	✓	✓	✓
VBF $\eta_0 \times \eta_1$	✓	✓	
$\Delta\phi_{jj}^{\text{VBF}}$	✓		
$\Delta R_{jj}^{\text{VBF}}$		✓	✓
$\Delta R_{\tau\tau}$	✓		
m_{HH}	✓		
f_2^a	✓		
C^a		✓	✓
m_{Eff}^a		✓	✓
f_0^c		✓	
f_0^a			✓
h_3^a			✓

bbbb NN reweighing

Normalise 2b to 4b only

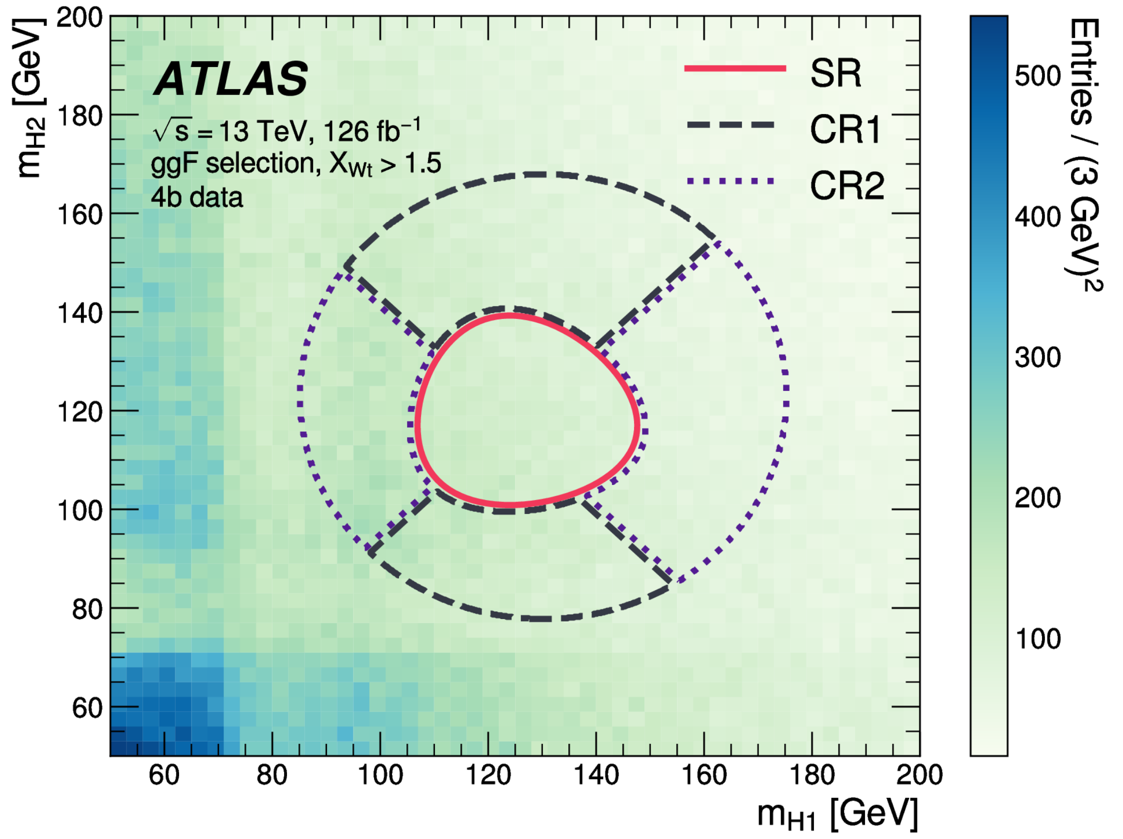

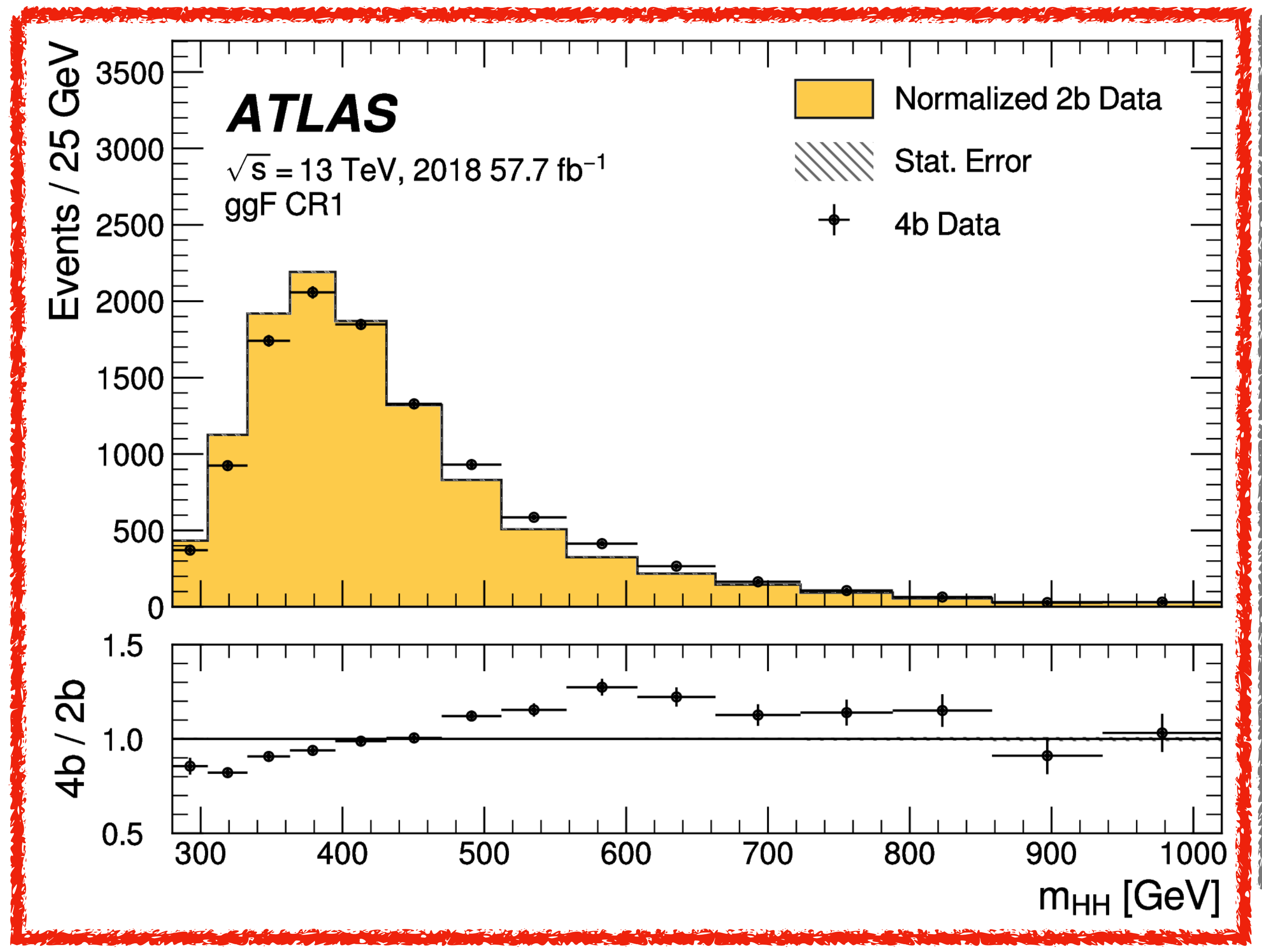

Reweight 2b with NN
+ normalise to 4b

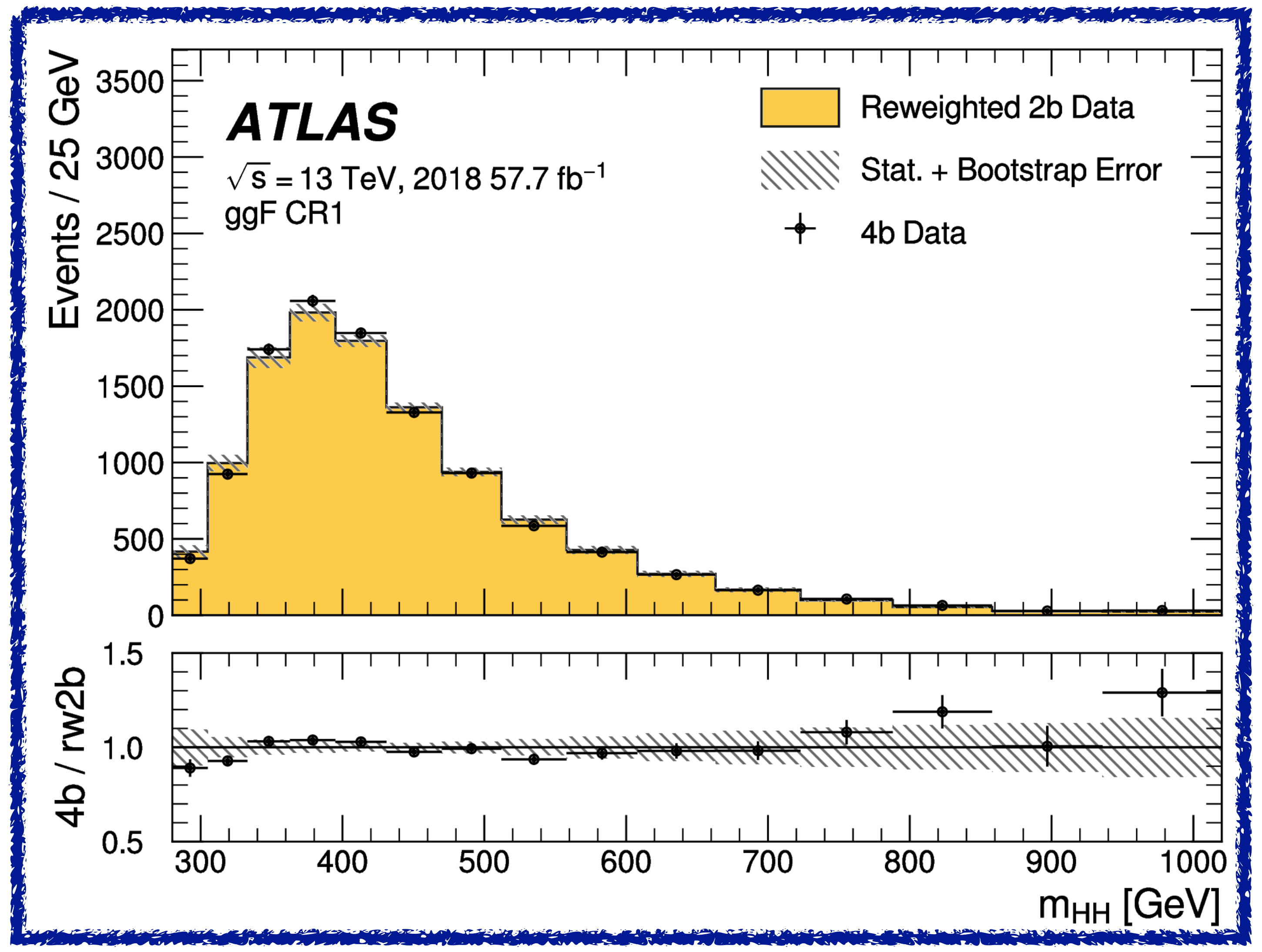

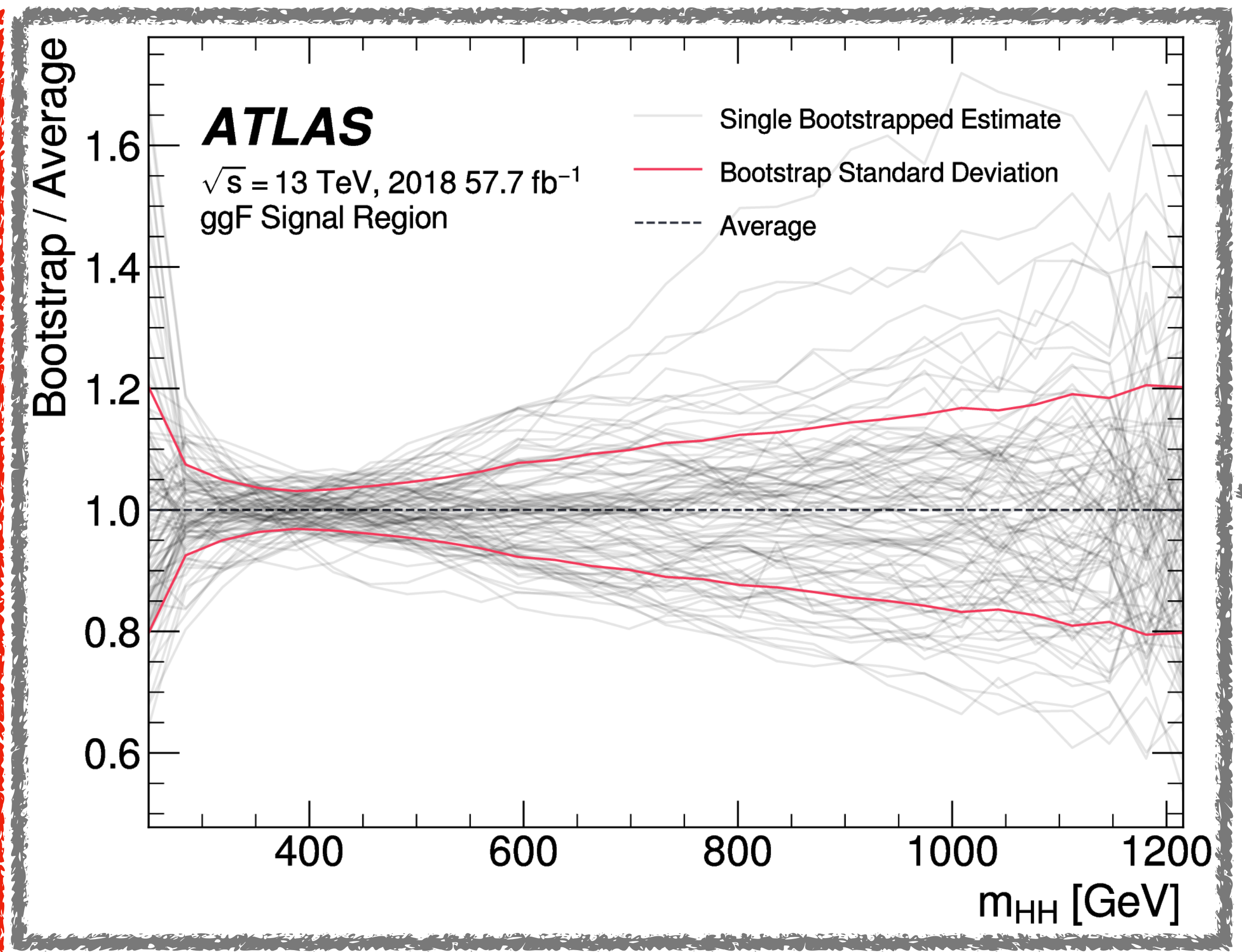

Mean/std deviation from 100 independent NN predictions

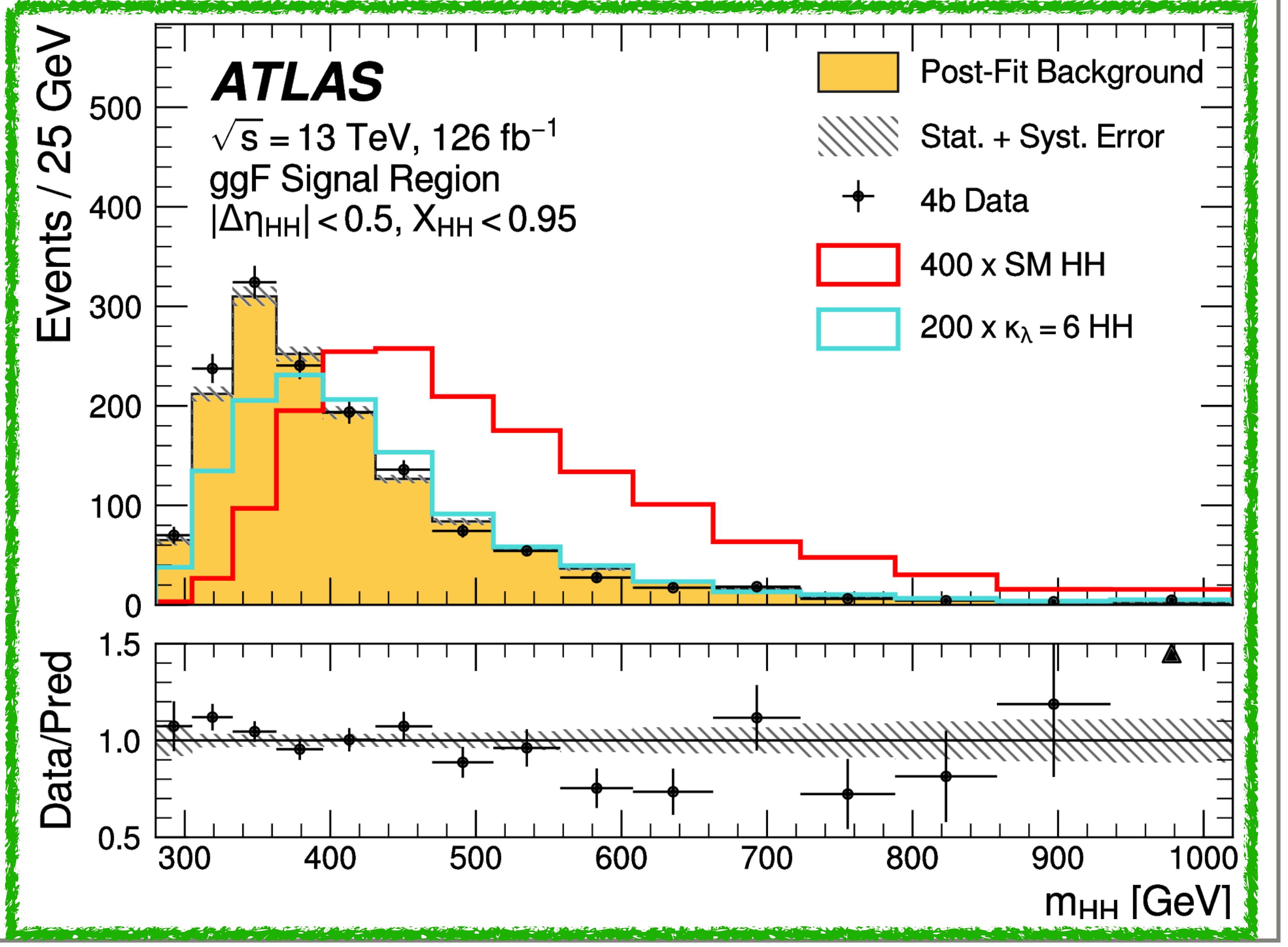

$bb\ell\ell + E_T^{miss}$ uncertainties

Uncertainty in region	Z+HF-CR (VBF)	Z+HF-CR (ggF)	Wt-CR (VBF)	Wt-CR (ggF)	$t\bar{t}$-CR (VBF)	$t\bar{t}$-CR (ggF)
Total Standard Model expectation	7320	88600	900	4940	39600	404000
Total statistical ($\sqrt{N_{exp}}$)	± 90	± 300	± 30	± 70	± 200	± 600
Total Standard Model systematic	$^{+130}_{-150}$	± 900	$^{+31}_{-35}$	$^{+90}_{-100}$	$^{+800}_{-1100}$	$^{+9000}_{-10000}$
Background normalization	$^{+180}_{-230}$	$^{+1200}_{-1600}$	± 60	$^{+180}_{-220}$	$^{+400}_{-1300}$	$^{+3500}_{-13000}$
Background theory	$^{+150}_{-50}$	$^{+1300}_{-500}$	$^{+50}_{-40}$	$^{+170}_{-110}$	$^{+1200}_{-310}$	$^{+12000}_{-3300}$
Experimental	$^{+180}_{-170}$	$^{+1200}_{-1100}$	± 28	± 110	$^{+130}_{-120}$	$^{+400}_{-500}$
Fake extraction	± 1.9	± 16	± 2.1	± 9	± 21	± 180
Signal normalization	$^{+0.05}_{-0.06}$	$^{+0.32}_{-0.35}$	± 0.0016	± 0.008	± 0.005	$^{+0.034}_{-0.04}$
Signal theory	$^{+0.004}_{-0.014}$	$^{+0.024}_{-0.08}$	± 0.00013	± 0.0006	± 0.0004	$^{+0.0026}_{-0.009}$
Template statistics	± 0	± 0	$^{+15}_{-15}$	± 0	± 0	± 0

Dominated in all regions by background & experimental systematics

Uncertainty in region	VBF-SR 5	VBF-SR 4	VBF-SR 3	VBF-SR 2	VBF-SR 1
Total Standard Model expectation	3430	920	123	8.8	1.3
Total statistical ($\sqrt{N_{exp}}$)	± 60	± 30	± 11	± 3.0	± 1.2
Total Standard Model systematic	± 120	$^{+40}_{-50}$	$^{+11}_{-13}$	± 1.7	$^{+0.5}_{-0.6}$
Background normalization	$^{+40}_{-100}$	$^{+11}_{-26}$	$^{+2.3}_{-3.3}$	$^{+0.20}_{-0.24}$	$^{+0.09}_{-0.10}$
Background theory	$^{+230}_{-170}$	$^{+90}_{-80}$	$^{+18}_{-15}$	$^{+0.9}_{-1.0}$	$^{+0.28}_{-0.4}$
Experimental	$^{+170}_{-190}$	$^{+70}_{-80}$	$^{+16}_{-18}$	± 1.4	$^{+0.30}_{-0.5}$
Fake extraction	± 2.4	± 0.7	± 0.08	± 0.04	± 0
Signal normalization	$^{+3.1}_{-3.4}$	$^{+2.9}_{-3.2}$	$^{+1.8}_{-1.9}$	$^{+0.6}_{-0.7}$	± 0.4
Signal theory	± 0.07	± 0.06	± 0.04	± 0.014	± 0.009
Template statistics	± 0	± 10	± 5	$^{+1.5}_{-1.3}$	$^{+0.26}_{-0.23}$

Uncertainty in region	ggF-SR 7	ggF-SR 6	ggF-SR 5	ggF-SR 4	ggF-SR 3	ggF-SR 2	ggF-SR 1
Total Standard Model expectation	550	363	209	123	60	39	15
Total statistical ($\sqrt{N_{exp}}$)	± 23	± 19	± 14	± 11	± 8	± 6	± 4
Total Standard Model systematic	$^{+28}_{-29}$	$^{+19}_{-18}$	$^{+13}_{-14}$	$^{+10}_{-12}$	± 6	± 5	± 4
Background normalization	$^{+6}_{-11}$	$^{+5}_{-8}$	$^{+3.5}_{-5}$	$^{+2.6}_{-3.2}$	$^{+1.5}_{-1.8}$	$^{+1.1}_{-1.3}$	$^{+0.5}_{-0.6}$
Background theory	$^{+40}_{-35}$	$^{+32}_{-27}$	± 21	$^{+19}_{-20}$	± 11	± 7	± 6
Experimental	$^{+40}_{-33}$	$^{+27}_{-19}$	$^{+13}_{-17}$	± 9	$^{+5}_{-6}$	± 4	± 1.8
Fake extraction	± 0.7	± 0.5	± 0.4	± 0.29	± 0.11	± 0.11	± 0.29
Signal normalization	$^{+5}_{-6}$	± 6	± 6	± 7	± 6	± 6	$^{+7}_{-8}$
Signal theory	$^{+0.4}_{-1.3}$	$^{+0.4}_{-1.5}$	$^{+0.5}_{-1.5}$	$^{+0.5}_{-1.8}$	$^{+0.5}_{-1.5}$	$^{+0.4}_{-1.5}$	$^{+0.6}_{-1.9}$
Template statistics	± 11	± 10	± 8	± 5	$^{+4}_{-4}$	$^{+4}_{-3.5}$	$^{+2.3}_{-2.1}$

$bb\ell\ell + E_{\mathrm{T}}^{\mathrm{miss}}$ MVA inputs

Input feature	Description
same flavour	unity if final state leptons are ee or $\mu\mu$, zero otherwise
p_{T}^{ℓ}, p_{T}^{b}	transverse momenta of the leptons, b-tagged jets
$m_{\ell\ell}$, $p_{\mathrm{T}}^{\ell\ell}$	invariant mass and the transverse momentum of the di-lepton system
m_{bb}, p_{T}^{bb}	invariant mass and the transverse momentum of the b-tagged jet pair system
m_{T2}^{bb}	stransverse mass of the two b-tagged jets
$\Delta R_{\ell\ell}$, ΔR_{bb}	ΔR between the two leptons and two b-tagged jets
$m_{b\ell}$	$\min\{\max(m_{b_0\ell_0}, m_{b_1\ell_1}), \max(m_{b_0\ell_1}, m_{b_1\ell_0})\}$
$\min \Delta R_{b\ell}$	minimum ΔR of all b-tagged jet and lepton combinations
$m_{bb\ell\ell}$	invariant mass of the $bb\ell\ell$ system
$E_{\mathrm{T}}^{\mathrm{miss}}$, $E_{\mathrm{T}}^{\mathrm{miss}}$-sig	missing transverse energy and its significance
$m_{\mathrm{T}}(\ell_0, E_{\mathrm{T}}^{\mathrm{miss}})$	transverse mass of the p_{T}-leading lepton with respect to $E_{\mathrm{T}}^{\mathrm{miss}}$
$\min m_{\mathrm{T},\ell}$	minimum value of $m_{\mathrm{T}}(\ell_0, E_{\mathrm{T}}^{\mathrm{miss}})$ and $m_{\mathrm{T}}(\ell_1, E_{\mathrm{T}}^{\mathrm{miss}})$
$H_{\mathrm{T2}}^{\mathrm{R}}$	measure for boostedness[1] of the two Higgs bosons

DNN (ggF)

Input feature	Description
η_{ℓ_0}, η_{ℓ_1}, ϕ_{ℓ_0}, ϕ_{ℓ_1}, $p_{\mathrm{T}}^{\ell_0}$, $p_{\mathrm{T}}^{\ell_1}$	η, ϕ, p_{T} of the p_{T}-(sub)leading lepton
η_{b_0}, η_{b_1}, ϕ_{b_0}, ϕ_{b_1}, $p_{\mathrm{T}}^{b_0}$, $p_{\mathrm{T}}^{b_1}$	η, ϕ, p_{T} of the p_{T}-(sub)leading b-tagged jet
η_{j_0}, η_{j_1}, ϕ_{j_0}, ϕ_{j_1}, $p_{\mathrm{T}}^{j_0}$, $p_{\mathrm{T}}^{j_1}$	ϕ, η, p_{T} of the p_{T}-(sub)leading non b-tagged jet
$E_{\mathrm{T}}^{\mathrm{miss}}$, $\phi^{E_{\mathrm{T}}^{\mathrm{miss}}}$, $E_{\mathrm{T}}^{\mathrm{miss}}$-sig	missing transverse energy, its ϕ and significance
p_{T}^{bb}, ΔR_{bb}, $\Delta\phi_{bb}$, m_{bb}	p_{T}, ΔR, $\Delta\phi$ and invariant mass of di-b-jet system
$p_{\mathrm{T}}^{\ell\ell}$, $\Delta R_{\ell\ell}$, $\Delta\phi_{\ell\ell}$, $m_{\ell\ell}$, $\phi_{\mathrm{centrality}}^{\ell\ell}$	p_{T}, ΔR, $\Delta\phi$, p_{T} and centrality[1] of di-leptons system
$p_{\mathrm{T}}^{bb\ell\ell}$, $m_{bb\ell\ell}$	p_{T} and invariant mass of the $bb\ell\ell$ system
$p_{\mathrm{T}}^{bb\ell\ell+E_{\mathrm{T}}^{\mathrm{miss}}}$, $m_{bb\ell\ell+E_{\mathrm{T}}^{\mathrm{miss}}}$	p_{T} and invariant mass of $bb\ell\ell + E_{\mathrm{T}}^{\mathrm{miss}}$ system
$m_{\ell\ell+E_{\mathrm{T}}^{\mathrm{miss}}}$	invariant mass of di-lepton + $E_{\mathrm{T}}^{\mathrm{miss}}$ system
$p_{\mathrm{T}}^{E_{\mathrm{T}}^{\mathrm{miss}}+\ell\ell}$, $\Delta\phi_{E_{\mathrm{T}}^{\mathrm{miss}},\ell\ell}$	p_{T} of and $\Delta\phi$ between $E_{\mathrm{T}}^{\mathrm{miss}}$ and di-lepton system
$p_{\mathrm{T}}^{\mathrm{tot}}$	p_{T} of $bb\ell\ell + E_{\mathrm{T}}^{\mathrm{miss}} + p_{\mathrm{T}}$-leading and -sub-leading jet
m_{tot}	invariant mass of $bb\ell\ell + E_{\mathrm{T}}^{\mathrm{miss}} + p_{\mathrm{T}}$-leading and -sub-leading jet
m_t^{KLF}	Kalman fitter top-quark mass
$\min \Delta R_{\ell_0 j}$, $\min \Delta R_{\ell_1 j}$	minimum ΔR between p_{T}-(sub)leading ℓ-j couples
$\sum m_{\ell j}$	sum of the invariant masses of all ℓ+jet combinations
$\max p_{\mathrm{T}}^{jj}$, $\max m_{jj}$	maximum p_{T} and invariant mass of any two non b-tagged jets
$\max \Delta\eta_{jj}$, $\max \Delta\phi_{jj}$	maximum $\Delta\eta$ and $\Delta\phi$ between any two non b-tagged jets
$\min \Delta R_{b\ell}$	minimum ΔR of all b-tagged jet and lepton combinations
$N_{\text{forward jets}}$, N_j	number of forward jets, number of non b-tagged jets
m_{T2}^{bb}	stransverse mass of the two b-tagged jets
m_{coll}	collinear mass (reconstruction of $m_{\tau\tau}$)
m_{MMC}	value of the MMC algorithm (reconstruction of $m_{\tau\tau}$)

BDT (VBF)

bb$\ell\ell$ + E_T^{miss} MVA scores

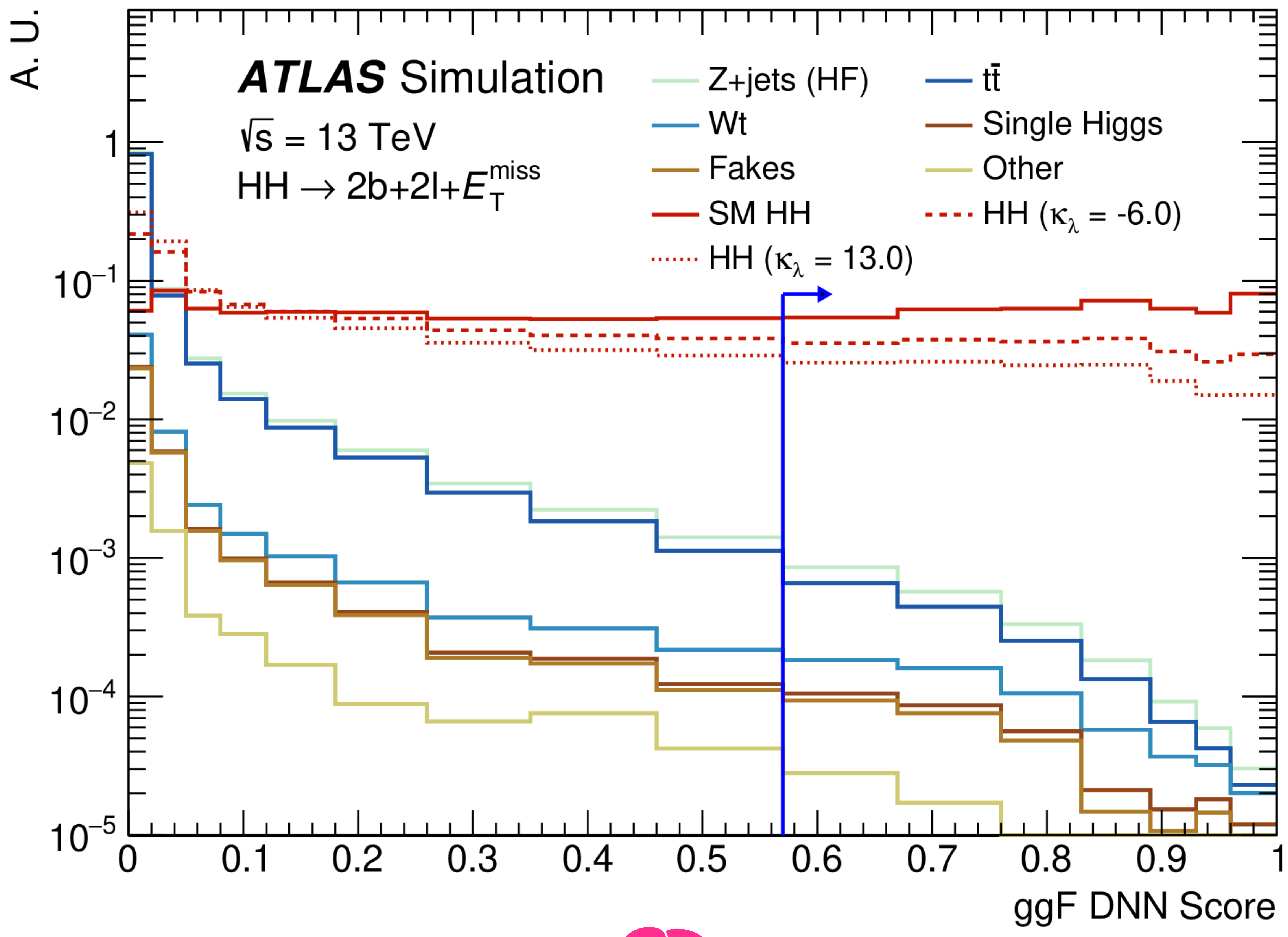

DNN
(ggF)

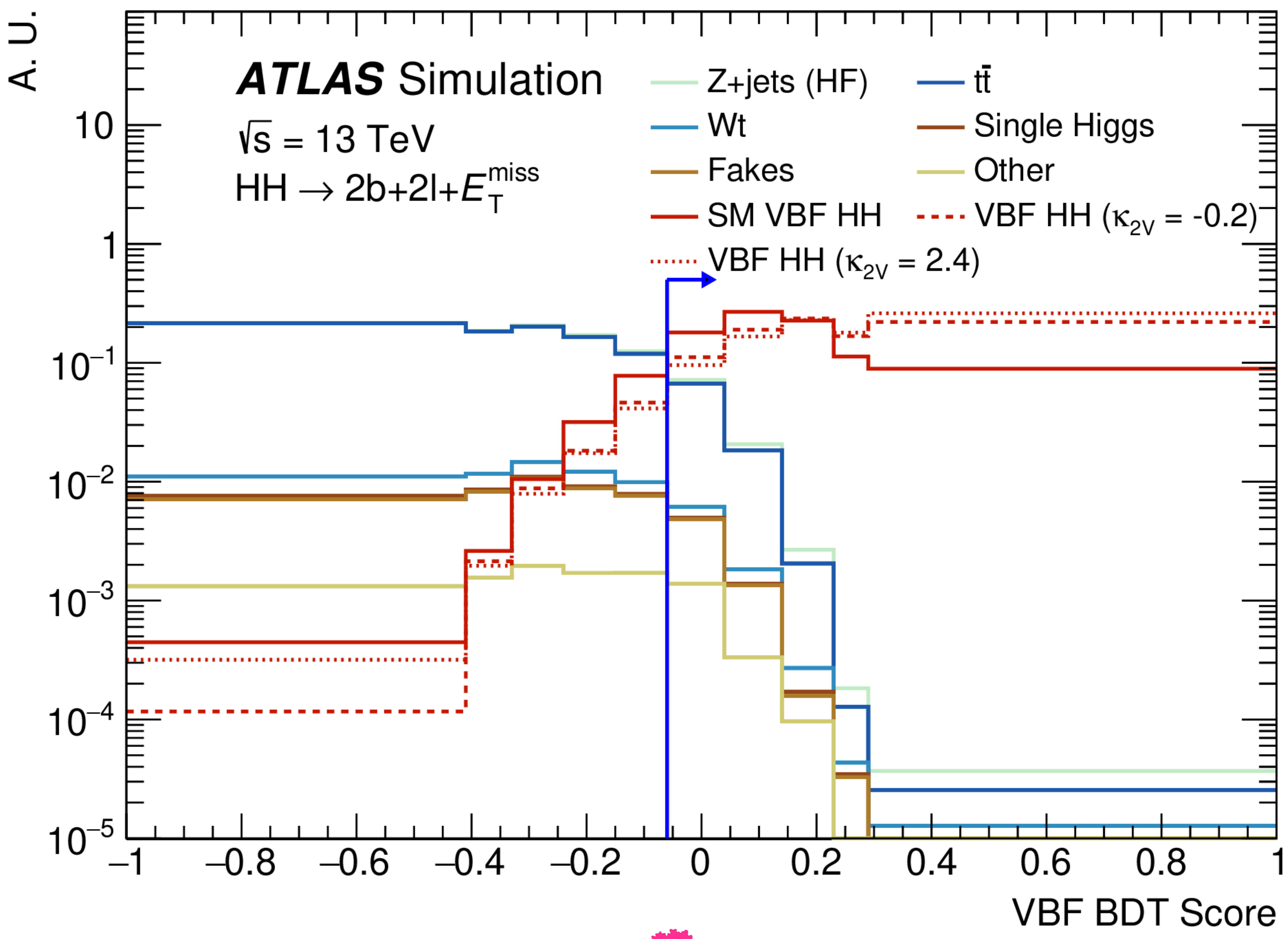

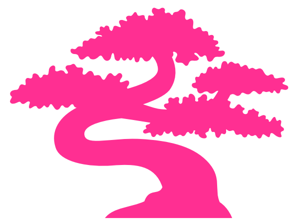

BDT
(VBF)

$bb\tau\tau$ additional limit plots

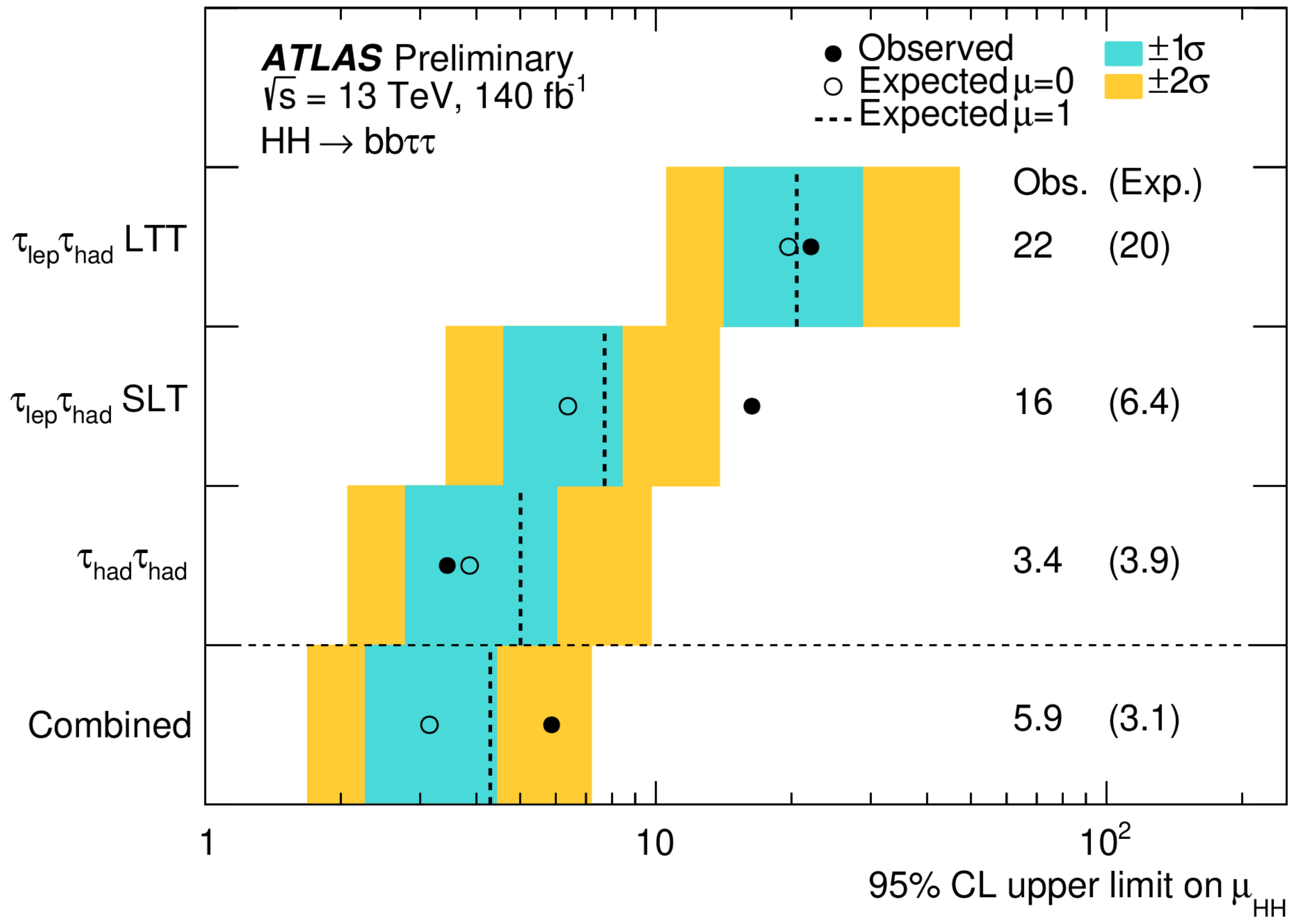

		μ_{HH}	μ_{ggF}	μ_{VBF}	μ_{ggF} (μ_{VBF}=1)	μ_{VBF} (μ_{ggF}=1)
$\tau_{had}\tau_{had}$	observed	3.4	3.6	87	3.5	80
	expected	3.9	4.0	103	3.9	101
$\tau_{lep}\tau_{had}$ SLT	observed	16.4	16.9	133	16.7	155
	expected	6.4	6.6	128	6.5	125
$\tau_{lep}\tau_{had}$ LTT	observed	22	18	767	21	731
	expected	20	21	323	20	317
Combined	observed	5.9	5.8	91	5.9	94
	expected	$3.1^{+1.3}_{-0.9}$	$3.2^{1.7}_{0.9}$	72^{+32}_{-20}	$3.2^{+1.7}_{-0.9}$	71^{+31}_{-20}

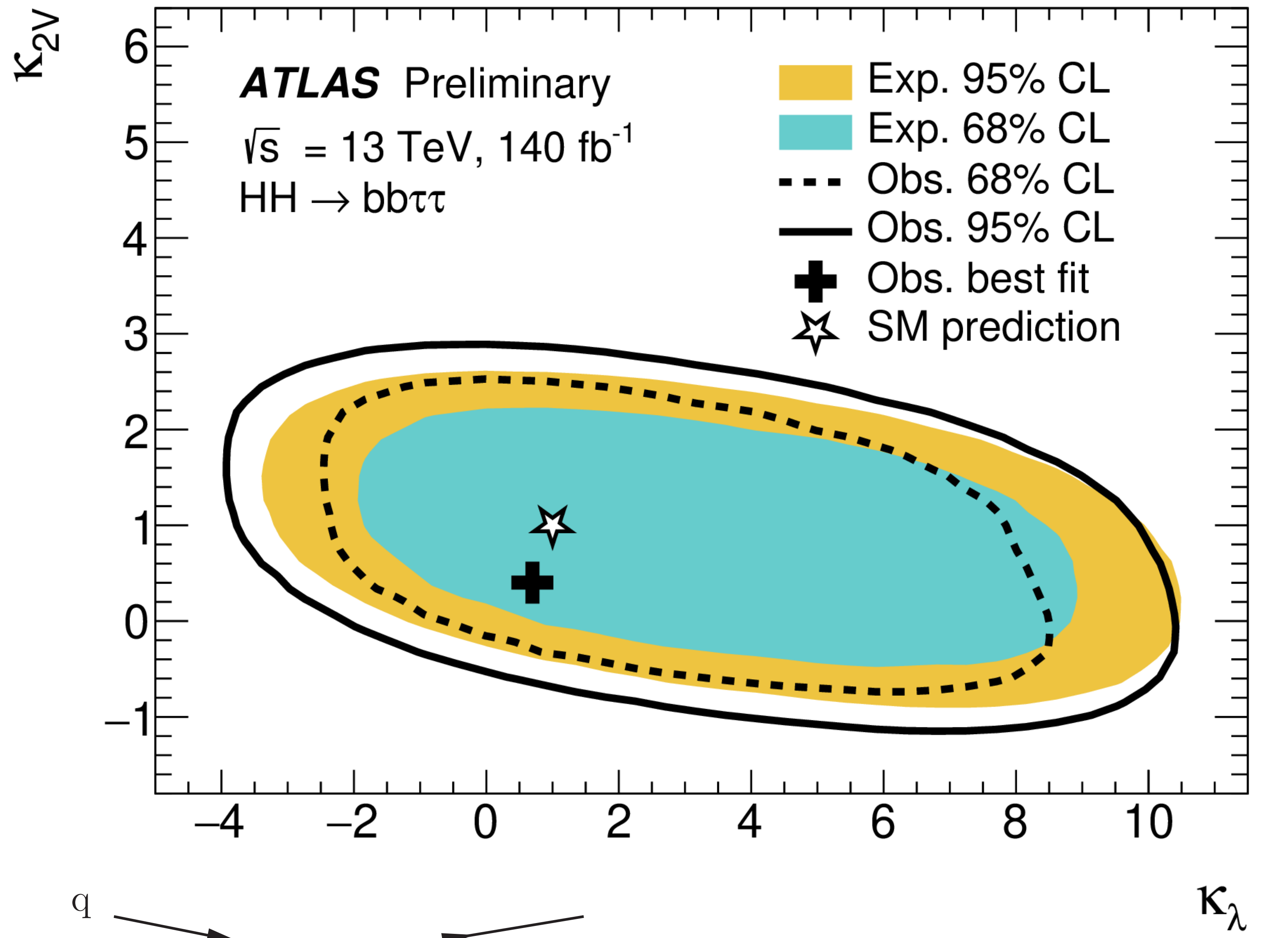

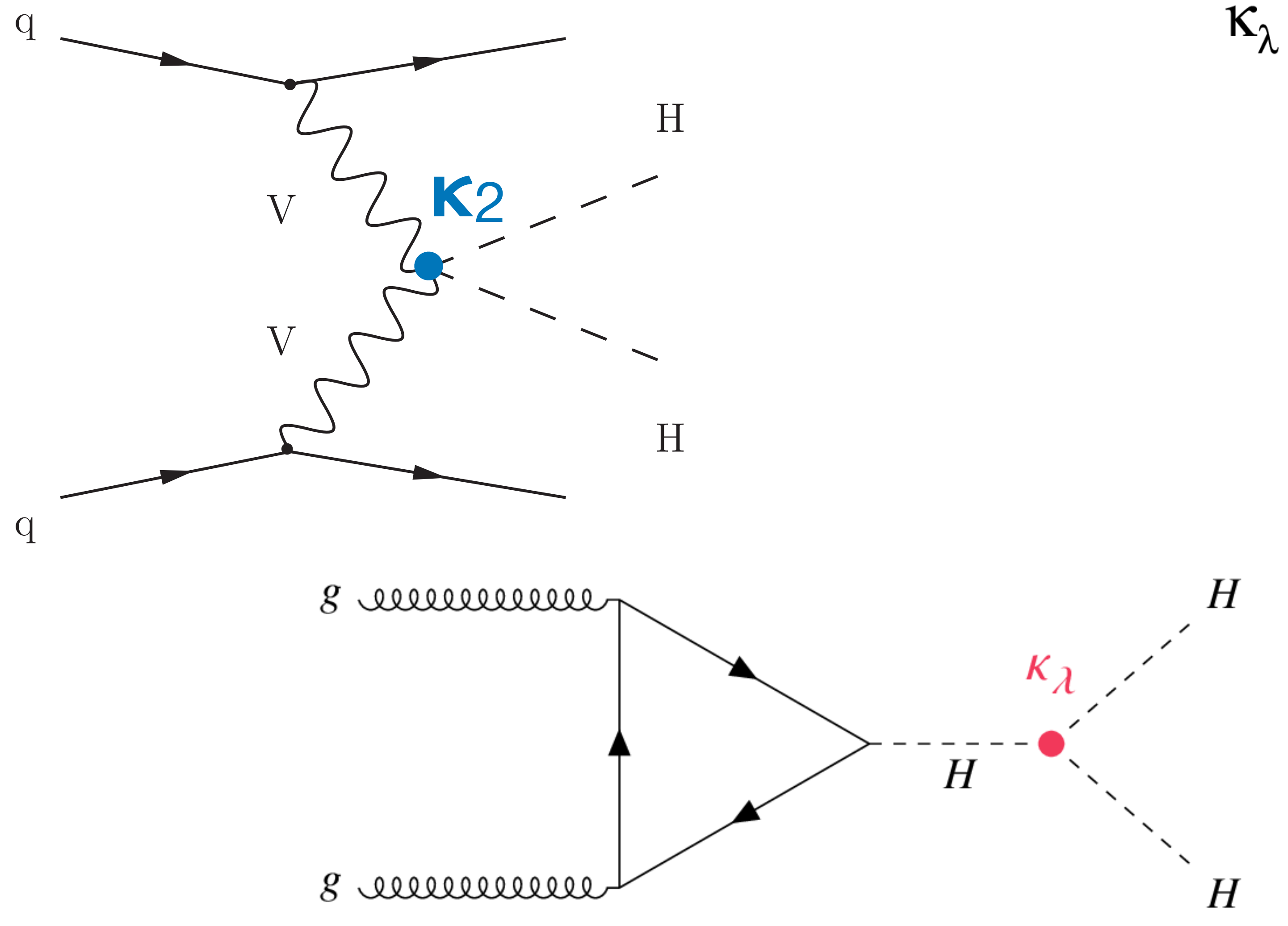

HEFT

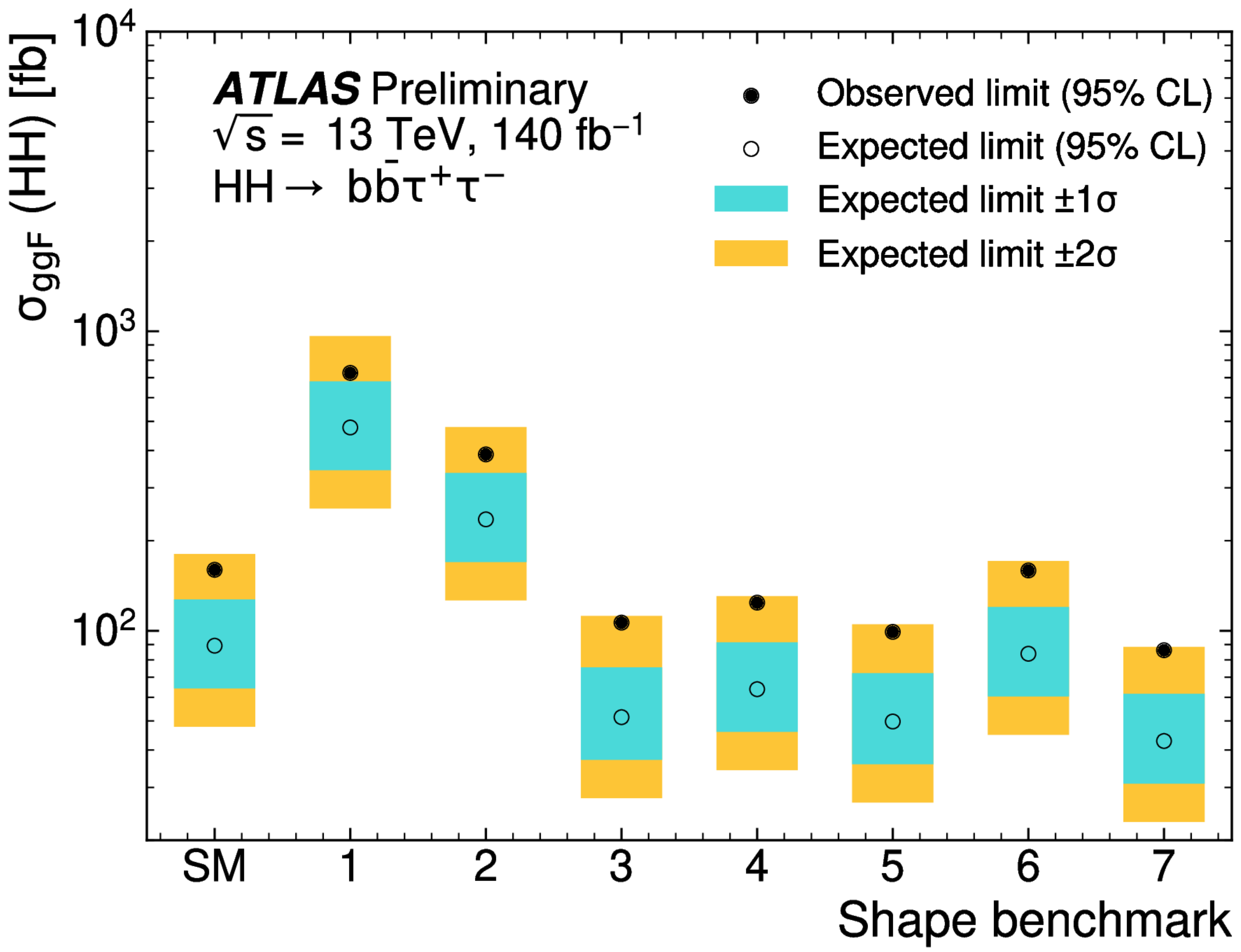

bbγγ additional limit plots

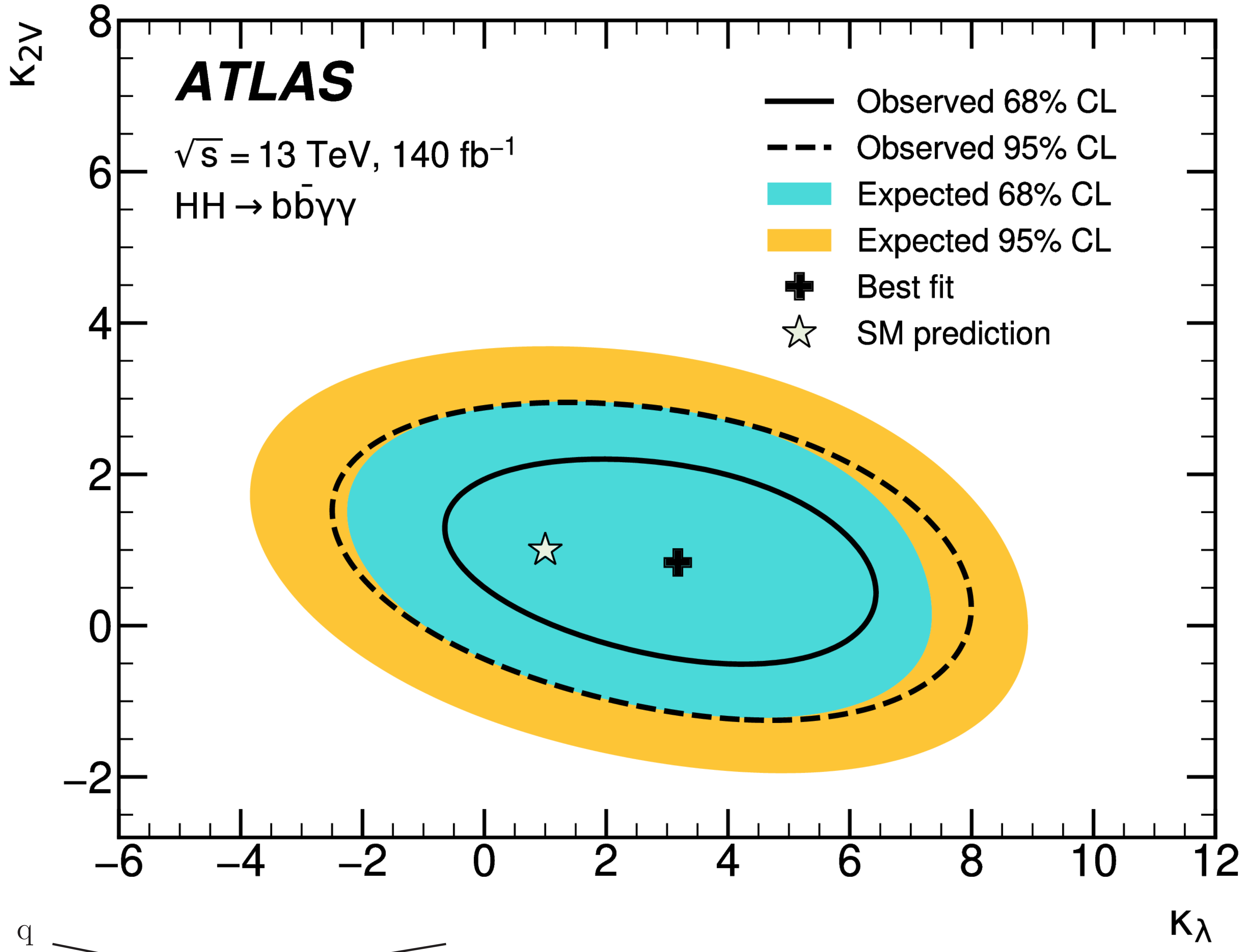

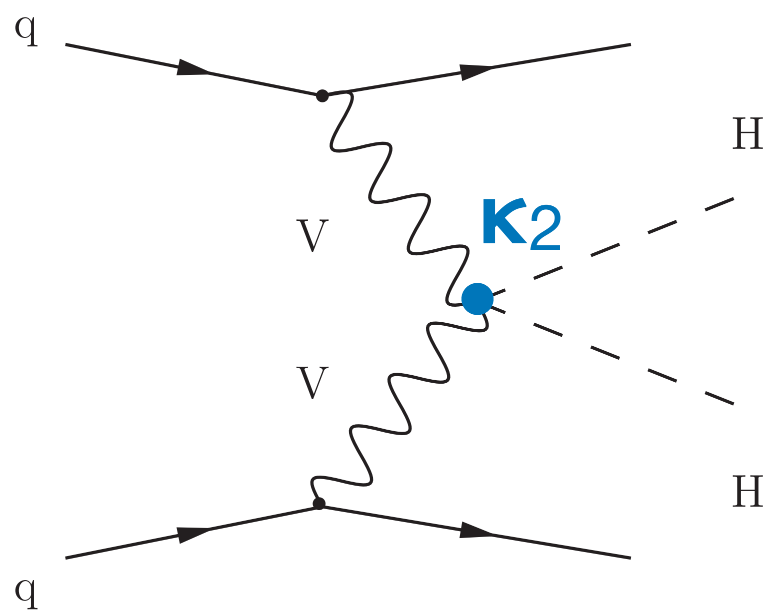

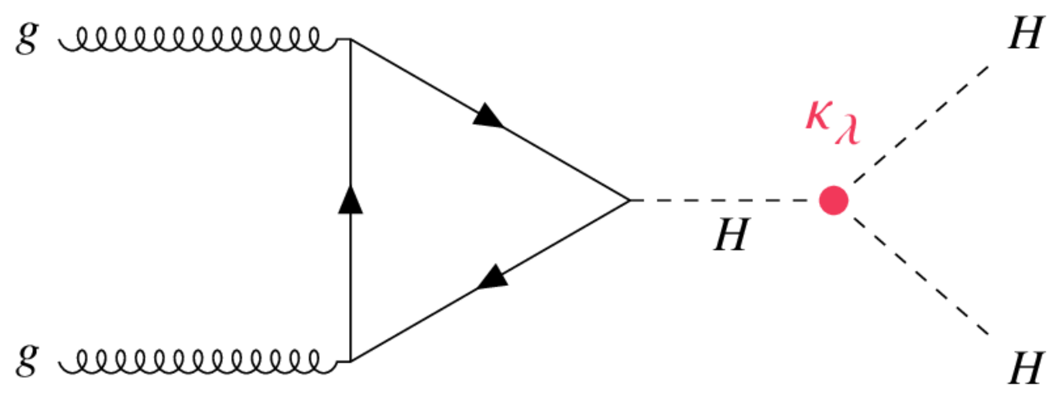

HEFT

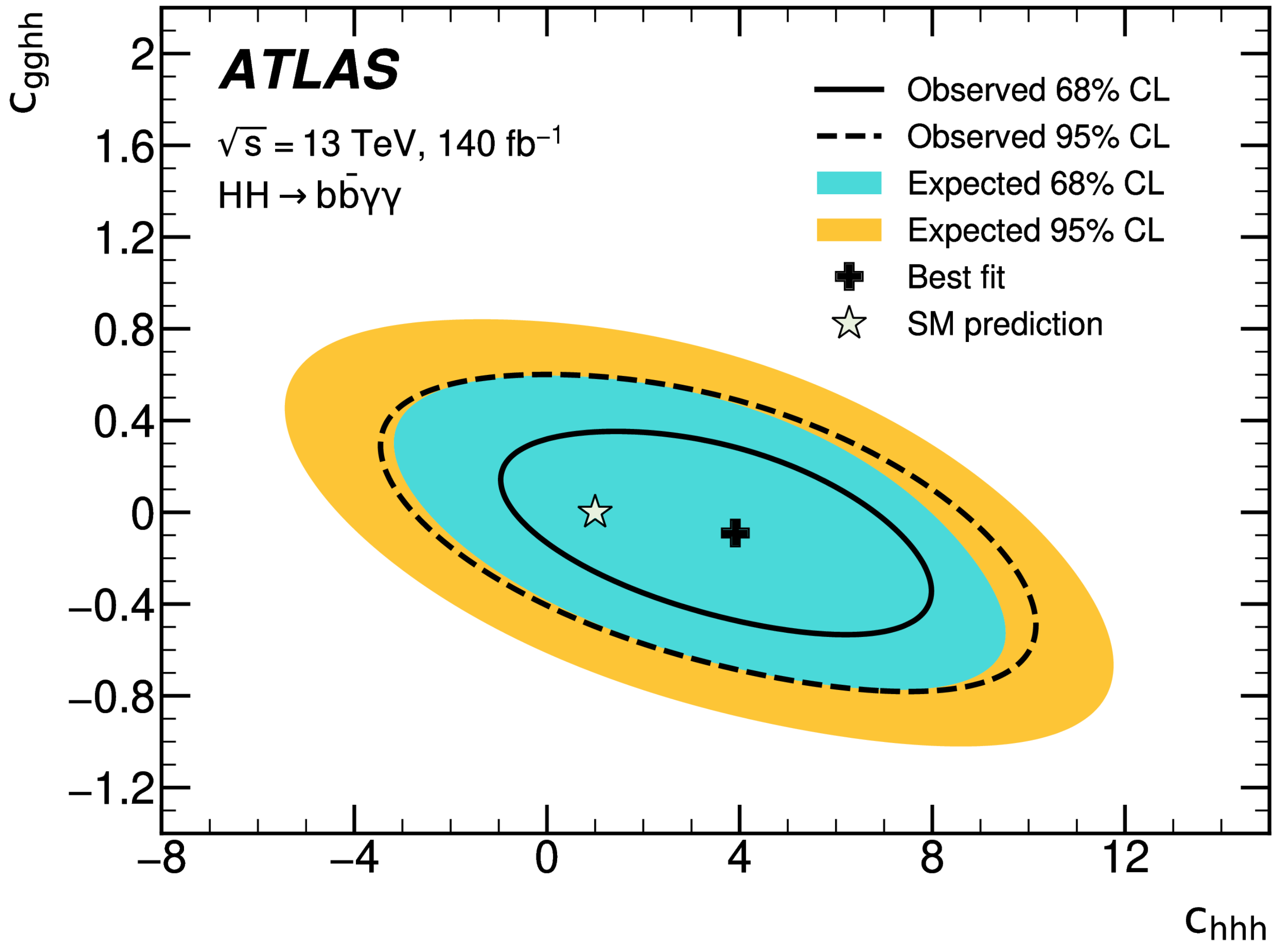

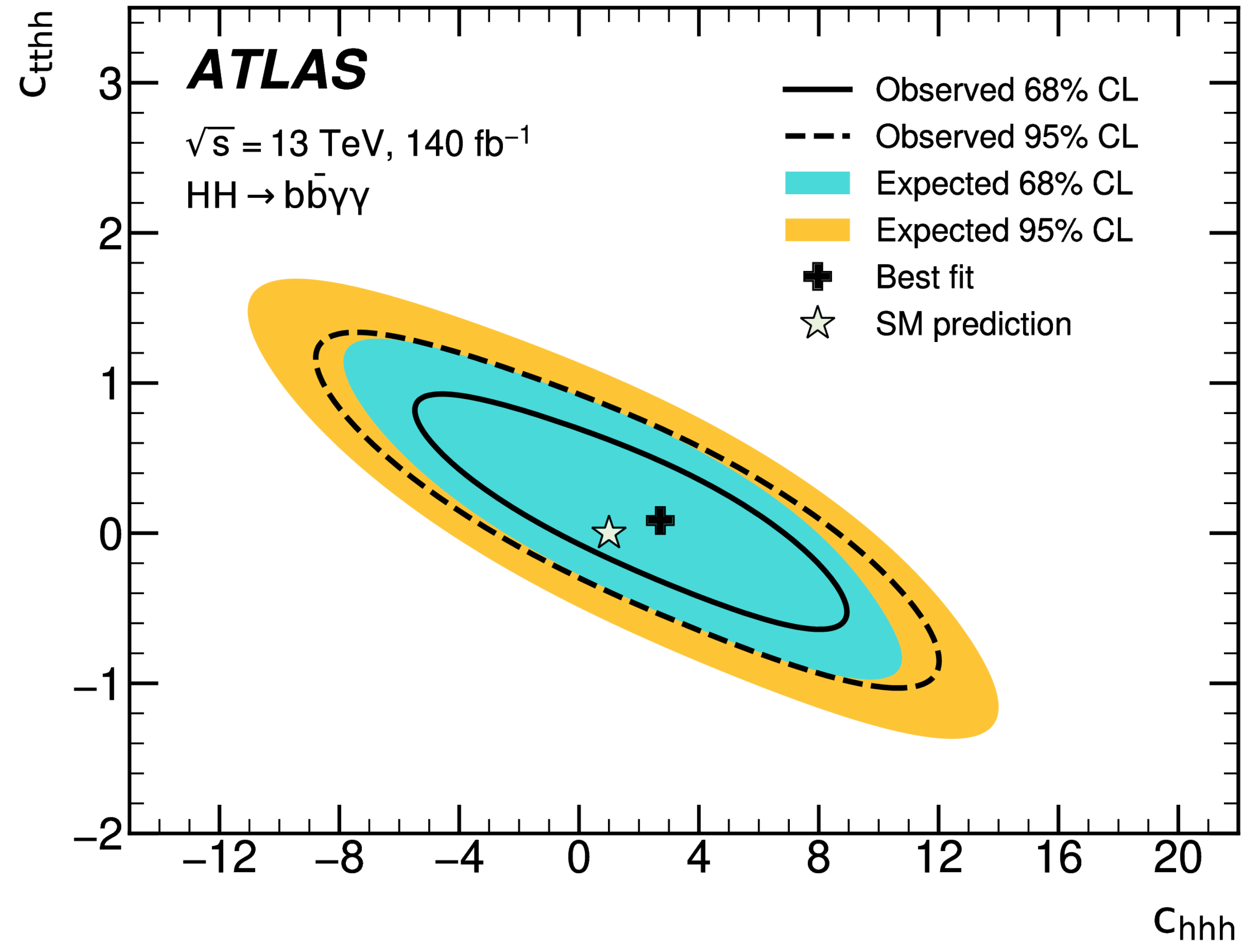

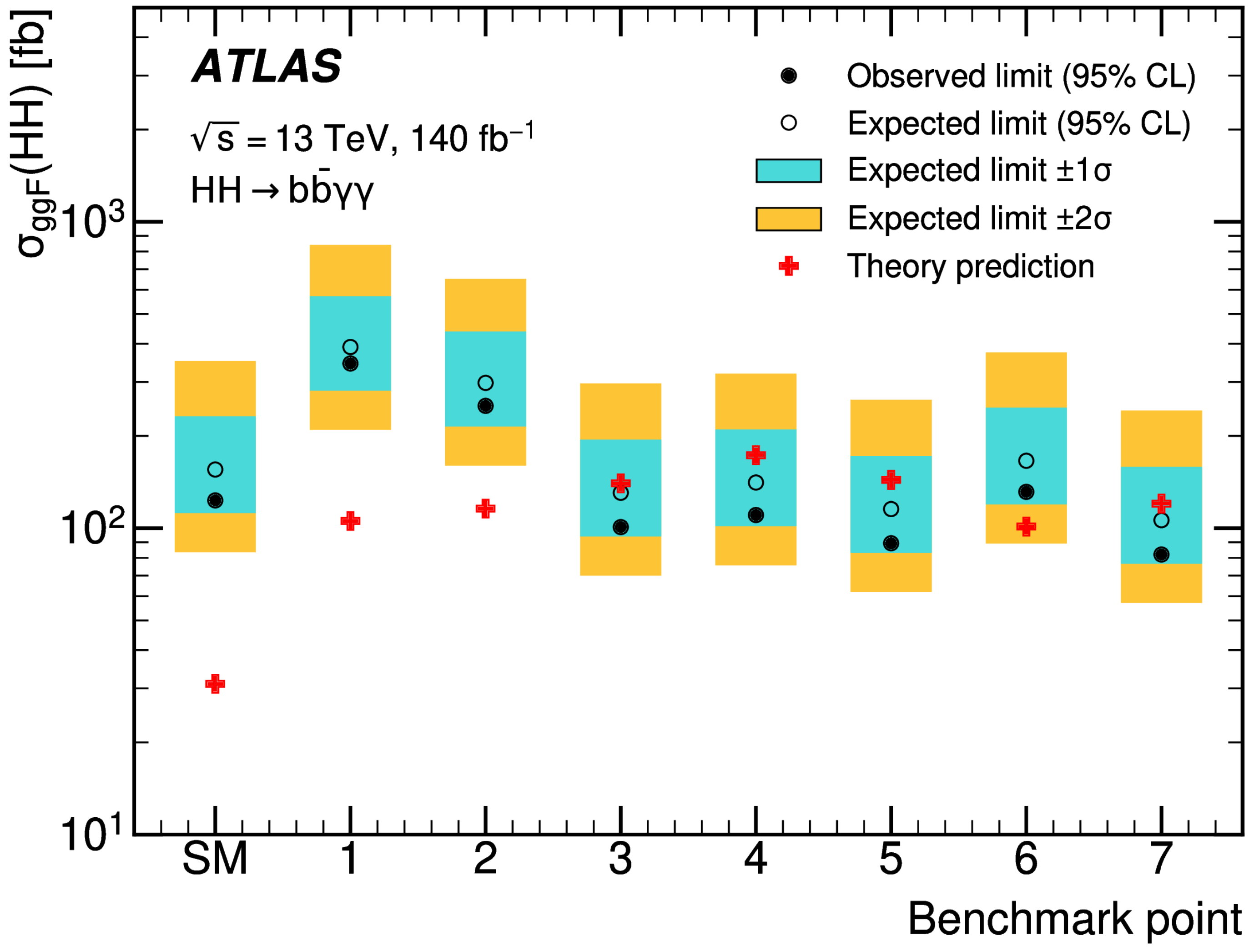

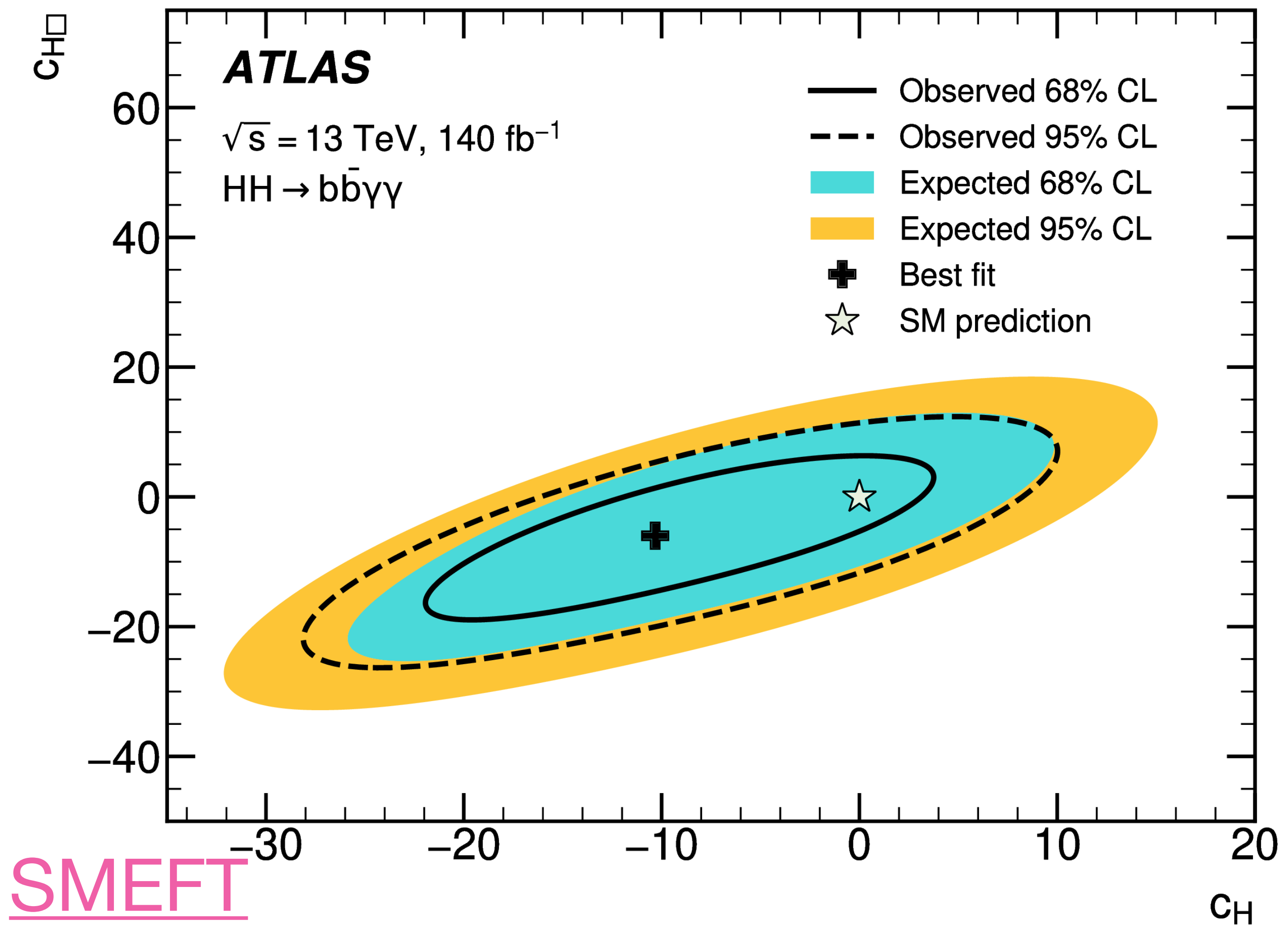

SMEFT

RosEFTa stone (HH operators)

HEFT

c_{hhh}, c_{tth}, c_{ggh}, c_{tthh}, c_{gghh}
c_{hhh}, c_{t}, c_{ggh}, c_{tt}, c_{gghh}
κ_{λ}, κ_{t}, c_{g}, c_{2}, c_{2g}

SMEFT

Relevant ggF HH operators

Warsaw operators	ATLAS STXS c_i/Λ^2	Alasfar & Gruber '19 c_i	SMEFiT '21 c_i/Λ^2	SMEFT@NLO c_i/Λ^2
Q_φ	C_H	c_H/Λ^2	C_6	cp
$Q_{\varphi G}$	C_{HG}	c_{HG}/Λ^2	$C_{\Phi G}$	cpG
$Q_{u\varphi}$	C_{tH}	c_{uH}/Λ^2	$C_{t\Phi}$	ctp
Q_{uG}	C_{tG}	-	C_{tG}	ctG
$Q_{\varphi\Box}$	$C_{H,\Box}$	$c_{H,kin}$	C_H	cdp
$Q_{\varphi D}$	C_{HD}	c_{HD}/Λ^2	-	cpDC

SMEFT → HEFT translation

L. Alasfar, LHC-HH

HEFT	SMEFT: SILH	SMEFT: Warsaw
c_{hhh}	$1+\bar{c}_6-\frac{3}{2}\bar{c}_H$	$1-2\frac{v^4}{m_h^2}C_H+3c_{H,kin}$
c_t	$1-\frac{\bar{c}_H}{2}-\bar{c}_u$	$1+c_{H,kin}-C_{uH}\frac{v^3}{\sqrt{2}m_t}$
c_{tt}	$-\left(\frac{3}{2}\bar{c}_u+\frac{\bar{c}_H}{2}\right)$	$-C_{uH}\frac{3v^3}{2\sqrt{2}m_t}+c_{H,kin}$
c_{ggh}	$\frac{128\pi^2}{g_2^2}\bar{c}_g$	$\frac{8\pi}{\alpha_s}v^2C_{HG}$
c_{gghh}	$\frac{64\pi^2}{g_2^2}\bar{c}_g$	$\frac{4\pi}{\alpha_s}v^2C_{HG}$

Where $C_{H,kin}=(C_{H,\Box}-\frac{1}{4}C_{HD})$

arXiv:1008.4884 arXiv:1008.4884

From L. Pereira Sanchez

HH → bb$\tau\tau$/bb$\gamma\gamma$ vs HEFT

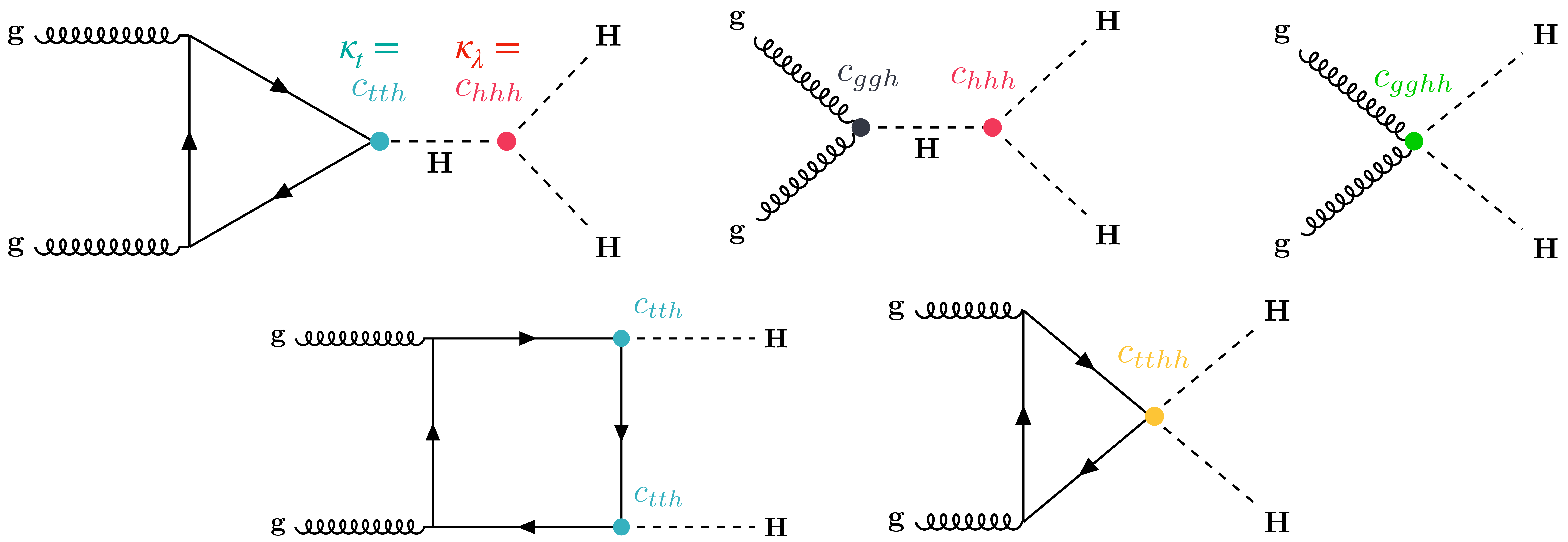

- Higgs Effective Field Theory [arXiv:1212.3305, arXiv:1312.5624]
  - Less stringent gauge (SU2) constraints on operators in H sector than SMEFT [arxiv.org:1308.2627]
  - Broader UV theories where e.g. BSM particles gain mass via EWSB (non-decoupling) [arXiv:1902.05936]
- Two Wilson coefficients (c_{tth}, c_{hhh}) correspond to Kappa framework (κ_t, κ_λ)

HH → bb$\tau\tau$/bb$\gamma\gamma$ vs HEFT

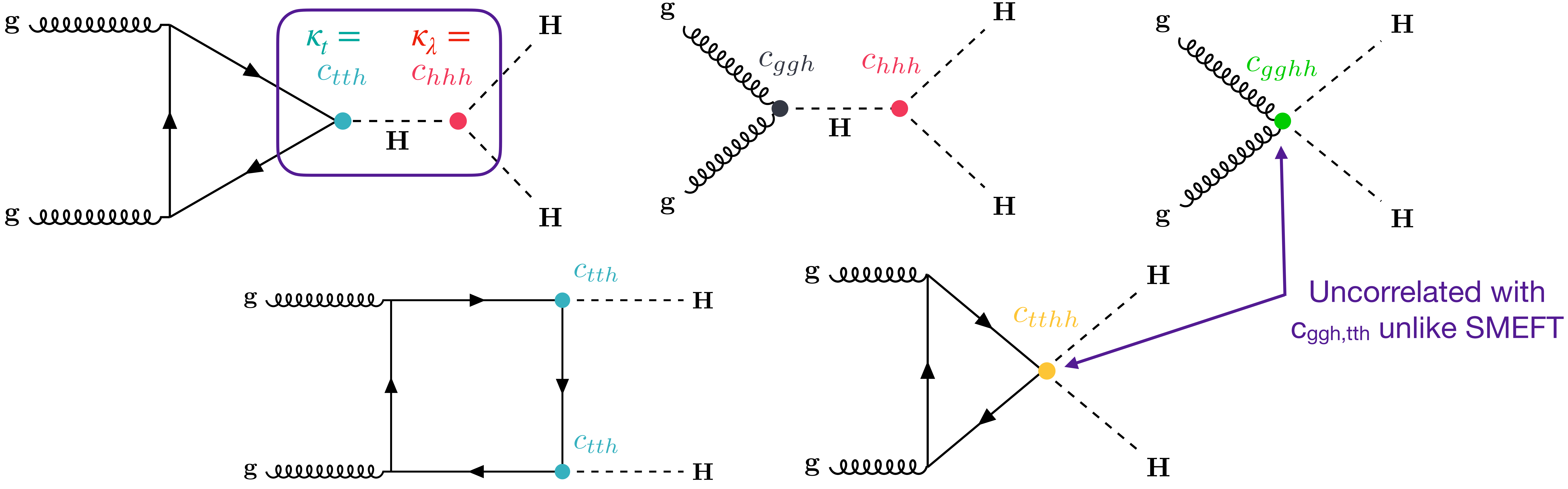

- Higgs Effective Field Theory [arXiv:1212.3305, arXiv:1312.5624]
  - Less stringent gauge (SU2) constraints on operators in H sector than SMEFT [arxiv.org:1308.2627]
  - Broader UV theories where e.g. BSM particles gain mass via EWSB (non-decoupling) [arXiv:1902.05936]
- Two Wilson coefficients (c_{tth}, c_{hhh}) correspond to Kappa framework (κ_t, κ_λ)

ATL-PHYS-PUB-2022-021

HH → bbττ/bbγγ vs HEFT

Limits set also on m_{HH} shape benchmarks
arXiv: 1908.08923

Constrain HH to gluon/top couplings via ggF cross-section

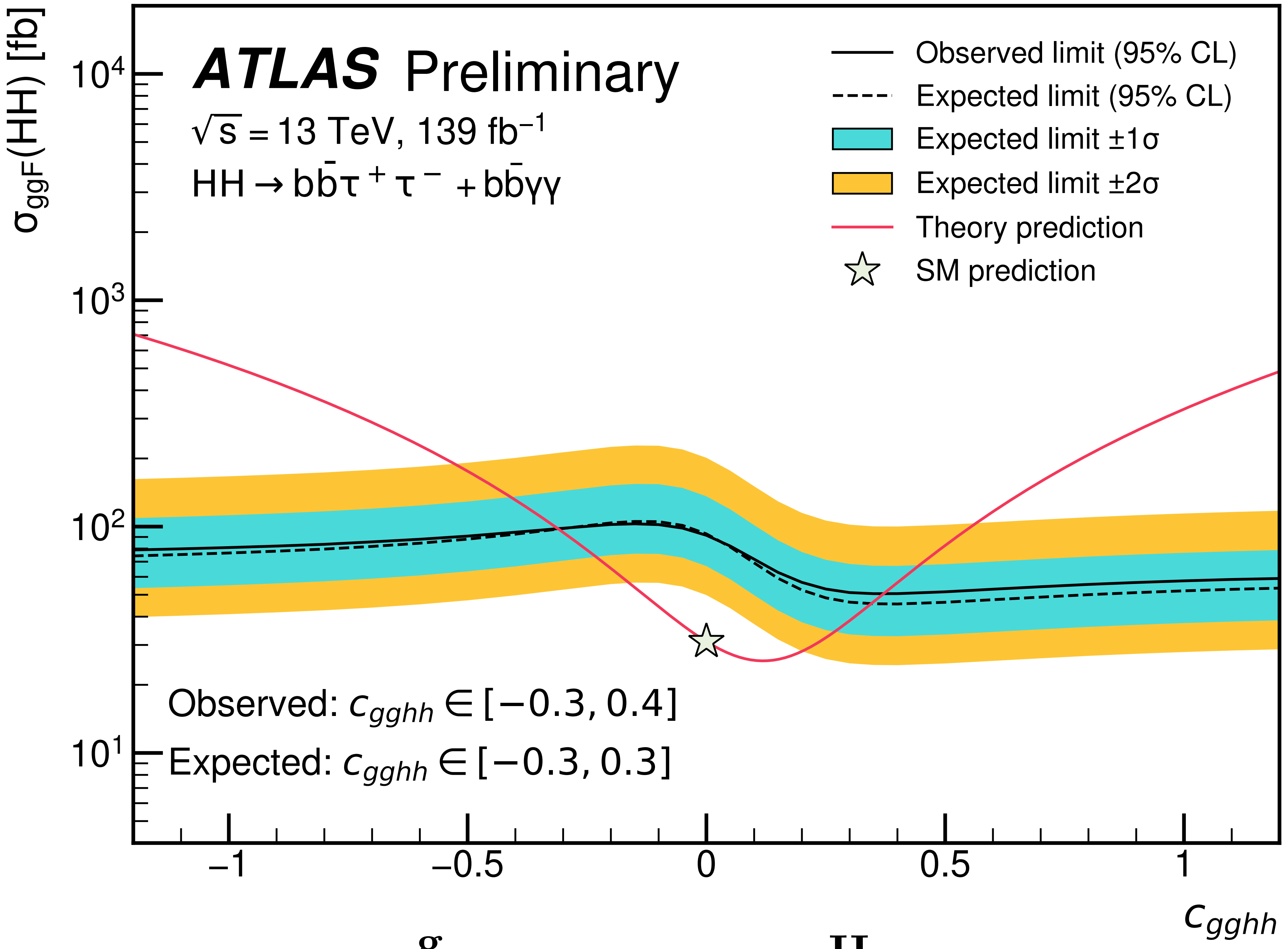

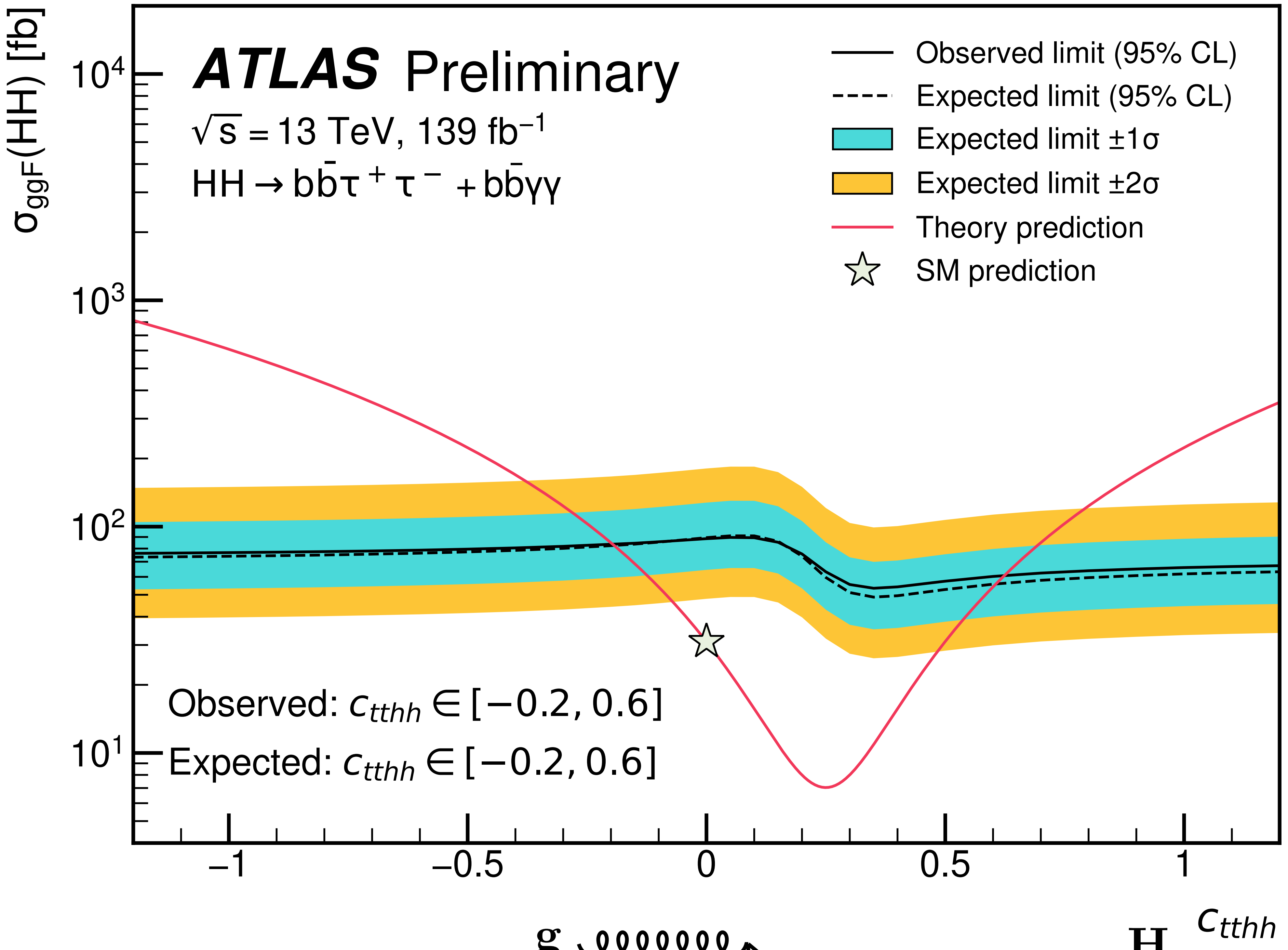

Decoupled from c_{ggh} unlike SMEFT

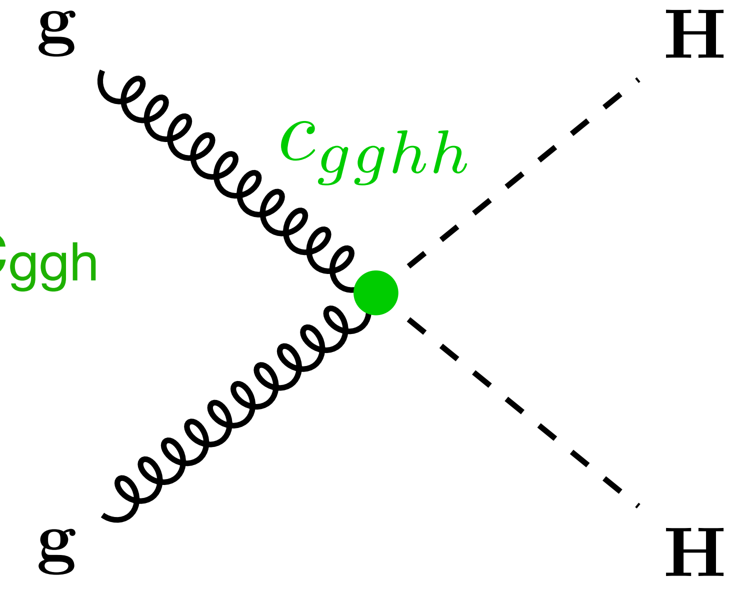

Decoupled from c_{tth} unlike SMEFT

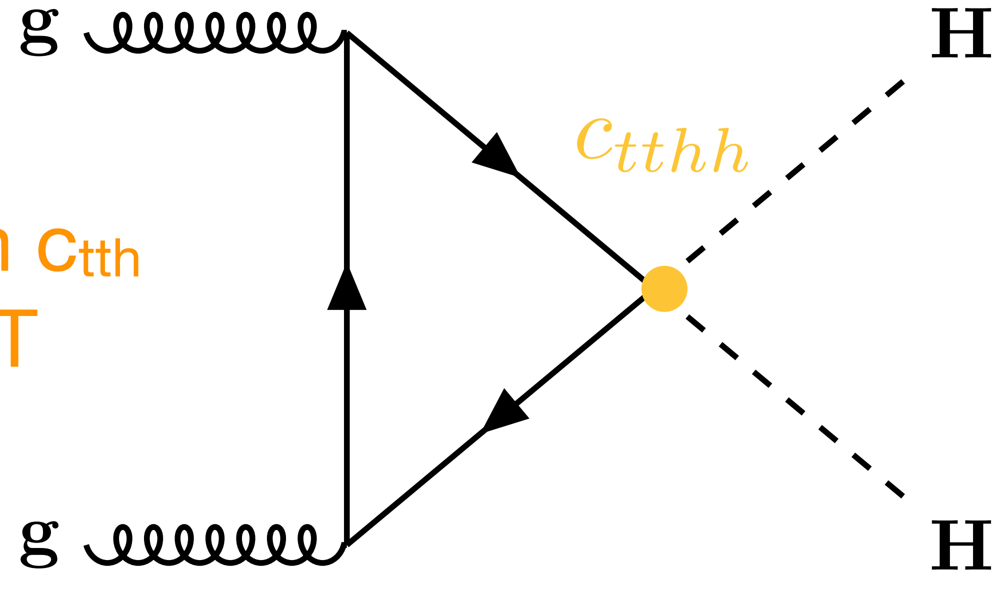

ATL-PHYS-PUB-2022-021

bbττ/bbγγ vs HEFT

Benchmark model	c_{hhh}	c_{tth}	c_{ggh}	c_{gghh}	c_{tthh}
SM	1	1	0	0	0
BM 1	3.94	0.94	1/2	1/3	−1/3
BM 2	6.84	0.61	0.0	−1/3	1/3
BM 3	2.21	1.05	1/2	1/2	−1/3
BM 4	2.79	0.61	−1/2	1/6	1/3
BM 5	3.95	1.17	1/6	−1/2	−1/3
BM 6	5.68	0.83	−1/2	1/3	1/3
BM 7	−0.10	0.94	1/6	−1/6	1

HEFT benchmarks via arXiv: 1908.08923

m_{HH} shapes representative of Wilson coeff variations

See e.g. CMS JHEP 03 (2021) 257
for SMEFT benchmarks

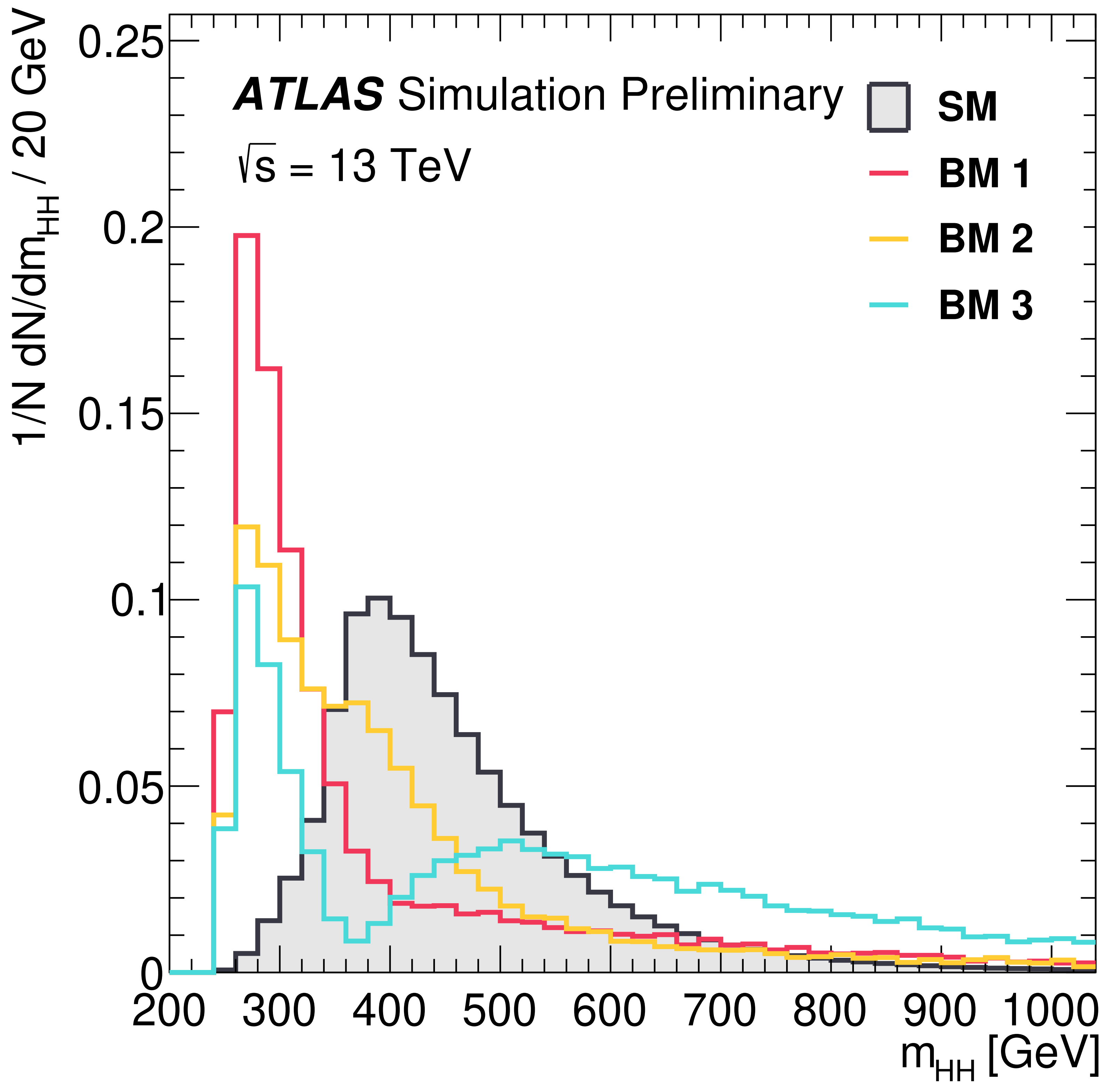

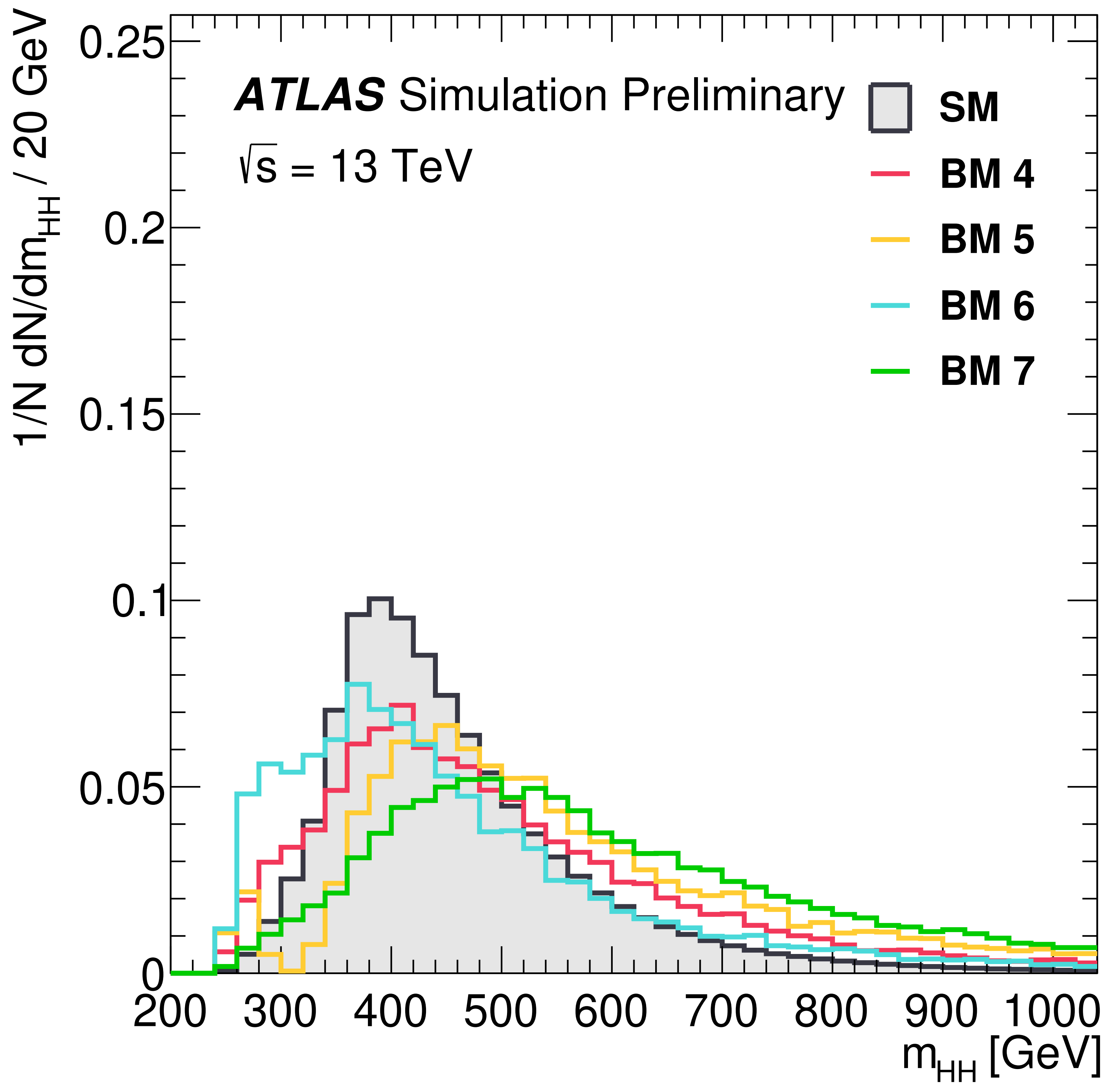

ATL-PHYS-PUB-2022-021, arXiv:2112.11876, ATLAS-CONF-2021-03